

Exploring the Mechanisms of Pacific Oyster Summer Mortality
in Baynes Sound Aquaculture

by

Malcolm Cowan

BSc, University of Victoria, 2016

A Thesis Submitted in Partial Fulfillment of the Requirements for the Degree of
MASTER OF SCIENCE
in the Department of Biology

© Malcolm Cowan, 2020

University of Victoria

All rights reserved. This thesis may not be reproduced in whole or in part, by photocopy or other means, without the permission of the author.

Exploring the Mechanisms of Pacific Oyster Summer Mortality
in Baynes Sound Aquaculture

by

Malcolm Cowan

BSc, University of Victoria, 2016

Supervisory Committee:

Dr. Patrick von Aderkas – Co-Supervisor
Department of Biology

Dr. Chris Pearce – Co-Supervisor
Department of Geography

Dr. Paul De La Bastide – Member
Department of Biology

Dr. Caren Helbing – Outside Member
Department of Biochemistry and Microbiology

Abstract

In recent years, mortalities of unknown aetiology have occurred in Pacific oyster aquaculture in Baynes Sound, BC during the summer. Field studies were conducted to examine environmental, reproductive and microbial factors that could be contributing to these mortalities. In 2017, oysters were observed at three sites from July 5 to September 15. Each intertidal site had three modules containing seven stacked trays with 80 oysters per tray. Final mortalities ranged from 9.3 ± 1.9 to $38.8 \pm 4.9\%$ per module. The mortality per module correlated significantly with gonad length and the proportion of oysters that were female in a multiple linear regression model ($R^2=0.824$, $p=0.002$). *Vibrio aestuarianus*, a well-documented pathogen of farmed Pacific oysters in France, was well represented in bacterial cultures from intertidal oysters in 2017 based on *recA* gene sequencing of 158 bacterial isolates. In 2018, juvenile Pacific oysters were monitored to characterize the onset of a summer mortality event in suspended culture. From May 11 to September 17, data on shell size, reproductive development, environmental conditions, and the microbial community of gill tissue was tracked at culture densities of 150, 300, 450, and 600 oysters tray⁻¹. The onset of mortality was associated with a period of rapid growth, reproductive development, and elevated temperatures. Cumulative mortality per tray ranged from 34 to 75%, with the highest density trays having significantly lower mortality ($p=0.023$), smaller shell width ($p=0.001$), smaller shell length ($p=0.002$) and smaller gonad length ($p=0.049$) than the lowest density trays in a linear mixed-effects regression. Histology of oysters from August 12, during the mortality event, showed a mixed microbial infection in peripheral gill tissue. High-throughput sequencing of the 16S rRNA gene and qPCR of *V. aestuarianus* using species-specific *recA* primers suggest *V. aestuarianus* is temporally associated with summer mortality. Mortalities observed in 2017 and 2018 occurred in different

age classes and with different oyster culture techniques, but all were associated with elevated water temperature, increased reproductive effort, and the presence of *V. aestuarianus*.

Table of Contents

Supervisory Committee.....	ii
Abstract.....	iii
Table of Contents.....	v
List of Tables.....	vii
List of Figures.....	viii
List of Abbreviations.....	x
Acknowledgments.....	xi
Chapter 1 Introduction to Summer Mortality and Pacific Oyster Aquaculture in Baynes Sound..	1
1.1 Aquaculture.....	1
1.2 Pacific Oysters.....	4
1.3 Pacific Oyster Aquaculture in British Columbia.....	5
1.4 Pacific Oyster Mortality and Disease.....	6
1.5 Emerging Summer Mortality in British Columbia.....	11
1.6 Objectives.....	11
Chapter 2 Assessing the roles of the <i>Vibrio</i> Community, Reproductive Effort, and Environmental Parameters in Intertidal Pacific Oyster Summer Mortality.....	13
2.1 Introduction.....	13
2.2 Materials and Methods.....	15
2.2.1 Study Sites and Experimental Design.....	15
2.2.2 Oyster Collection and Bacterial Isolation and Identification.....	18
2.2.3 Sample Oyster Collection and Tissue Histology Preparation and Analysis.....	20
2.2.4 Environmental Factors.....	22
2.2.5 Statistical Analyses and Visualization.....	23
2.3 Results.....	25
2.3.1 Environmental Factors.....	25
2.3.2 Histology.....	26
2.3.3 Mortality Models.....	28
2.3.4 Bacterial Species Isolated from Oysters.....	35
2.4 Discussion.....	40
2.4.1 Reproductive Effort and Summer Mortality.....	40
2.4.2 Pathogens and Bacterial Identification.....	42
2.4.3 Environmental Monitoring.....	43
2.4.4 Conclusions.....	47
Chapter 3 <i>Vibrio aestuarianus</i> , temperature, and stocking density are associated with summer mortality of juvenile Pacific oysters (<i>Crassostrea gigas</i>) in suspended culture.....	48
3.1 Introduction.....	48
3.2 Materials and Methods.....	50
3.2.1 Study Site and Experimental Design.....	50
3.2.2 Environmental Factors.....	53
3.2.3 Oyster Monitoring and Sample Collection.....	53
3.2.4 Histology.....	54
3.2.5 DNA Extraction.....	55
3.2.6 Microbial Composition.....	56
3.2.7 Quantification of <i>Vibrio aestuarianus</i>	57
3.2.8 Potentially Harmful Phytoplankton.....	58

3.2.9 Statistical Analyses and Visualization.....	59
3.3 Results:	60
3.3.1 Effects of Stocking Density	60
3.3.2 Growth and Reproductive Development	64
3.3.3 Observed Mortality	66
3.3.4 Environmental Observations	68
3.3.5 Histopathology	68
3.3.6 Analysis of Microbial Composition	70
3.3.7 Quantification of <i>Vibrio aestuarianus</i>	74
3.3.8 Phytoplankton.....	76
3.4 Discussion	78
3.4.1 Effect of Stocking Density	78
3.4.2 Environmental Factors.....	79
3.4.3 Bacterial Composition and the Occurrence of <i>Vibrio aestuarianus</i>	80
3.4.4 Reproductive Effort	82
3.4.5 Conclusion	84
Chapter 4 Conclusion and Perspectives	85
4.1 Summary of Pacific Oyster Summer Mortality in Baynes Sound	85
4.2 Mitigating Pacific Oyster Summer Mortalities	86
4.3 Conclusion.....	90
Literature Cited.....	91

List of Tables

Table 1.1: Annual yields of mussels, oysters, scallops, and clams in metric tonnes of live weight from global aquaculture production (1980, 2000, 2016), as well as from Canada (2016), and China (2016). Data from FishStatJ (Anon, 2018). Values in brackets represent % of global production by weight.	3
Table 2.1: Model selection for a binomial generalized linear mixed-effects model using a cloglog link function to describe Pacific oyster survival over time. All models include date, a date offset, 494 residual degrees of freedom, and the random effects of trays nested in modules. Factors examined were site, temperature (Temp), tide exposure (Tide), tray height (Tray), proportion of oysters that were female (PF), gonad length (GL), gonadosomatic index (GSI), and proportion of oysters with ripe gonads (PR). Model 4, shown in bold, has the lowest ΔAIC value.....	30
Table 2.2: Model 4 fixed effects from Table 2.1. Describing the most parsimonious binomial generalized linear mixed-effects model with a cloglog link describing intertidal Pacific oyster mortality during the summer of 2017. This model has 9 degrees of freedom, 497 residual degrees of freedom, and includes the nested random effects of trays within modules.	31
Table 2.3: Multiple linear regression AIC model selection. Models explained the variation in cumulative mortality per module based on gonad characteristics. Model 4 is the most parsimonious, with the lowest AIC value. GSI: gonadosomatic index, GL: gonad length, OA: oyster area, GA: gonad area, PF: proportion female.....	33
Table 2.4: Summary of recA nucleotide sequence BLAST queries from NCBI database in November, 2018 for 158 cultured bacterial isolates from intertidal Pacific oyster homogenate during the summer of 2017.	36

List of Figures

- Figure 1.1: Interactions among the primary hypothesized factors that influence Pacific oyster summer mortality. Positive (+) and negative (–) interactions between factors are indicated. 10
- Figure 2.1: Left: Map of greater region with Baynes Sound shown as a square. Right: Baynes Sound with Buckley Bay (◆), Fanny Bay (▲), Ship’s Point (●), Metcalf Bay (■), and Chrome Island (□). 17
- Figure 2.2.2: Proportion of Pacific oyster gonads in each reproductive developmental phase throughout the summer of 2017, as determined from hematoxylin and eosin stained histological cross sections. Classification of development phases was based on Steele and Mulcahy (1999). 27
- Figure 2.3: Survival curve for intertidal Pacific oysters from July 12 to September 15, 2017. Each point represents an observation of a tray of 80 oysters. Points are jittered around the sampling date to prevent overlap. Data are fitted with a binomial model using a cloglog link function, with standard error shown in grey. 29
- Figure 2.4: Linear regressions for the average cumulative mortality per module with the explanatory variables (A) gonad length (GL) and (B) proportion of individuals that are female (PF). (C) fitted values from the most parsimonious linear regression in Table 2.3 (Model 4). Average mortality per module was measured on September 15, 2017. Sites are indicated by different shapes; Buckley Bay (●), Fanny Bay (▲), and Ship’s Point (■).. 34
- Figure 2.5: Neighbor-joining tree showing clusters of identified bacterial isolates from Pacific oysters in Baynes Sound, based on the nucleotide sequence of the recA gene (~800 bp). The number of isolates that cluster together with >96.3% within-group mean nucleotide identity (N) is indicated (Table 2.4). Numbers on nodes represent support generated from 500 bootstrap replicates. Scale bar represents p-distance. 39
- Figure 3.1: Left: Map of Pacific Northeast with the field site location shown with a square. Right: Baynes Sound with Metcalf Bay (■), Fanny Bay (▲), and Chrome Island (●) shown. 51
- Figure 3.2: Experimental design of juvenile Pacific oyster trays in suspended culture. Each block of four trays contained one replicate unit at each of the four densities (150, 300, 450, and 600 oysters tray⁻¹). All blocks were suspended at 5 m depth in Metcalf Bay off a shellfish aquaculture raft, following standard industry practices. 52
- Figure 3.3: Final-end measurements of density dependent effects on Pacific oyster shell size. Oysters were grown at four starting stocking densities 150, 300, 450, and 600 oysters tray⁻¹ from May 11 to September 17, 2018. Values represent the average of four replicate trays at each density with 10 observations from each tray, and error bars represent standard error. 61
- Figure 3.4: Final-end measurements of reproductive characteristics measured from Pacific oyster histological cross sections. Oysters were grown at four starting stocking densities (150, 300, 450, and 600 oysters tray⁻¹) from May 11 to September 17, 2018. Values represent the average of four replicate trays at each density with one observation from each tray, error bars represent standard error. 62
- Figure 3.5: Final-end observations of Pacific oyster cumulative mortality observed in suspended culture at Metcalf Bay, Baynes Sound on September 17, 2018. Oysters were grown at four starting stocking densities (150, 300, 450, and 600 oysters tray⁻¹) from May 11 to

	September 17, 2018. Values represent the average of four replicate trays at each density with 100 observations from each tray, and error bars represent standard error.....	63
Figure 3.6:	Each point represents a replicate tray containing 150, 300, 450, or 600 Pacific oysters. PC1 of oyster size variables described 98.3% of the variation in shell height, width, and length. PC1 of oyster reproductive development described 79.4% of variation in oyster gonad length, gonad area, gonadosomatic index, and gonad developmental phase.	65
Figure 3.7:	Pacific oyster survival by starting stocking density and water temperature during summer, 2018. Densities were 150, 300, 450, and 600 oysters tray ⁻¹ at the onset of the experiment on May 11, 2018. Daily water temperatures were acquired from DFO monitoring at Chrome Island Lighthouse (Fig. 3.1) (Anon, 2019a). Fitted curves are smoothed conditional means using local polynomial regression fitting.	67
Figure 3.8:	Example histopathology cross sections from August 12, 2018 sampling of the Pacific oyster summer mortality event. Top: low magnification of necrosis in gills and epithelium with healthy labial palps on the left. Bottom: high magnification of mixed microbial infection in peripheral tissue necrosis. Staining done with H&E (A and C) and Gram stain (B and D). In the Gram stain gram-negative bacteria are pink to light purple and gram-positive bacteria are blue.	69
Figure 3.9:	Stacked bar plot of Pacific oyster bacterial microbiome. Shown identities are the nearest result from AMPtk 16S rRNA gene data base using AMPtk taxonomy with 97% nucleotide clustering.	72
Figure 3.10:	Bacterial composition using Bray Curtis dissimilarities of the V4 region of the 16S rRNA gene rarified to 9150 reads. Ellipses indicate 95% confidence intervals for each cluster.	73
Figure 3.11:	Quantitative polymerase chain reaction results for juvenile Pacific oyster gill tissue. Group averages are shown with gray bars. Four moribund and two weak individuals were collected during the mortality event on August 12, 2018. The red point is from the same oyster with a mixed microbial infection shown in Figure 3.8.	75
Figure 3.12:	Concentration of the most abundant species per samples and all potentially harmful plankton species detected at 5 m depth in Metcalf Bay.....	77
Figure 4.1:	Hypothesized mechanisms of Pacific oyster summer mortality and potential mitigative actions (shown in grey filled boxes). Positive (+) and negative (-) interactions between factors are indicated.....	87

List of Abbreviations

AIC – Akaike Information Criterion
BC – British Columbia
BLAST – Basic Local Alignment Search Tool
DFO – Department of Fisheries and Oceans
EtOH – Ethanol
GA – Gonad Area
GL – Gonad Length
GLMM – Generalized Linear Mixed-Effects Model
GSI – Gonadosomatic Index
H&E – Hematoxylin and Eosin
HABs - Harmful Algal Blooms
NCBI – National Center for Biotechnology Information
NMDS – Non-Metric Multidimensional Scaling
OA – Oyster Area
OTU – Operational Taxonomic Unit
PCA – Principle Component Analysis
PC1 - Principle Component One
PERMANOVA – Permutational Multivariate Analysis of Variance
PF – Proportion of Oysters that are Female
POMS – Pacific Oyster Mortality Syndrome
PR – Proportion Ripe
QGIS – Quantum Geographic Information System
qPCR – Quantitative Polymerase Chain Reaction
SIMPER – Similarity Percentage Analysis
VGH – Viral Gametocytic Hypertrophy

Acknowledgements

I am incredibly thankful for the support and community at Mac's Oysters Ltd.

Thank you to the Aquaculture Collaborative Research and Development Program (ACRDP) at the Department of Fisheries and Oceans Canada and Mac's Oysters Ltd. for the financial support for this project.

I'd like to thank my committee members for the input and guidance throughout this project: Dr. Patrick von Aderkas, Dr. Chris Pearce, Dr. Paul de la Bastide, and Dr. Caren Helbing.

Thank you to the support from the following collaborators: Chris Pearce, Paul de la Bastide, Terrie Finston, Gary Meyer, Rob Marshall, Tim Green, Terri Sutherland, Jon Van Hamme, Eric Bottos, Breanne McAmmond, Wiley Evans, and Will Hintz.

I am also very grateful to my family, friends, fellow students, and the staff in the UVic Biology Department for their support during these years; most notably Priscilla Tetley, Emily Warren, Élyse Gaudreau, and Michelle Shen.

Chapter 1 **Introduction to Summer Mortality and Pacific Oyster Aquaculture in Baynes Sound**

1.1 Aquaculture

Aquaculture is the practice of farming aquatic species and generally includes stocking, feeding, and containment of animals. Since the 1960s, the global consumption of seafood has increased dramatically from 9.9 to over 19.7 kg per capita (Anon, 2016a). Today, aquaculture produces over half of the seafood for human consumption, up from only 7% in 1974. This expansion in aquaculture was led by China, which accounts for roughly 60% of the global aquaculture activity. In 2014, aquaculture produced 73.8 million tonnes of food, equating to an estimated US\$160.2 billion farm-gate value (the price at first point of sale by the harvester); finfish, crustaceans, and molluscs represent 67.7, 21.7, and 9.8% of that value, respectively. Of this tonnage, 30.8% are non-fed animals, predominantly carp, bivalves, and other filter feeders.

Seafood accounts for at least 15% of the animal protein consumed by humans, and is high in essential fats, vitamins, and minerals. As the global population trends towards 9.7 billion people by 2050 there will be an ever-growing need for protein and nutrient-rich food. Increasing terrestrial protein production is becoming increasingly costly due to limited arable land (Flachowsky *et al.*, 2017) and food production from wild fisheries has been stagnant due to degradation and limitation of wild stocks (Pauly *et al.*, 2002; Garcia *et al.*, 2010; Godfray *et al.*, 2010; Anon, 2016a). Conversely, aquaculture is the largest growing food sector in the world (Anon, 2016a). The economic growth of aquaculture, however, is limited by changing environmental conditions, disease, the use of wild fish in feed, and the externalities on natural stocks and local habitats (Smith *et al.*, 2010; Anon, 2016a).

Shellfish aquaculture provides several ecosystem services and it is often considered a sustainable form of food production (Shumway *et al.*, 2003). Unlike most terrestrial forms of farming, shellfish aquaculture is generally integrated within the marine ecosystem. This promotes biodiversity and biomass of species in the habitat through increased spatial complexity and nutrient cycling (Shumway *et al.*, 2003; Coen *et al.*, 2007; Lemasson *et al.*, 2017). Shellfish filter feeding also improves water quality and can regulate concentrations of microorganisms and plankton (Shumway *et al.*, 2003; Coen *et al.*, 2007). Additionally, shellfish aquaculture provides essential economic sustainability in coastal communities, and its success is evident in global shellfish production (Shumway *et al.*, 2003; Anon, 2018) (Table 1.1).

Table 1.1: Annual yields of mussels, oysters, scallops, and clams in metric tonnes of live weight from global aquaculture production (1980, 2000, 2016), as well as from Canada (2016), and China (2016). Data from FishStatJ (Anon, 2018). Values in brackets represent % of global production by weight.

	Global 1980	Global 2000	Global 2016	Canada 2016	China 2016
Mussels	563,373	1,307,243	2,007,507	24,584 (1.22 %)	878,771 (43.8 %)
Oysters	906,371	3,610,867	5,594,822	13,824 (0.25 %)	4,834,527 (86.4 %)
Scallops	40,653	1,047,884	2,126,930	38 (0.00 %)	1,879,097 (88.3 %)
Clams	276,522	2,354,730	5,570,141	1,962 (0.03 %)	5,363,442 (96.2 %)
Total	1,786,919	8,320,724	15,299,400	40,408 (0.26 %)	12,955,837 (84.7 %)

1.2 Pacific Oysters

The preferred scientific name for Pacific oysters, also known as Japanese or miyagi oysters, is *Crassostrea gigas* (Quayle, 1988; Bayne *et al.*, 2019), but the name *Magallana gigas* has recently been proposed (Salvi *et al.*, 2014). These cupped oysters are a species of bivalve molluscs endemic to Northeast Asia (Quayle, 1988). They can grow in a broad range of temperatures (3 to 35°C) and salinities (10 to 35‰) (Quayle, 1988; Strand and Lindergarth, 2014). There is marked variability in the size, shape, and colour of Pacific oysters (Quayle, 1988). Generally, adult Pacific oysters are 10–15 cm in height (the longest dimension), have a grey exterior shell with purple fluting and have a smooth mauve or white inner shell surface (Galstoff, 1964; Quayle, 1988). The shell of Pacific oysters is nearly bilaterally symmetrical with two valves parallel to its surface, and interlocking teeth along its shell margins (Galstoff, 1964). Pacific oysters typically grow as intertidal reefs on rocky substrates, but can also proliferate in intertidal mudflats and subtidal habitats (Quayle, 1988).

Pacific oysters are protandrous hermaphrodites that change sex erratically: they can possess male and female gametes (Pauley *et al.*, 1988). Fecundity of Pacific oysters rivals most bivalves (Troost, 2010). For example, adult female Pacific oysters contain over 100 million eggs (Royer *et al.*, 2008), whereas the Eastern oysters (*Crassostrea virginica*) have no more than 350 thousand eggs per spawn (Mroch *et al.*, 2012). Water temperatures from 20 to 23°C induce broadcast spawning (Quayle, 1988). Once fertilized, the spherical eggs of roughly 0.05 mm diameter begin rapid cell division. After 48 h the larvae possess newly developing organ systems and a rapidly growing shell. Depending on the temperature, after 18-30 days larvae reach a size of 0.30 mm in length. At this point, they begin the process of setting, i.e. adhering to a solid surface. The remainder of their life cycle is sessile.

Pacific oysters have highly developed stress tolerance mechanisms that allow adaptation to both daily and seasonal fluctuations in biotic and abiotic conditions within the intertidal environment. These fluctuations include temperature, salinity, hypoxia, pathogens, and wave action (Zhang *et al.*, 2016). The rapid adaptive divergence, and high phenotypic plasticity of Pacific oysters' have contributed to their success as an invasive species (Troost, 2010; Wendling and Wegner, 2015; Li *et al.*, 2018). Today, they are present in most coastal countries as a result of both deliberate and accidental introductions (Gillespie *et al.*, 2012; Anon, 2018). Due to their rapid growth, large size, and success in many environments, they are one of the most widely cultured bivalve species in the world (Quayle, 1988; Gillespie *et al.*, 2012; Anon, 2018).

1.3 Pacific Oyster Aquaculture in British Columbia

Pacific oyster aquaculture has been an important industry and cultural component in British Columbia (BC) for over a century (Quayle, 1988; Gillespie, 2012). Following a precipitous decline in the stocks of the native Olympia oyster (*Ostrea lurida*), Pacific oysters were introduced from Japan around 1912 (Quayle, 1988). These initial oysters were planted in Ladysmith Harbour and Fanny Bay. By 1942, over four million oyster seed had been introduced to areas such as Pender Harbour, Boundary Bay, and Baynes Sound. In 2016, BC oyster aquaculture production was 8,757 tonnes with a value of CA\$14.8 million (Anon, 2016b).

Today, Baynes Sound – the site of this research project – is extensively farmed. There are 137 shellfish tenures covering 90% of the intertidal area (Bendell, 2019). Commercial shellfish production in Baynes Sound accounts for 39% of the cultured oysters and 55% of the cultured clams in BC (Emmet, 2002). Production of Pacific oysters in the area generally uses hatchery supplied seed that is grown in suspended culture, followed by shell conditioning in the intertidal

for the half-shell market. The area also has a diverse ecological landscape that includes spawning habitat for salmonids and herring (Bendell, 2019).

1.4 Pacific Oyster Mortality and Disease

Pacific oysters are susceptible to a number of parasites and pathogens of regional concern, described by Bower (2017). These include viruses (causing viral gametocytic hypertrophy), bacteria (*Nocardia crassostrea*), protists (*Mikrocytos* spp., *Haplosporidium nelsoni* [MSX]), fungi (*Ostracoblable implexa*), flukes (*Gymnophalloides tokiensis*, *Bucephalus* spp.), copepods (*Mytilicola orientalis*), and crabs (*Pinnotheres* spp., *Pinnixa littoralis*) (Bower, 2017).

There are a few disease pathologies of Pacific oysters that have caused major mortalities and have been the target of systematic research for decades, including Pacific Oyster Mortality Syndrome (POMS), Denman Island Disease, and summer mortality. POMS, also referred to as summer mortality syndrome, is caused by the *Ostreid herpesvirus* μ Var 1 (OsHV-1), which infects hemocytes (de Kantzow *et al.*, 2017; de Lorgeril *et al.*, 2018). Oysters become immunocompromised and develop fatal bacteremia, due to infections by opportunistic pathogens (de Lorgeril *et al.*, 2018). Mortalities of up to 100% have occurred in France (Anon, 2015). Sudden extreme losses due to POMS occurred in New South Wales, Australia in 2010 (Jenkins *et al.*, 2013), Tasmania, Australia in 2016 (Whittington *et al.*, 2016; de Kantzow *et al.*, 2017), and California, USA (Burge *et al.*, 2006). OsHV-1 has not been detected in BC (Anon, 2017a).

Denman Island Disease is named after Denman Island, which borders Baynes Sound. The causal agent of this disease is a small intracellular protistan called *Mikrocytos mackini* (Bower *et al.*, 1997) and is easily identified by the presence of green pustules on the surface of gonad tissue

(Quayle, 1988). Oysters affected by Denman Island Disease are generally more than two years of age. Historically, outbreaks of Denman Island Disease caused mortalities of roughly 30%, typically occurring between April and July when water temperatures are between 9 and 18°C. Furthermore, temperatures above 15°C may prevent disease progression of *M. mackini* in Pacific oysters (Bower *et al.*, 1997).

Pacific oyster summer mortality describes OsHV-1-free mortalities that is most commonly associated with elevated water temperature, elevated reproductive effort, and the presence of opportunistic pathogens. Observations fitting this definition of summer mortality were first described in Japan in the 1940s (Imai *et al.*, 1965; Renault *et al.*, 2005). Summer mortality has been described and is a major challenge for shellfish aquaculture in many countries, including Australia (Go *et al.*, 2017), Canada (Meyer, 2013), Mexico (Chávez-Villalba *et al.*, 2007), Ireland (Cotter *et al.*, 2010), France (Gouletquer *et al.*, 1998; Renault *et al.*, 2005; Garnier *et al.*, 2007), Germany (Watermann *et al.*, 2008), and the USA (Katkansky and Warner, 1974)

Summer mortality typically occurs during the hottest period of the summer when water temperatures are above 20 °C (e.g. Imai *et al.*, 1965; Garnier *et al.*, 2007; Watermann *et al.*, 2008; Go *et al.*, 2017). Elevated temperatures induce gametogenesis and spawning in Pacific oysters, increasing their susceptibility to summer mortality (De Decker *et al.*, 2011; Wendling and Wegner, 2013). Gametogenesis is an energetically costly process (Malham *et al.*, 2009; Wendling *et al.*, 2014). During gametogenesis, oyster gonads can occupy over 50% of their body volume, a state that is often referred to as a high condition or fatness (Imai *et al.*, 1965; Quayle, 1988). As a result of the metabolic demand of gametogenesis, oysters may develop a disorder in glycogen metabolism (Patrick *et al.*, 2006). Oyster growing areas with higher food availability

have increased reproductive effort and more severe summer mortalities (Imai *et al.*, 1965; Perdue, 1983). Similarly, oysters fed more in a controlled environment have higher reproductive investment and higher cumulative mortalities than controls (Delaporte *et al.*, 2007). Ripe and spawning oysters also have a lower density of circulating hemocytes, and those hemocytes have reduced phagocytic activity and adhesive capabilities (Delaporte *et al.*, 2006; Li *et al.*, 2007; Wendling *et al.*, 2014). Additionally, oysters with increased reproductive effort are more susceptible to *Vibrio* infections (De Decker *et al.*, 2011; Wendling and Wegner, 2013).

Vibrio is a well-studied genus that includes a number of Pacific oyster pathogens. It is a genus of Gammaproteobacteria with over 100 species, including at least 12 human pathogens (most notably *V. cholerae*) and many finfish and invertebrate pathogens (Colwell and Grimes, 1984; Percival and Williams, 2014; Travers *et al.*, 2015; Baker-Austin *et al.*, 2018). They generally grow in warm brackish waters and can have notably short doubling times of 8–9 min under optimal conditions (Joseph *et al.*, 1982; Baker-Austin *et al.*, 2018). *Vibrio* genomes include two circular chromosomes that have been heavily shaped by recombination events, horizontal gene transfer, and bacteriophages (Baker-Austin *et al.*, 2018). Due to the sensitivity of their growth and virulence to ambient water temperatures, they are also considered an indicator species for climate change (Kimes *et al.*, 2012; Vezzulli *et al.*, 2016; Baker-Austin, 2017).

During the 1970s in Washington State, a *Vibrio* sp. was frequently isolated from Pacific oysters during summer mortality events and thought to be the etiological agent (Katkansky and Warner, 1974; Brown, 1977). Associated challenge studies demonstrated that an isolated species with similar biochemical markers to *V. parahaemolyticus* caused significant mortalities (Brown, 1977). *Vibro aestuarianus* and *V. splendidus* are also pathogens of Pacific oysters associated with summer mortality based on field observations (Garnier *et al.*, 2007), and laboratory

challenge studies (Lacoste *et al.*, 2001; Azéma *et al.*, 2016). Additionally, *Nocardia crassotrea* has been identified as the causative agent of some cases of Pacific oyster summer mortality in Washington State and British Columbia (Elston *et al.*, 1987; Friedman *et al.*, 1991, 1998; Friedman and Hendrick, 1991). Other factors, such as the toxin producing dinoflagellate *Alexandrium catenella* (Abi-Khalil, 2016), reduced dissolved oxygen levels (Cheney *et al.*, 2000), organic pollution (Imai *et al.*, 1965), and harmful algal blooms (HABs) (Cassis *et al.*, 2011) have all been considered as important or causative factors in observations of Pacific oyster mortalities. Factors and interactions that are most commonly implicated in Pacific oyster summer mortality events are summarized below (Fig. 1.1)

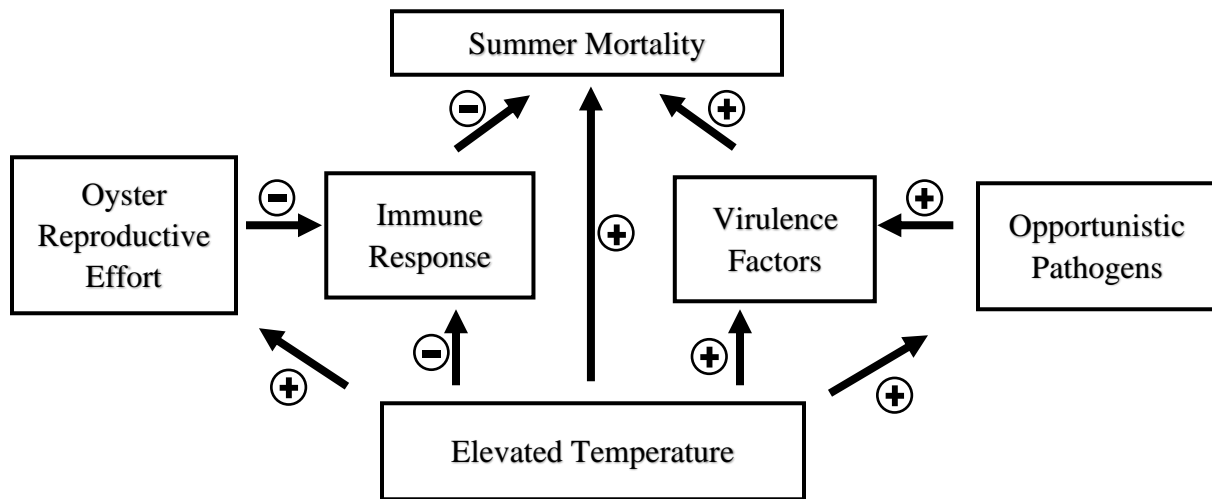


Figure 1.1: Interactions among the primary hypothesized factors that influence Pacific oyster summer mortality. Positive (+) and negative (-) interactions between factors are indicated.

1.5 Emerging Summer Mortality in British Columbia

In 1988, Daniel Quayle, the foremost expert in BC bivalve culture and Pacific oysters wrote: “In British Columbia there has been little evidence of [summer mortalities] in the Pacific oyster since it was first introduced. Very few mass mortalities have been reported, and these have all occurred in Boundary Bay during summers warmer than usual.” (Quayle, 1988). The mortalities he had noted were explored in depth in Washington State (Pauley *et al.*, 1988); contributing factors included elevated temperature, the onset of reproductive effort (Perdue, 1983), and potentially the presence of an unknown pathogenic *Vibrio* sp. (Brown, 1977). Recent Pacific oyster summer mortalities in BC have caused losses of approximately 80% in Redonda Bay (Meyer, 2013) and Sykes Island (Cassis *et al.*, 2011). Furthermore, there was a notable outbreak of foodborne gastroenteritis from *V. parahaemolyticus* in oysters during the summer of 2015, which suggests that other *Vibrio* spp. may have been accumulating during mortality events that summer (Anon, 2016c).

1.6 Objectives

The primary objective of this thesis is to monitor and describe summer mortality of Pacific oysters in Baynes Sound. A number of factors will be discussed in the context of the biological rationale for impacting oyster health. The following questions will be investigated:

- 1) How prevalent are Pacific oyster summer mortalities in Baynes Sound?
- 2) What potentially pathogenic *Vibrio* spp. are present during the observed mortalities and are they more abundant during periods of mortality?
- 3) Are there elevated concentrations of potentially harmful phytoplankton species associated with mortality events?

4) What environmental factors appear to contribute to the incidence of summer mortality in Baynes Sound?

Chapter 2 Assessing the roles of the *Vibrio* Community, Reproductive Effort, and Environmental Parameters in Intertidal Pacific Oyster Summer Mortality

2.1 Introduction

Summer mortality of Pacific oysters was first described in Japan in the 1940s and currently represents a major challenge for aquaculture around the world (Renault *et al.*, 2005). Summer mortality events have occurred in coastal regions of many countries, including Australia (Go *et al.*, 2017), France (Gouletquer *et al.*, 1998; Renault *et al.*, 2005), and the USA (Katkansky and Warner, 1974). Pacific oyster (*Crassostrea gigas*) summer mortality is generally considered a result of complex interactions amongst opportunistic pathogens, environmental conditions, and the extent of reproductive effort (e.g. Renault *et al.*, 2005; Garnier *et al.*, 2007; Watermann *et al.*, 2008; Cotter *et al.*, 2010; Wendling and Wegner, 2013; Go *et al.*, 2017). Due to the multifaceted nature of the disease, the aetiology of summer mortality is disputed, but it generally occurs in the hottest period of the summer when water temperatures are above 20°C. Elevated water temperature can reduce the immune response of oysters, induce gametogenesis and spawning, and increase the growth and virulence of pathogenic bacteria (Malham *et al.*, 2009; Wendling *et al.*, 2014; Baker-Austin *et al.*, 2018).

Vibrio spp. are opportunistic pathogens of many marine organisms, including Pacific oysters (Baker-Austin *et al.*, 2018). For example, *V. aestuarianus* and *V. splendidus* have frequently been isolated from Pacific oyster summer mortality events in France (Garnier *et al.*, 2007). Challenge experiments with both *V. splendidus* (Lacoste *et al.*, 2001) and *V. aestuarianus* (Azéma *et al.*, 2016) have demonstrated their pathogenicity to Pacific oysters. The diversity of *Vibrio* spp. within BC, however, is not well understood, despite their significance as pathogens in other regions. *Vibrio anguillarum* and *V. ordalii*, which cause mortality in salmon, are

endemic to the region (Morrison and Saksida, 2013). *Vibrio parahaemolyticus*, *V. fluvialis*, *V. vulnificus*, *V. damsela*, and *V. hollisae* were previously cultured from oysters in BC (Kelly and Stroh, 1989). Additionally, unknown *Vibrio* spp. were associated with up to 80% mortality of Pacific oysters in Redonda Bay, BC and challenge experiments suggested that they may contribute to summer mortality in BC (Meyer, 2013).

Harmful algal blooms (HABs) can produce toxic metabolites or have spiny projections that could contribute to the susceptibility of Pacific oysters to summer mortality. For instance, *Protoceratium reticulatum* blooms, producing yessotoxin, have been associated with mortalities of Pacific oysters in BC (Cassis, 2005). Saxitoxin produced by *Alexandrium* spp. and domoic acid produced by *Pseudo-nitzschia* can have adverse sub-lethal effects on the digestion and energy balance of bivalves (Pazos *et al.*, 2017; Mat *et al.*, 2018). Furthermore, saxitoxin-producing *Alexandrium cantenella* increases the susceptibility of Pacific oysters to pathogenic *Vibrio* spp. and, in turn, could increase the severity of mortality events (Abi-Khalil *et al.*, 2016).

Gametogenesis is a stressful period that can compromise the thermo-tolerance and anti-microbial activity of oyster hemocytes (Li *et al.*, 2007; Huvet *et al.*, 2010; Wendling and Wegner, 2013). The process is thermo-regulated and induced by increasing temperatures during the summer months (Quayle, 1988). During gametogenesis, nutrient reserves of glycogen-rich connective tissue are replaced by proliferating reproductive cells that are high in lipids and proteins. Gametogenesis can cause physiological disorders in which lipid synthesis stops and carbohydrate anabolism occurs (Patrick *et al.*, 2006; Huvet *et al.*, 2010). Ripe and spawning oysters also have a lower density of circulating hemocytes, and reduced phagocytic activity and adhesive capabilities, which increases host susceptibility to opportunistic pathogens (Delaporte *et al.*, 2006; Li *et al.*, 2007; Wendling *et al.*, 2014).

Research on summer mortality of Pacific oysters in the USA during the 1960's and 70's sought to find a causative pathological agent (Lipovsky and Chew, 1972; Katkansky and Warner, 1974). Some evidence emerged that a *Vibrio* sp. was the aetiological factor, however, periodic culturing of bacteria from moribund oysters provided inconsistent results, leading to an alternate hypothesis that physiological stress associated with gametogenesis causes summer mortality (Lipovsky and Chew, 1972; Katkansky and Warner, 1974; Brown, 1977; Perdue, 1983). It was demonstrated that high mortality growing areas had increased reproductive effort, when compared to low mortality areas (Perdue, 1983).

The present study collected baseline data on intertidal summer mortality of cultured Pacific oysters in Baynes Sound, BC to address four knowledge gaps for this region. (1) How abundant are mortalities? (2) What culturable *Vibrio* spp. are present in Pacific oysters? (3) Are mortalities correlated with reproductive effort and/or specific environmental conditions throughout the summer? (4) Is there a significant difference in mortality between the selected intertidal sites?

2.2 Materials and Methods

2.2.1 Study Sites and Experimental Design

Baynes Sound is a small passage located between Vancouver Island and Denman Island and is home to a large portion of the province's shellfish aquaculture (Fig. 2.1). For this study, three intertidal sites were selected in Baynes Sound at Buckley Bay (49.527° N, 124.850° W), Fanny Bay (49.507° N, 124.829° W), and Ship's Point (49.492° N, 124.692° W). Buckley Bay is an exposed gravel beach, located near a large passenger cable-ferry and beach-front properties.

Fanny Bay is a narrow, sheltered and silty beach near a commercial wharf. Ship's Point is a gravel beach in a protected bay with low aspect and abundant oyster production.

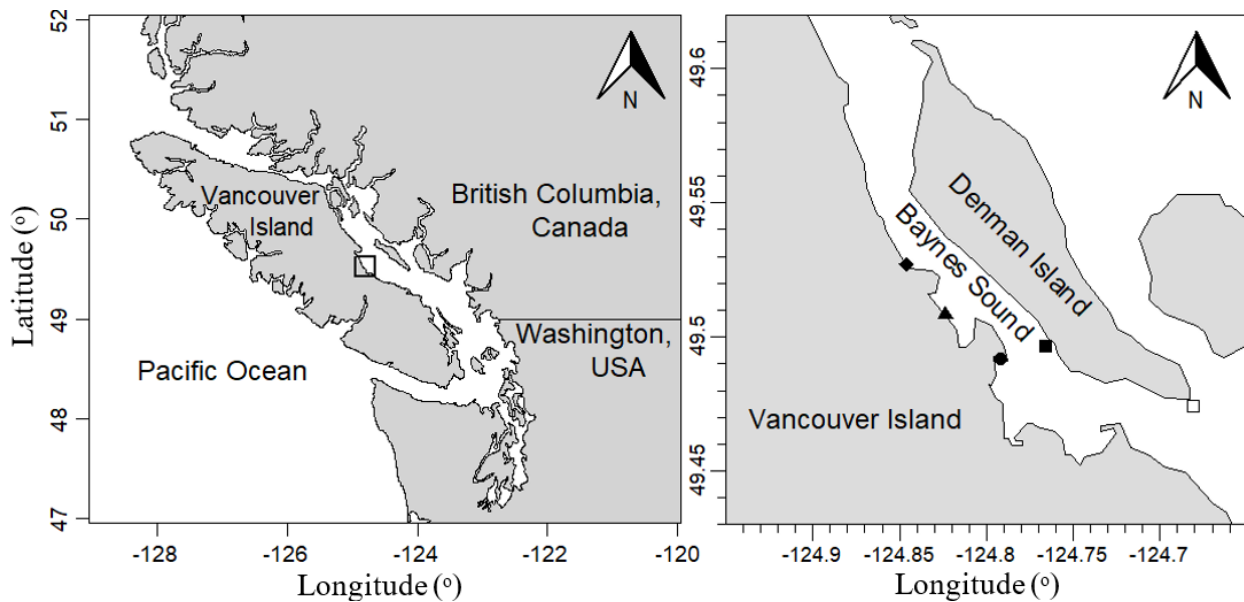


Figure 2.1: Left: Map of Pacific Northwest with the field site location shown as a square. Right: Baynes Sound with Buckley Bay (◆), Fanny Bay (▲), Ship's Point (●), Metcalf Bay (■), and Chrome Island (□).

All oysters used for the study had been reared in suspended culture at Metcalf Bay (49.250° N, 124.456° W) in Baynes Sound at a depth of 5 m using Dark Sea trays (LxWxH: 69x69x9 cm) (Dark Sea Enterprises Inc., Vancouver, BC, Canada). To populate the experiment, dead oysters were removed and live ones (shell height mean \pm SD: 96.0 \pm 13.2 mm, 15 months of age) were transferred to clean Dark Sea trays, free of biofouling, at a density of 80 oysters tray⁻¹ (190 oysters m⁻²). Each site had three replicate modules 3 m apart. Each module consisted of a metal rack containing seven stacked Dark Sea trays with 80 oysters in each ($N_{\text{Tray}}=80$, $N_{\text{Module}}=560$, $N_{\text{Site}}=1,680$). The bottom trays were at 1.70 m and the top trays at 2.65 m elevation above 0-m tidal height. Near weekly, from July 5, 2017 to September 15, 2017, dead oysters were counted in every tray, but left in their tray, to mimic industry practices. Each oyster was observed on sampling dates to track mortality. Oysters were considered dead if they had empty shells or no shell-closing response. Sampling occurred twice during the low tide cycle on the first and last day with a minimum tide height of 1.7 m.

2.2.2 Oyster Collection and Bacterial Isolation and Identification

Two live oysters were haphazardly chosen from each module at each sample interval for the isolation and culture of bacteria. Additionally, two oysters were haphazardly collected on June 25 and 30 from Metcalf Bay. Oysters were scrubbed of biofouling with a bristle brush and opened with a shucking knife and scalpel that were sterilized before use for approximately 2 min in 8% v/v bleach. The liquor from each individual oyster was drained and the soft tissue weighed and homogenized 3:1 v/w in phosphate-buffered saline with a sterile Waring blender on high for 30 s until homogenized. For each oyster processed, a 20- μ l volume of homogenate was plated onto either thiosulfate citrate bile salts sucrose agar, lysogeny broth agar, or marine agar, to increase the diversity of bacteria cultured, and incubated overnight at 30°C. Colonies were

selected to maximize the diversity of bacterial isolates, based on colony size, shape, and colour. Selected colonies were cultured for 12 h at 30°C in both 10 ml of alkaline peptone water (pH: 8.5) and lysogeny broth (pH: 8.5), after which 1 ml of turbid culture for each isolate was transferred to a 1.7-ml microcentrifuge tube. Tubes were centrifuged at 5,000 rcf for 5 min, the liquid phase decanted, and the pellet re-suspended in 1 ml of sterile, distilled water. Cell suspensions were transferred to a 95°C heat block for 20 min for cell lysis and then stored at -20°C for use in DNA amplification and sequence analysis.

Bacterial cultures were identified by sequence analysis of the *recA* gene, which encodes the DNA recombination/repair protein RecA. The primer set 222F (5' TGARAARCARTTYG GTAAAGG 3') and 1040R (5' TCRCNTTRTAGCTR TACC 3') was used to amplify this diagnostic gene sequence (Thompson *et al.*, 2005). All PCR reactions were prepared in a final volume of 40 µl containing 1x buffer, 0.2 mM dNTPs (Thermo Fisher Scientific, Waltham, MA, USA), 0.5 µM forward and reverse primers, 2 units of Dream Taq DNA polymerase (Invitrogen, Carlsbad, CA, USA), and 10 ng of extracted genomic DNA in sdH₂O. Amplification conditions were 5 min at 95°C, followed by 35 cycles at 95°C (35 s), 55°C (75 s), and 72°C (75 s), with a final elongation step at 72°C (7 min) using a StepOnePlus Real-time PCR System (Applied Biosystems, Foster City, CA, USA). For all PCR reactions, 5 µl of product was loaded on a 1.5% (w/v) agarose gel that included a 100-bp DNA ladder (New England Biolabs, Ipswich, MA, USA). After electrophoresis at 80 volts for 35 min, the gel was stained for 45 min in GelRed nucleic acid gel stain (150 µl GelRed, 50 ml 1-M NaCl, 450 ml dH₂O) (Biotium, Hayward, CA, USA) and visualized with UV light using the Bio-Rad GelDoc XR+ Gel Documentation System (Bio-Rad, Hercules, CA, USA). Following the confirmation of expected band size, the remaining 35 µl of product was purified with the ABM column-pure PCR clean-up kit (Applied Biological

Materials, Richmond, BC, Canada) and Sanger sequenced by Eurofins MWG Operon (Operon, Huntsville, AL, USA).

A consensus sequence for each isolate was created by comparing the forward and reverse sequence chromatograms, trimming nucleotides, and aligning sequences by default ClustalW on Mega 10 (Kumar *et al.*, 2015). Reference sequences of *recA* were acquired from the National Center for Biotechnology Information (NCBI). All sequences were aligned by ClustalW on MEGA10, and then aligned manually using BioEdit 7.2.5 (Hall, 2005), and used to generate a neighbor-joining tree using p-distances with 500 bootstrap replicates on MEGA10.

Identifications of isolates were based on the percent nucleotide identity within and between clustering groups on the neighbor-joining tree and a nucleotide basic local alignment search tool (BLAST) analysis (NCBI), with gap costs of existence=5, extension=2, match score=1, and mismatch score=-2. Isolates were identified to species level classification in conditions with only one voucher species with >97% nucleotide identity in NCBI BLAST results.

2.2.3 Sample Oyster Collection and Tissue Histology Preparation and Analysis

During sampling, one haphazardly chosen oyster was collected from the bottom, middle, and top trays of each module at each site for histological analysis ($N_{\text{Module/Site/Week}}=3$, $N_{\text{Site/Week}}=9$, $N_{\text{Week}}=27$). All sampled oysters were replaced from an extra replicate module at each site to maintain the density of 80 oysters tray⁻¹. Oysters were shucked and a cross section of tissue was taken at approximately one third the distance from the dorsal end, perpendicular to the dorsal-ventral margin. A thin section was transferred to a histology cassette and fixed in Davidson's solution (Howard *et al.*, 2004). Tissue was processed and embedded in paraffin by routine histological techniques using a Tissue Tek-TEC embedder (Sakuras, Torrance, CA, USA). Five-

µm thick sections of tissue, prepared via microtome, were de-paraffinized and rehydrated, stained with Harris' modified hematoxylin and eosin (H&E), dehydrated, and cover slips added and sealed with Permount (Thermo Fisher Scientific, Waltham, MA, USA).

H&E-stained histology slides were examined and imaged via light microscopy to record the sex, phase of gonad maturity (GM), maximal gonad length (GL), gonad area (GA), and total oyster tissue area (OA) for each tissue cross section. Traces of GA and OA were prepared using Quantum Geographic Information System (QGIS) (Anon, 2020a). For each tissue sample, the GA, OA, and GL were quantified with ImageJ (Schneider *et al.*, 2012) and the gonadosomatic index (GSI) was calculated as:

$$\text{Gonadosomatic index} = \frac{\text{gonad area (mm}^2\text{)}}{\text{oyster area (mm}^2\text{)}}$$

The gill and mantle were excluded from traces to reduce the variability between oysters resulting from histological preparation.

The phase of gonad maturity was categorized according to the scale of Steele and Mulcahy (1999) and included undifferentiated (0), early active (1), late active (2), ripe (3), partially spent (4), totally spent (5), post-spawning (6), and resorption (7) phases. Sex was categorized as female, male, hermaphrodite, or undifferentiated. The proportion of oysters that were female was calculated as a ratio of females to males excluding hermaphrodites and undifferentiated oysters due to their low occurrence. For quantitative analysis of gonad development, the proportion of ripe oysters (PR), including the late active and ripe stages, to the total number of oysters was used.

2.2.4 Environmental Factors

From July 1 to September 20, 2017, a YSI EXO2 sonde (YSI, Yellow Springs, OH, USA) was deployed at 5.0 m depth to record water temperature, salinity, dissolved oxygen, and chlorophyll *a* at 10 min intervals at Buckley Bay, Fanny Bay, and Metcalf Bay. The data from Metcalf Bay was used as a proxy for Ship's Point, which did not have a floating construct to attach the sonde to. HOBO temperature Tidbits (Onset, Bourne, MA, USA) recorded the temperature at the bottom of the middle module at each intertidal site at 10-min intervals.

Historic water temperatures data were acquired from Chrome Island (49.496°N, 124.765°W, Fig. 2.1) (Anon, 2019a). Local daily minimum tide height data were acquired from the Department of Fisheries and Oceans (DFO), Canada (Anon, 2017b).

Phytoplankton samples were collected at each sampling period 275–310 m offshore from each site at 1 and 5 m depths using a Van Dorn bottle. Samples were preserved with concentrated Lugol's iodine (Thermo Fisher Scientific). Prior to analysis, samples were suspended by gentle shaking. The absolute concentration (cells ml⁻¹) of each potentially harmful phytoplankton species was determined visually via a compound microscope using 1 ml per sample on a Sedgewick-Rafter slide. Phytoplankton species observed were identified to the lowest taxonomic level possible, based on morphology (Hasle, 1978). Quantified potentially harmful algal species included *Alexandrium* spp., *Ceratium fusus*, *Dicthyocha speculum*, *Dinophysis* spp., *Heterosigma akashiwo*, *Protoceratium reticulatum*, *Pseudo-nitzschia* spp., and *Rhizosolenia setigera* (Cassis *et al.*, 2011).

One discrete water sample for carbonate chemistry was collected in a 350-ml soda-lime glass bottle from surface water at each site during every sampling, with care taken to limit the introduction of air bubbles (Evans *et al.*, 2019). Bottles were preserved with 200 µl of a saturated

mercuric chloride solution and capped with polyurethane-lined metal caps. Samples were analyzed using a Burke-o-Lator (Hales *et al.*, 2004) and partial pressure of carbon dioxide (pCO₂), temperature-adjusted hydrogen ion concentration (pH_T), and aragonite saturation state (Ω_{arag}) were computed using the CO2SYS program on MATLAB (Van Heuven *et al.*, 2011; Evans *et al.*, 2019). The saturation state (Ω) of calcium carbonate was calculated as:

$$\Omega = \frac{[Ca^{2+}][CO_3^{2-}]}{K'_{sp}},$$

where K'_{sp} represents the thermodynamic solubility of a calcium carbonate (CaCO₃) mineral, either aragonite or calcite (Gazeau *et al.*, 2007).

2.2.5 Statistical Analyses and Visualization

Data analysis was completed using R (Anon, 2020b) and the packages referenced herein. The statistical significance in this study was defined with an alpha of 0.05. All data are presented as average ± standard error, unless otherwise indicated. Figures were made using the ggplot2 package (Wickham, 2016) and Microsoft Excel 2016 (Microsoft, Redmond, WA, USA). Maps of the field area were created using the maps (Becker *et al.*, 2018a), mapdata (Becker *et al.*, 2018b), PBSmapping (Schnute *et al.*, 2019), and prettymapR (Dunnington, 2017) packages in R statistical language. Data were manipulated in R using the data.table package (Dowle and Srinivasan, 2019).

To examine which variables correlated with mortality, a binomial generalized linear mixed-effects model (GLMM) was used with a complimentary log log link function using the lme4 package (Bates *et al.*, 2019). In this model, hazard is the conditional probability of each oyster dying between observations given that it was alive at the previous observation. The binomial GLMM used a cloglog link function expressed as:

$$\log\left(-\log\left(1 - \lambda(t_j|x_i)\right)\right) = \alpha_j + xb_1 + xb_n$$

with the explanatory variables b_1 to b_n , λ the discrete hazard for individual x_i at time t_j given that it survived until t_{j-1} , and α_j being the cloglog transformation of the baseline hazard.

For the binomial model, tray was nested within module as a random effect, with tray height and site as fixed factors. Due to the interval-censored observations of mortality in this study, all models include a date offset factor to account for variations in the number of days between observations. Explanatory variables were scaled and centered, with missing data using the average throughout the experiment. Variables that were measured continuously throughout the study, such as temperature and minimum tide height, were averaged over the interval between two observations of mortality. Discrete data, such as oyster gonad characteristics, which were collected on the same day as observed mortality were averaged with the previous weeks to better reflect the period in which mortalities occurred. Assumptions of the binomial GLMM are that it is a binomial response, that the number of oysters is fixed across the study, and that the observed events occur independently. For this model, p -values used Z -statistics from Wald chi-square tests computed for each parameter in the model. Conditional coefficients of determination are reported for each model generated using the MuMIn package (Bartoń, 2020).

The effect of module variation on average final cumulative mortality was investigated using multiple linear regression in comparison to average values for GA, GL, GSI, OA, PR, and the proportion female. The assumptions of normality and homoscedasticity for a linear model were met based on the Shapiro-Wilk test and Levene's test, respectively. Model selection used backwards parameter selection based on Akaike Information Criterion (AIC): $AIC = 2k - 2 \ln(L)$, where k is the number of parameters in the model and L is the maximum value for

likelihood function of the model. Models with the lowest AIC value represent the most parsimonious model.

2.3 Results

2.3.1 Environmental Factors

Average temperatures at the modules from July 5 to September 15, 2017 were 19.59 ± 0.02 , 19.42 ± 0.02 , and $19.33 \pm 0.04^\circ\text{C}$ for Buckley Bay, Fanny Bay, and Ship's Point, respectively, with a range of daily averages of $13.50\text{--}23.36 \pm 2.07^\circ\text{C}$ across all sites. Based on the Chrome Island data set the average daily water temperatures for July (17.5°C) and August (18.0°C) were on average the 45.2 and 50.8 percentile, respectively, in comparison to the last 30 years of the same dates. The average salinities throughout the study at Buckley Bay, Fanny Bay, and Metcalf Bay were 26.15 ± 0.01 , 26.80 ± 0.02 , and $27.06 \pm 0.02\text{‰}$, respectively, with a range of observations of $21.52\text{--}31.4\text{‰}$ across all times and sites. Daily average oxygen saturation at Buckley Bay and Fanny Bay was 118.51 ± 17.07 and $114.73 \pm 0.18\%$, respectively (no data were recorded at Metcalf Bay). The lowest observed daily average oxygen saturation occurred on August 15 with 69.50 and 88.57% at Buckley Bay and Fanny Bay, respectively. The averages for chlorophyll *a* throughout the study at Buckley Bay, Fanny Bay, and Ship's Point were 12.31 ± 0.14 , 14.49 ± 0.16 , and $11.06 \pm 0.06 \mu\text{g l}^{-1}$, respectively, with daily averages ranging from 0.91 to $35.51 \mu\text{g l}^{-1}$ across all sites and times. A total of 41 samples were collected to examine ocean acidification parameters. Across all times and sites, the average pH was 8.14 ± 0.04 (min: 7.95, max: 8.24), average Ω_{arag} was 2.32 ± 0.04 (min: 1.55, max: 2.71), and average pCO_2 was $268.62 \pm 7.07 \mu\text{ATM}$ (min: 208.97 μATM , max: 441.86 μATM). There were no HABs observed during this study. Observed potentially harmful phytoplankton species (Cassis *et al.*, 2011)

included *Rhizosolenia setigera* (average: 217.2 ± 27.4 cells ml^{-1} , max: 1,000 cells ml^{-1}), *Pseudo-nitzschia pungens*-type (54.1 ± 13.0 , 600 cells ml^{-1}), *Heterosigma akashiwo* (5.7 ± 2.3 , 150 cells ml^{-1}), and *Alexandrium* spp. (0.10 ± 0.04 , 2 cells ml^{-1}).

2.3.2 Histology

A total of 272 oysters were collected for histology throughout the study, of which 96 were male, 154 were female, 12 were hermaphrodites, and 10 were undifferentiated. The only observed pathology of regional concern was viral gametocytic hypertrophy (VGH) which was observed in four oysters (not shown) (Bower, 2017). Most oysters throughout the study had late active (36%) or ripe (50%) gonads, with the prevalence of oysters with partially spent, post-spawning, and resorption gonad phases increasing towards the end of the summer (Fig. 2.2).

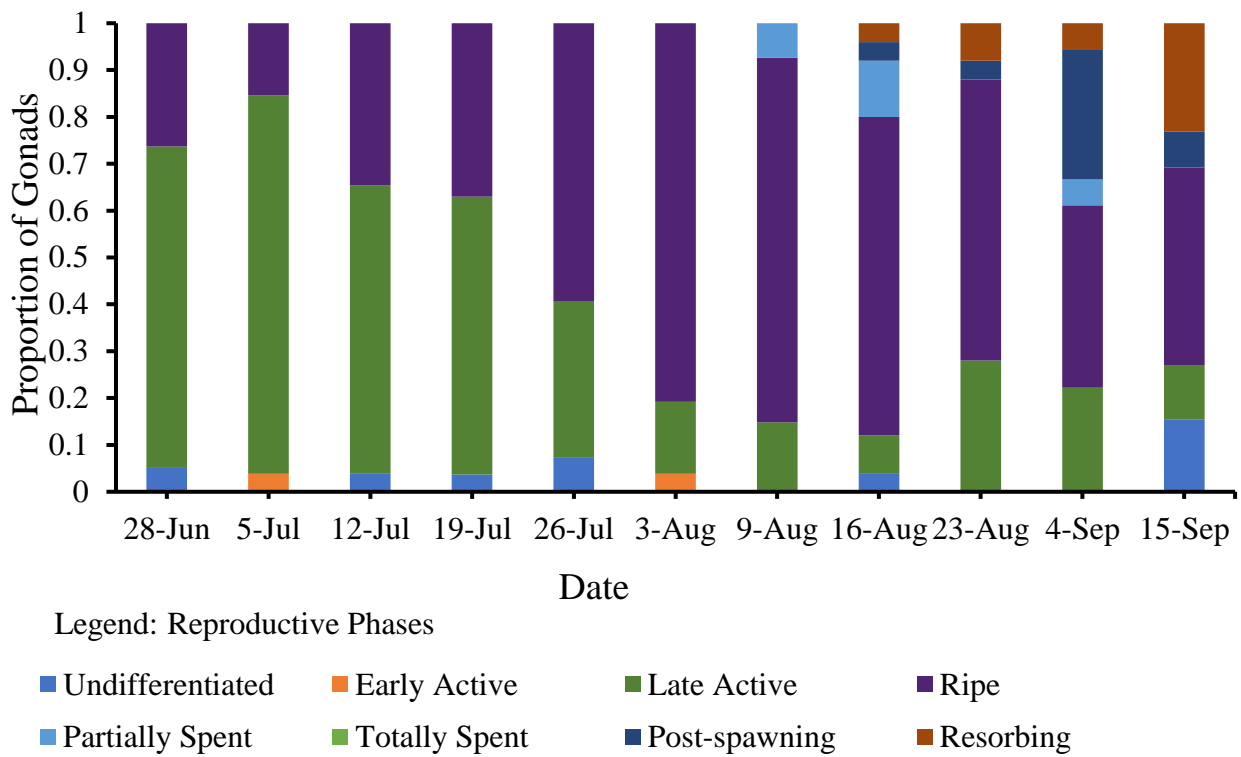


Figure 2.2.2: Proportion of Pacific oyster gonads in each reproductive developmental phase throughout the summer of 2017, as determined from hematoxylin and eosin stained histological cross sections. Classification of development phases was based on Steele and Mulcahy (1999).

The average values, across time and modules, for GL, OA, GA, and GSI were 18.4 ± 0.2 mm, 186.8 ± 4.4 mm², 103.9 ± 3.5 mm², and $0.52 \pm 0.17\%$, respectively. The observed gonad characteristics across all sampling points varied between modules. For example, observations of GL per module ranged from 16.4 ± 0.6 to 20.8 ± 0.8 mm. Similarly, the proportion of oysters that were female ranged from 0.4 ± 0.1 to 0.8 ± 0.10 per module. The effect of this variation in reproductive effort between modules on mortality was examined with a multiple linear regression model below.

2.3.3 Mortality Models

The average cumulative mortality among all sites measured on September 15, 2017 was $22.7 \pm 1.8\%$, with 16.5 ± 1.9 , 18.0 ± 2.5 , and $35.1 \pm 3.2\%$ at Buckley Bay, Fanny Bay, and Ship's Point sites, respectively (Fig. 2.3). In total, there were nine intervals of observation for mortality and environmental data for the GLMM. Data from seven of the 63 replicate trays was excluded from the study, based on the assumption of constant number of individuals. Factors included in the full model were temperature and its interaction with minimum tide height, proportion of oysters that are female, GL, GSI, site, and tray height. All models included date, tray nested within module as a random effect, and a date offset to account for interval censoring (Table 2.1). Tray height, proportion of oysters that were female, GL, and site were excluded based on AIC model selection. Model 4, the most parsimonious one, included the interaction of temperature and tide, as well as GSI and PR, and had a $R_m^2 = 0.046$ that excludes the random effects of tray height nested in module (Table 2.2). The conditional coefficient of determination for model 4 was $R_c^2 = 0.265$ (Table 2.2).

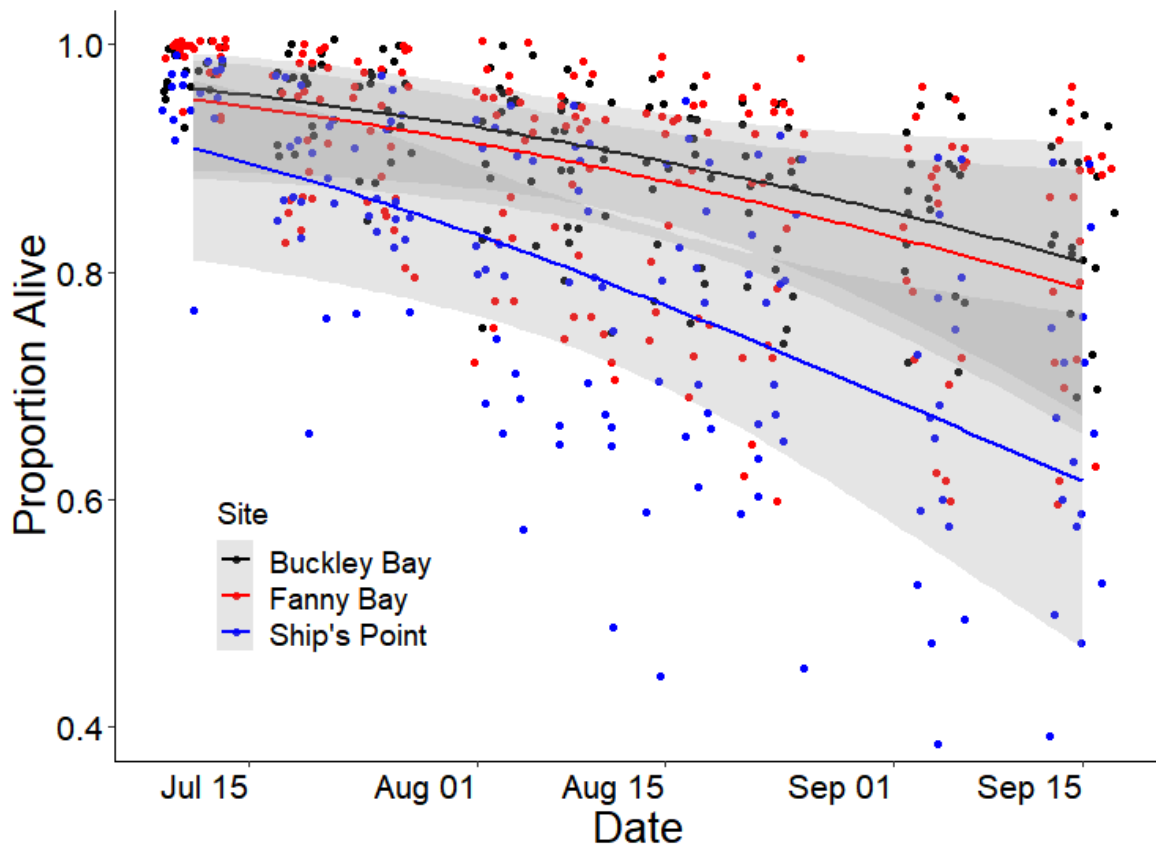


Figure 2.3: Survival curve for intertidal Pacific oysters from July 12 to September 15, 2017. Each point represents an observation of a tray of 80 oysters. Points are jittered around the sampling date to prevent overlap. Data are fitted with a binomial model using a cloglog link function, with standard error shown in grey.

Table 2.1: Model selection for a binomial generalized linear mixed-effects model using a cloglog link function to describe Pacific oyster survival over time. All models include date, a date offset, 494 residual degrees of freedom, and the random effects of trays nested in modules. Factors examined were site, temperature (Temp), tide exposure (Tide), tray height (Tray), proportion of oysters that were female (PF), gonad length (GL), gonadosomatic index (GSI), and proportion of oysters with ripe gonads (PR). Model 4, shown in bold, has the lowest ΔAIC value.

Model	df	ΔAIC	R_m^2	R_c^2	Explanatory Factors
Model 0	19	12.51	0.102	0.264	Tray + GL + Site + Temp x Tide + GSI + PR
Model 1	13	3.01	0.0997	0.264	PF + GL + Site + Temp x Tide + GSI + PR
Model 2	12	1.207	0.0993	0.264	GL + Site + Temp x Tide + GSI + PR
Model 3	11	0.503	0.101	0.258	Site + Temp x Tide + GSI + PR
Model 4	9	0	0.046	0.265	Temp x Tide + GSI + PR
Model 5	7	0.72	0.045	0.260	Tide + GSI + PR
Model 6	7	9.07	0.043	0.260	Temp + GSI + PR
Model 7	8	1.38	0.044	0.256	Temp x Tide + PR
Model 8	8	5.69	0.043	0.257	Temp x Tide + GSI

Table 2.2: Model 4 fixed effects from Table 2.1. Describing the most parsimonious binomial generalized linear mixed-effects model with a cloglog link describing intertidal Pacific oyster mortality during the summer of 2017. This model has 9 degrees of freedom, 497 residual degrees of freedom, and includes the nested random effects of trays within modules.

Fixed Effects	Estimate	SE	Z value	p-value
Date	-0.448	0.055	-8.184	<2.74E-16
Proportion Ripe	-0.166	0.059	-2.817	0.0048
Gonadosomatic Index	0.082	0.044	1.869	0.0615
Temperature	0.007	0.052	0.143	0.8866
Tide	0.136	0.040	3.351	0.0008
Temperature x Tide	-0.084	0.044	-1.906	0.0566
Intercept	-5.875	0.222	-26.453	<2.74E-16

Average percent cumulative mortality per module ranged from 9.3 ± 1.9 to $38.8 \pm 4.9\%$. There was variability in mortality and gonad characteristics between supposed replicate modules. Multiple linear regression models demonstrated that the average final cumulative percent mortality per module correlated significantly with average values for gonad characteristics (Table 2.3). The multiple linear regression Model 4, containing GL and PF, was selected based on AIC. The equation for Model 4, describing the average cumulative mortality per module is: $y = 0.059 \text{ mm} \times \text{GL} + 0.338 \times \text{PF} - 1.11$, and has an R^2_{adj} of 0.824, and a p -value of 0.002 (Fig. 2.4).

Table 2.3: Multiple linear regression AIC model selection. Models explained the variation in cumulative mortality per module based on gonad characteristics. Model 4 is the most parsimonious, with the lowest AIC value. GSI: gonadosomatic index, GL: gonad length, OA: oyster area, GA: gonad area, PF: proportion female.

Model	df	ΔAIC	R^2_{adj}	p -value	Explanatory Factors
Model 0	8	4.54	0.640	0.246	GA, OA, PR, GSI, PF, GL
Model 1	7	2.75	0.754	0.087	OA, PR, GSI, PF, GL
Model 2	6	2.45	0.777	0.034*	PR, GSI, PF, GL
Model 3	5	1.61	0.797	0.011*	GSI, PF, GL
Model 4	4	0	0.824	0.002*	PF, GL
Model 5	3	5.71	0.644	0.006*	GL
Model 6	3	9.18	0.476	0.024*	PF

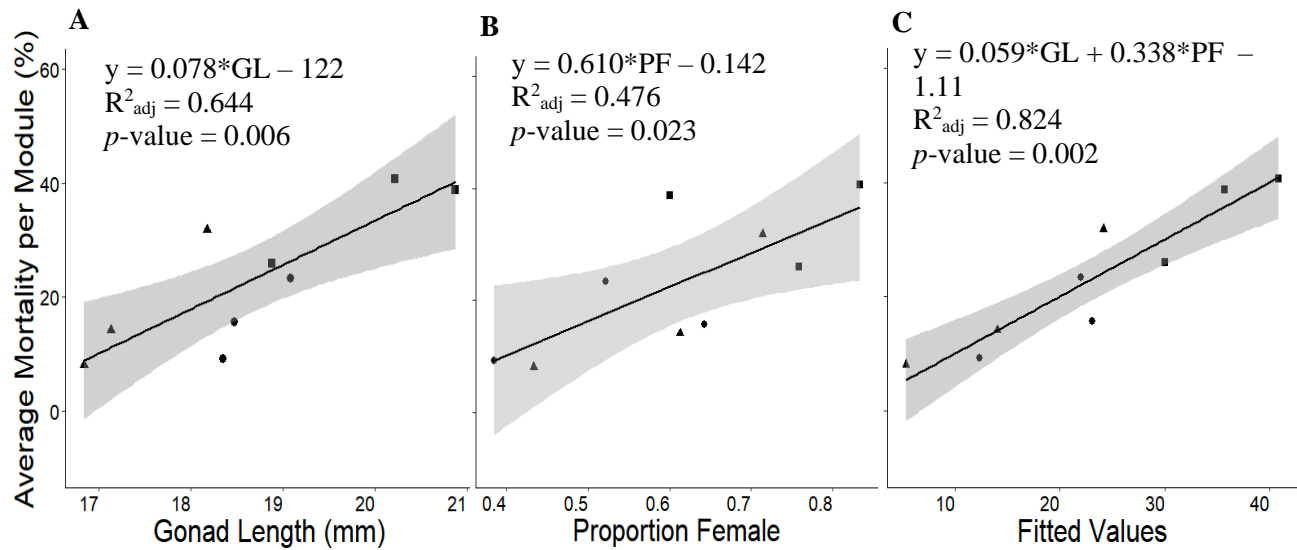


Figure 2.4: Linear regressions for the average cumulative mortality per module with the explanatory variables (A) gonad length (GL) and (B) proportion of individuals that are female (PF). (C) fitted values from the most parsimonious linear regression in Table 2.3 (Model 4). Average mortality per module was measured on September 15, 2017. Sites are indicated by different shapes; Buckley Bay (●), Fanny Bay (▲), and Ship's Point (■).

2.3.4 Bacterial Species Isolated from Oysters

A total of 158 bacterial isolates were obtained from the homogenate of sampled oysters collected from June 25 to September 15, 2017 and were putatively identified by sequencing a portion of the *recA* gene (Table 2.4; Fig. 2.5). Species level identification was assigned to 129 isolates based on the amplified region and these sequences had an average nucleotide identity of 98.9% to reference sequences available in the NCBI database. A total of 147 isolates were considered members of the genus *Vibrio*, based on >97% nucleotide identity with only *Vibrio* spp. in BLAST. *Vibrio parahaemolyticus* was the most prevalent species with 39 isolates and $97.2 \pm 0.3\%$ within-group mean nucleotide identity. Other commonly isolated species included: *V. aestuarianus* (N=27 isolates, within-group mean nucleotide diversity of $99.1 \pm 0.1\%$), *V. diabolicus* (N=21, $97.6 \pm 0.3\%$), *V. alginolyticus* (N=15, $96.7 \pm 0.3\%$), *Serratia marcescens* (N=7, $98.2 \pm 0.3\%$), and *V. pelagius* (N=6, $98.0 \pm 0.3\%$). The *recA* gene of isolates which clustered in the Harveyi (N=15), Anguillarum (N=3), and Splendidus (N=2) clades did not closely match any single species on NCBI. For example, two isolates had 97.1, 96.9, and 96.6% nucleotide identity with *V. celticus*, *V. crassostrea*, and *V. splendidus*, and were therefore designated as unknown *Vibrio* spp. in the Splendidus clade.

Table 2.4: Summary of recA nucleotide sequence BLAST queries from NCBI database in November, 2018 for 158 cultured bacterial isolates from intertidal Pacific oyster homogenate during the summer of 2017.

N	Putative species identification with >97% recA NCBI BLAST nucleotide identity	Number of isolates	Nearest NCBI BLAST results	Percent nucleotide identity	Query Coverage
1	<i>Vibrio parahaemolyticus</i>	39	<i>Vibrio parahaemolyticus</i> – gi 1220464799 MF066645.1	100%	100%
2	<i>Vibrio aestuarianus</i>	27	<i>Vibrio aestuarianus</i> – gi 157100334 AM884018.1	99%	99%
3	<i>Vibrio diabolicus</i>	21	<i>Vibrio diabolicus</i> – gi 1345471481 CP014036.1	98%	100%
4	<i>Vibrio alginolyticus</i>	15	<i>Vibrio alginolyticus</i> – gi 1345482739 CP014045.1	99%	99%
5	N/A – Harveyi clade (genus <i>Vibrio</i>)	11	<i>Vibrio jasicida</i> – gi 1329988821 CP025792.1 <i>Vibrio hyugaensis</i> – gi 1329988819 CP025794.1	99% 98%	100% 100%
6	<i>Serratia marcescens</i>	7	<i>Serratia marcescens</i> – gi 1511327077 CP033504.1	99%	99%
7	<i>Vibrio pacinii</i>	4	<i>Vibrio pacinii</i> – gi 58415603 AJ842487.1	99%	99%
8	<i>Vibrio pelagius</i>	6	<i>Vibrio pelagius</i> – gi 54792173 AJ580872.1	99%	96%
9	<i>Vibrio harveyi</i>	3	<i>Vibrio harveyi</i> – gi 215271619 FM204795.1	99%	100%
10	<i>Vibrio cyclitrophicus</i>	2	<i>Vibrio cyclitrophicus</i> – gi 809278768 LN832792.1	100%	100%
11	<i>Vibrio chagasii</i>	2	<i>Vibrio chagasii</i> – gi 58415400 AJ842385.1	99%	99%
12	N/A – Splendidus clade (genus <i>Vibrio</i>)	2	<i>Vibrio crassostreae</i> – gi 809278756 LN832786.1 <i>Vibrio celticus</i> – gi 809278712 LN832764.1	97% 97%	100% 100%
13	<i>Vibrio bivalvicida</i>	1	<i>Vibrio bivalvicida</i> – gi 452084891 HF568940.1	99%	100%
14	<i>Vibrio rotiferianus</i>	1	<i>Vibrio rotiferianus</i> – gi 1214539220 CP018312.1	99%	99%

N	Putative species identification with >97% recA NCBI BLAST nucleotide identity	Number of isolates	Nearest NCBI BLAST results	Percent nucleotide identity	Query Coverage
15	<i>Vibrio portersiae</i>	1	<i>Vibrio porteresiae</i> – gi 146742339 EF547199.1 <i>Vibrio tritonius</i> – gi 156106874 EU072029.1	97% 91%	88% 98%
16	N/A (genus <i>Vibrio</i>)	1	<i>Vibrio parahaemolyticus</i> – gi 193221978 EU770348.1	85%	81%
17	N/A (genus <i>Vibrio</i>)	1	<i>Vibrio jasicida</i> – gi 1329988821 CP025792.1	93%	97%
18	N/A (genus <i>Vibrio</i>)	1	<i>Vibrio jasicida</i> – gi 1329988821 CP025792.1	93%	88%
19	N/A (genus <i>Vibrio</i>)	1	<i>Vibrio jasicida</i> – gi 1329988821 CP025792.1	96%	91%
20	N/A (genus <i>Vibrio</i>)	1	<i>Vibrio jasicida</i> – gi 1329988821 CP025792.1 <i>Vibrio hyugaensis</i> – gi 1329988819 CP025794.1	92% 92%	86% 86%
21	N/A (genus <i>Vibrio</i>)	1	<i>Vibrio celticus</i> – gi 1042053030 CP016228.1	86%	100%
22	<i>Vibrio fortis</i>	1	<i>Vibrio fortis</i> – gi 58415474 AJ842422.1	99%	100%
23	N/A (genus <i>Photobacterium</i>)	1	<i>Photobacterium</i> sp. – gi 213012321 EU716943.1 <i>Photobacterium sanquinancrui</i> – gi 1005672319 KU681321.1	99% 89%	75% 97%
24	N/A (genus <i>Vibrio</i>)	1	<i>Vibrio parahaemolyticus</i> – gi 1379020998 CP022552.2	92%	99%
25	N/A (genus <i>Vibrio</i>)	1	<i>Vibrio parahaemolyticus</i> – gi 1388769464 CP028342.1	89%	98%
26	<i>Shewanella algae</i>	1	<i>Shewanella algae</i> – gi 1464292657 CP018456.1	99%	100%
27	N/A (genus <i>Shewanella</i>)	1	<i>Shewanella algae</i> – gi 1511681841 CP033575.1	96%	100%
28	N/A	1	<i>Shewanella japonica</i> – gi 1171874157 CP020472.1 <i>Providencia rustigianii</i> – gi 1540094082 LR134396.1 <i>Shewanella halifaxensis</i> – gi 167351963 CP000931.1	80% 81% 80%	97% 88% 91%

N	Putative species identification with >97% recA NCBI BLAST nucleotide identity	Number of isolates	Nearest NCBI BLAST results	Percent nucleotide identity	Query Coverage
29	N/A	1	<i>Shewanella sp.</i> – gi 113886955 CP000444.1	83%	94%
30	N/A (genus <i>Vibrio</i>)	1	<i>Vibrio anguillarum</i> – gi 1220461175 CP022468.1	99%	97%
			<i>Vibrio ordalii</i> – gi 58415591 AJ842481	98%	96%

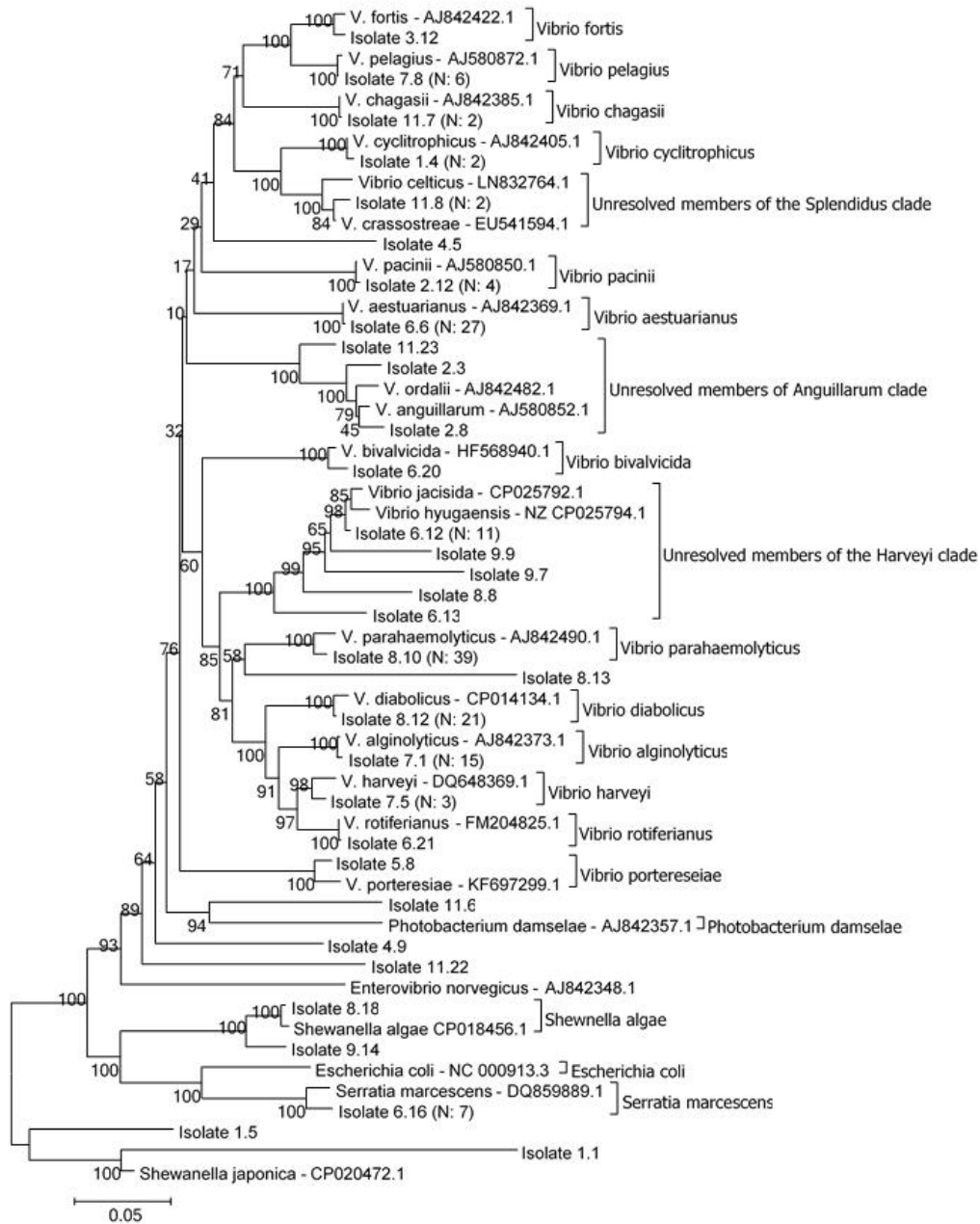


Figure 2.5: Neighbor-joining tree showing clusters of identified bacterial isolates from Pacific oysters in Baynes Sound, based on the nucleotide sequence of the *recA* gene (~800 bp). The number of isolates that cluster together with >96.3% within-group mean nucleotide identity (N) is indicated (Table 2.4). Numbers on nodes represent support generated from 500 bootstrap replicates. Scale bar represents p-distance.

2.4 Discussion

2.4.1 Reproductive Effort and Summer Mortality

A number of factors are associated with Pacific oyster summer mortality, most notably; temperature, microbial pathogens, and reproductive effort (Malham *et al.*, 2009; Wendling *et al.*, 2014; Green *et al.*, 2019). In this chapter, intertidal cumulative mortalities of adult Pacific oysters correlated with observations of oyster reproductive effort. This finding is consistent with those in other studies on oysters. For instance, Perdue (1983) observed a similar correlation; growing areas with abundant summer mortalities also had elevated reproductive effort. In addition, Cotter *et al.* (2010) concluded that elevated growth rates, gonadal development, and spawning may increase oyster susceptibility to summer mortality. Similarly, families of Pacific oysters susceptible to summer mortality were found to have higher reproductive effort and early partial spawning, relative to resistant families (Samain *et al.*, 2007). Furthermore, controlled challenge experiments with variable nutrient conditions demonstrated the influence of reproductive effort on summer mortalities (Delaporte *et al.*, 2007). Oysters on a higher feeding regime (12% compared to 4% of oyster soft-tissue dry weight in algal dry weight per day) showing increased mortality, with a positive correlation between increased reproductive investment and mortality (Delaporte *et al.*, 2007). Field observations suggest that temperature regulates the timing of gametogenesis and that nutrient availability regulates the intensity of gonad development (Enríquez-Díaz *et al.*, 2009).

Pacific oysters have a complex and dynamic sex-determination mechanism. They are protandric hermaphrodites all juveniles are male until their first spawning season and then, subsequently, a portion of the population will become female (Pauley *et al.*, 1988). Guo *et al.* (1998) observed females making up 37, 55, and 77% of Pacific oysters in one-, two- and three-

year-old oysters, respectively, whereas the proportion of 15-month-old of observed oysters that were female ranged from 0.40 ± 0.10 to 0.81 ± 0.07 per module and correlated with mortality ($R^2=0.476$, $p=0.023$). Transition between sexes may occur during the early spring as a result of nutrient-dense phytoplankton blooms (Lango-Reynoso *et al.*, 2006). Perdue *et al.* (1981) also observed higher mortalities in female than male oysters. There is evidence, from the American oyster (*Crassostrea virginica*), that females require more nutrients than males, due to their increased metabolic activity (Choi *et al.*, 1993), and they may have significantly faster growth rates than males (Baghurst and Mitchell, 2002).

Sex determination in Pacific oysters is an interaction between environmental conditions and genetics (Guo *et al.*, 1998; Zhang *et al.*, 2014). In the present study, all oysters came from the same hatchery brood stock, therefore, the variation in observed gonad characteristics within each module are likely due to an unidentified environmental variable or handling bias in suspended culture before the experiment began. Further research should examine the role of Pacific oysters' sex in summer mortality, as it may be a useful parameter for selective breeding. The Molluscan Broodstock Program at Oregon State University has selected oysters since 1996 for increased yield (Anon, 2019b) and may have inadvertently selected for higher proportions of females, due to their faster growth rates (Baghurst and Mitchell, 2002; de Melo *et al.*, 2016). The analysis of reproductive effort and bacterial cultures in this chapter only examined live and healthy individuals and, therefore, survivorship bias may have influenced observations of gonad tissue.

2.4.2 Pathogens and Bacterial Identification

The only observed pathology present in the histological data was VGH and it was present in four of 272 oyster cross sections examined in this study. Cheslett *et al.* (2009) used transmission electron microscopy to examine VGH in Pacific oysters during mortality. They observed that the virus particles were 50 nm and appeared similar to viruses in the *Polyomaviridae* family. The low observed frequency of VGH, and the lack of host response suggests that VGH is unlikely to have a significant role in mortalities of Pacific oysters (Garcia *et al.*, 2006; Cheslett *et al.*, 2009).

Bacterial isolates collected were putatively assigned to either species or genus, based on nucleotide sequence variation in the *recA* gene. This gene provides higher resolution in phylogenetic analysis than the 16s rRNA region and is supported by extensive public sequence database resources (Thompson *et al.*, 2005).

Vibrio aestuarianus, *V. harveyi*, and members of the Splendidus clades are recognized opportunistic pathogens of Pacific oysters. *Vibrio aestuarianus* was first isolated from estuarine waters, oysters, and crabs in Oregon (Tison and Seidler, 1983) and has frequently been detected during summer oyster mortalities in France (Garnier *et al.*, 2007). Laboratory challenge experiments have confirmed its pathogenicity (Azéma *et al.*, 2016). *Vibrio harveyi* has also been described as a causative agent of mortality in Pacific oysters and a number of other marine species (Austin *et al.*, 2003). It has also been considered a putative pathogen for Pacific oysters in a laboratory simulated heatwave (Green *et al.*, 2019). Raising the water temperature from 20 to 25°C resulted in 77.4% mortality after 6 days, whereas oysters treated with penicillin and streptomycin only had 4.3% mortality. Research in BC has demonstrated that an unknown *Vibrio* spp. from Redonda Bay oyster mortalities caused death in Pacific oyster laboratory bath

exposures (Meyer, 2013). These results, combined with those from the current study, suggest that they are strong candidate bacterial pathogens of Pacific oysters and require further analysis.

A number of observed isolates in the Splendidus clade did not closely match any single species on NCBI. This suggests that these may be novel strains or species within this clade. *Vibrio splendidus* is a causative agent of juvenile Pacific oyster mortalities in France and has demonstrated pathogenicity for early life stages of mussels (*Mytilus edulis* and *Perna canaliculus*), clams (*Ruditapes decussatus*), and scallops (*Pecten maximus*) (Lacoste *et al.*, 2001; Dubert *et al.*, 2017). Two other common bacterial species identified in this study also have human pathogenic variants, namely *V. parahaemolyticus* and *Serratia marcescens*. The clustering of the *V. parahaemolyticus* isolates into three distinct groups may reflect differences in their pathogenicity. Further resolution of *V. parahaemolyticus* strain diversity is critical to assessing risk, since two strains (O3:K6 and ST36) are pandemic and highly virulent human pathogens (Baker-Austin *et al.*, 2018). *Serratia marcescens*, a common nosocomial infection, is present in the coastal environment and often occurs in untreated human waste water (Burge *et al.*, 2016). This bacterium also causes white-pox disease in corals. To my knowledge, this pathogen has not been previously detected in BC oceans and its virulence, hosts, and abundance are unknown; however, it may be associated with failing septic systems and hazardous waste disposal in the area.

2.4.3 Environmental Monitoring

The most parsimonious model from the GLMM described little of the variation in observed mortality over time with a marginal coefficient of determination (R^2_M) of 0.046. This may be due to the short period of observation that only included a period of mortality. Several

factors were excluded from the GLMM because the range of observations was within the optimal range for oyster health and there was no biological rationale for their inclusion. Regionally, ocean acidification (Moore-Maley *et al.*, 2017) and harmful phytoplankton abundance (Cassis, 2005; Cassis *et al.*, 2011) have been hypothesized as potential contributing factors to oyster mortalities in Baynes Sound. The following section discusses the rationale for excluding these factors from the GLMM based on the lack of scientific evidence within published data for their adverse effects on oyster health within the present study's observed ranges.

Aragonite and calcite are two allomorph mineral forms of calcium carbonate that are used to form shell in marine systems (Stenzel, 1963). The shells of oysters (Family Ostreidae) are formed mainly by conchiolin and calcite, whereas most bivalve molluscs use conchiolin and aragonite (Stenzel, 1963). Calcite is less soluble than aragonite with experimental tests suggesting Ω_{calcite} is approximately 1.8 times larger than Ω_{arag} (Gazeau *et al.*, 2007). This is why the net calcification of Pacific oysters is higher than mussels (*Mytilus edulis*) in modelled impacts of ocean acidification. Values of Ω less than one, for both aragonite and calcite, represent conditions that are corrosive to their respective forms of calcium carbonate; in other words, the rate of dissolution is greater than the rate of calcium carbonate precipitation (Waldbusser *et al.*, 2016). Controlled laboratory experiments are increasingly able to decouple pH, pCO₂, and Ω_{arag} and demonstrate the importance of aragonite saturation for early larval shell formation in Pacific oysters (Waldbusser *et al.*, 2014). Due to their dependency on aragonite, post-fertilization larvae experience acute effects on development at Ω_{arag} values of ~1.2–1.5 and below (Waldbusser *et al.*, 2014). Low aragonite saturations can negatively affect larval bivalve survival and growth because, at this life stage, aragonite is used for shell production (Barton *et*

al., 2012; Waldbusser *et al.*, 2014; Boulais *et al.*, 2017), whereas adults predominantly use the calcite form of calcium carbonate (Stenzel, 1963).

For the present study, the average values for pH, pCO₂, and Ω_{arag} were 8.14 ± 0.04 , $268.60 \pm 7.07 \mu\text{ATM}$, 2.32 ± 0.04 , respectively. Based on the variance of the observed values in this study, the life stages affected, and the extensive literature on summer mortality from other regions, there is limited scientific rationale for the direct association of ocean acidity changes with summer mortality in Baynes Sound. However, an interesting question may be raised regarding the role of oyster liquor pH in oyster health, particularly during low tide when anaerobic respiration may affect the immune response of intertidal oysters to infections. Allen and Burnett (2008) demonstrated that 4 h at an ambient air temperature of 30°C resulted in a hemolymph pH of 6.84 compared to a pH of 7.52 at 18°C. This suggests that the daily minimum in oyster liquor pH is likely lower than that in the observed sea surface water samples.

As intertidal organisms, Pacific oysters are well known for their ability to optimize their metabolism in response to hypoxia (Sussarellu *et al.*, 2013; Zhang *et al.*, 2016). Oxygen consumption rates for Pacific oysters increase additively with temperature and tissue dry weight (Bourgrier *et al.*, 1995). Bourgrier *et al.* (1995) examined oxygen consumption of 5 to 200 g wet weight Pacific oysters and found that at 5°C they consumed $0.2 \text{ mgO}_2 \text{ h}^{-1}$, whereas at 32°C the oxygen consumption was $1.9 \text{ mgO}_2 \text{ h}^{-1}$. Gouletquer *et al.* (1998) also observed a similar range of oxygen consumption with 0.96 and $0.81 \text{ mgO}_2 \text{ h}^{-1}$ in stressed and control oysters respectively. Le Moullac *et al.* (2007) identified a critical threshold of oxygen concentration that induces anaerobic respiration in Pacific oysters 3.02 to 3.43 mg l^{-1} at 15 to 25°C. Low levels of oxygen, less than 4 mg l^{-1} , have coincided with summer mortality in Puget Sound (Cheney *et al.*, 2000). In contrast, others did not observe the occurrence of mortality with persistent reduced oxygen

saturation of 3.8 mg l⁻¹ (Chávez-Villalba *et al.*, 2010). The observed values of dissolved oxygen at 5 m depth from this study suggest dissolved oxygen did not contribute to summer mortality of intertidal Pacific oysters in 2017.

The concentrations of potentially harmful phytoplankton species observed were magnitudes lower than other investigations that showed negative effects of microalgae on oyster health (Cassis, 2005; Abi-Khalil, 2016). Laboratory exposure of *H. akashiwo* (11,000 cells ml⁻¹) can have negative sublethal effects on the hepatopancreas of *Crassostrea virginica* (Keppler *et al.*, 2005). I observed a maximum *H. akashiwo* concentration of only 150 cells ml⁻¹ (average: 5.7±2.3 cells ml⁻¹). Similarly, exposure to the paralytic shellfish toxin-producing algal species *Alexandrium catenella* at concentrations of 2,000 cells ml⁻¹ for 24 h increased *V. tasmaniensis* associated mortality of Pacific oysters (Abi-Khalil, 2016). I observed a maximum of only 2 cells ml⁻¹ of *Alexandrium* sp. Additionally, this study did not examine whether any of the observed phytoplankton species were toxin producing variants.

Rhizosolenia setigera was the most abundant potentially harmful phytoplankton species, as defined by Cassis *et al.* (2011), in the present study, with a maximum concentration of 1,000 cells ml⁻¹ being observed (average: 217.0 ± 27.4 cells ml⁻¹). This species is a long, needle-like centric diatom of 100–500 µm (Horner, 2002) that may cause physical damage to oysters (Cassis, 2005). After consumption of *R. setigera* in a challenge study, the pallial cavity of oyster seed (shell height: 1–10 mm) rapidly rejects the particles as aggregated pseudo-faeces (Cassis, 2005). Therefore, a prolonged bloom of this species may limit feeding and reduce oyster seed growth. The oysters in this study averaged 97 mm in height, suggesting they have fully functional gill particle processing and selection, which develops in oysters between 10 and 24 mm (Cannuel and Beninger, 2006). In contrast, evidence from grazing experiments with adult

oysters (shell length: 5 cm) suggests that *R. setigera* is highly retained and an important food source for Pacific oysters (Dupuy *et al.*, 2000). In cases where HABs are reported to have adversely affected Pacific oyster health, they have generally been present for weeks or months and affected earlier life-stages (Cassis, 2005; Cassis *et al.*, 2011). It was demonstrated by Cassis (2005) that, preceding a mortality event in oyster seed (shell height: 1–10 mm), they were exposed for two weeks to approximately 7.5×10^5 cells ml⁻¹ of *Protoceratium reticulatum*. Analyses of adult Pacific oyster summer mortalities in other regions have demonstrated that it is unlikely for phytoplankton to be a contributing factor (e.g. Katkansky and Warner, 1974; Anon, 2015; Go *et al.*, 2017). The observed concentrations, and the conclusions from other studies of shellfish summer mortality, suggest that potentially harmful algal species are typically not a contributing factor for adult Pacific oyster summer mortality in Baynes Sound.

2.4.4 Conclusions

This study examined a wide range of factors that could have potentially contributed to intertidal adult Pacific oyster summer mortalities in Baynes Sound, BC, Canada. I observed continuous mortality from July 5 to September 15, 2017, with a mean cumulative mortality of 22.7% across the three experimental sites. The average cumulative mortality per module had a high correlation with observations of oyster reproductive effort per module. This is the first study to provide a qualitative description of *Vibrio* spp. associated with Pacific oysters in BC during a period of summer mortality. A number of potential disease-causing agents were putatively identified, including *V. aestuarianus*. Future research on summer mortality in Baynes Sound should quantitatively examine changes in the oyster microbiome associated with the onset of summer mortality.

Chapter 3 *Vibrio aestuarianus*, temperature, and stocking density are associated with summer mortality of juvenile Pacific oysters (*Crassostrea gigas*) in suspended culture

3.1 Introduction

Pacific oysters (*Crassostrea gigas*) are one of the most extensively cultured bivalve species in the world (Anon, 2018). In BC they have been an important farmed species for over a century and have a significant socioeconomic impact on coastal communities (Quayle, 1988; Anon, 2013). Pacific oyster aquaculture in Baynes Sound, BC generally uses hatchery-produced seed grown in suspended culture for their first year, followed by shell conditioning in the intertidal before being brought to the half-shell market. Baynes Sound is a small passage between Vancouver Island and Denman Island that is extensively farmed, with 137 shellfish tenures that includes 90% of the intertidal area (Bendell, 2019). In recent years, the BC oyster aquaculture industry has been faced with recurring summer mortalities of unknown aetiology. Temperature, reproductive development, and opportunistic pathogens are well-studied factors that are implicated in Pacific oyster summer mortality in other regions of the world (Katkansky and Warner, 1974; Garnier *et al.*, 2007; Wendling and Wegner, 2013; Azéma *et al.*, 2016; Green *et al.*, 2019).

Altering the culture density of oysters may be a potential method to mitigate summer mortalities. High culture density reduces the growth rate of oysters by limiting food availability and space (Chávez-Villalba *et al.*, 2010). A reduction in food availability also reduces the reproductive effort of oysters, and decreases summer mortalities in controlled experiments (Delaporte *et al.*, 2007; Enríquez-Díaz *et al.*, 2009). Conversely, higher densities could contribute to higher mortalities due to increased transmission of pathogenic agents between hosts (Baker-Austin *et al.*, 2018).

Bacterial pathogens have been considered an important factor in some Pacific oyster summer mortality events. The most well-documented of the bacterial pathogens associated with oyster mortality include *V. aestuarianus* and *V. splendidus*, both described in mass mortalities in France (Lacoste *et al.*, 2001; Garnier *et al.*, 2007; Solomieu *et al.*, 2015; Azéma *et al.*, 2016), and *N. crassostrea*, described in the USA (Elston *et al.*, 1987; Friedman *et al.*, 1991, 1998; Friedman and Hendrick, 1991). The genus *Vibrio* contains a number of opportunistic pathogens of humans and many marine species (Baker-Austin *et al.*, 2018). *Vibrio aestuarianus* can cause significant mortalities in Pacific oysters, and older oysters are more susceptible (Azéma *et al.*, 2016). Recently, *V. aestuarianus* cultures were obtained from Pacific oysters in Baynes Sound, BC and identified based on the sequence of the *recA* gene (see Chapter 2). Due to the inherent bias in culture-based isolation techniques, however, little is known about the composition of the broader bacterial community in Pacific oysters from Baynes Sound. In other regions of the world, changes in the oyster microbial community during summer mortalities, particularly the abundance of *Vibrio* spp., have provided evidence for the association of *Vibrios* with summer mortality events (Green *et al.*, 2019; King *et al.*, 2019a, 2019b).

Microbiomes promote homeostasis and can protect their host from pathogens and disease (Kamada *et al.*, 2013). Pacific oyster microbiomes typically decrease in diversity when disease symptoms are observed (Lokmer and Wegner, 2015; Green *et al.*, 2019; King *et al.*, 2019a). The use of high-throughput sequencing targeting the 16S rRNA gene provides an effective way to assess changes in the microbial community associated with Pacific oyster summer mortality (Wendling *et al.*, 2014; Green *et al.*, 2019; King *et al.*, 2019a). For example, King *et al.* (2019a) demonstrated an increase in rare operational taxonomic units (OTUs) in oyster microbiomes associated with a diseased state relative to healthy oysters. These OTUs aligned with *Vibrio*

harveyi and another unidentified *Vibrio* sp., implicating this genus in the 2013–2014 oyster summer mortality in Australia.

This chapter evaluates the growth and reproductive development of juvenile Pacific oysters grown in suspended culture at four different densities. Two key questions were addressed: (1) How will culture density influence the development and mortality of the oyster, and (2) how does the microbiome of oyster gill tissue change throughout the summer and during periods of mortality.

3.2 Materials and Methods

3.2.1 Study Site and Experimental Design

The experiment was conducted at a commercial oyster raft in Metcalf Bay, Baynes Sound, BC (49.250°N, 124.456°W) from May 11 to September 17, 2018 (Fig. 3.1). Juvenile Pacific oysters were grown under the same conditions prior to the beginning of the experiment. Oysters at the start of the experiment were 14.2 ± 0.5 , 4.7 ± 0.2 , and 11.0 ± 0.3 mm (mean \pm SD) in shell height, width, and length, respectively, and 8 months in age. They were placed into Dark Sea oyster trays (LxWxH: 69x69x9 cm) at four different stocking densities (150, 300, 450, and 600 oysters tray⁻¹) with four replicate trays per density; for a total of four blocks in a Latin–square design (Fig. 3.2). The blocks of trays were suspended in the water column with their midpoint at a 5 m depth and 1.5 m apart.

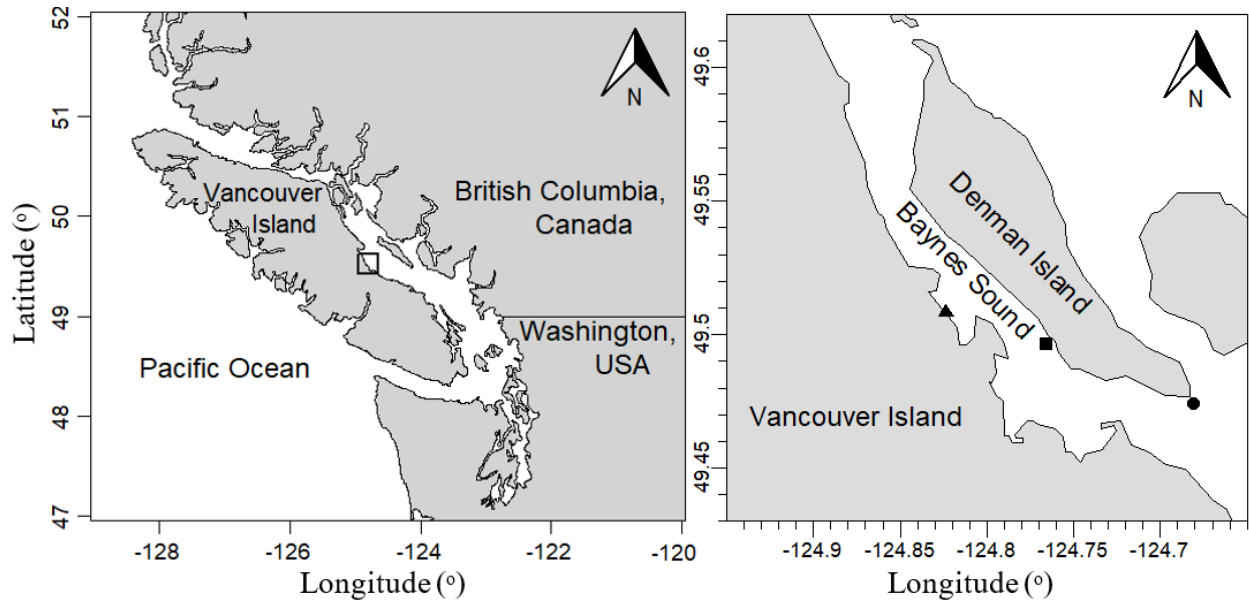


Figure 3.1: Left: Map of Pacific Northwest with the field site location shown with a square.
 Right: Baynes Sound with Metcalf Bay (■), Fanny Bay (▲), and Chrome Island (●) shown.

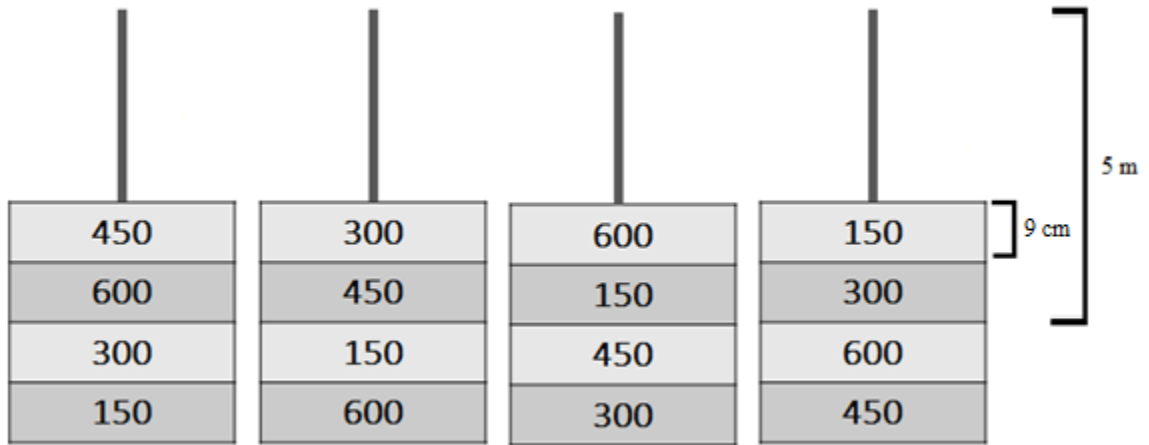


Figure 3.2: Experimental design of juvenile Pacific oyster trays in suspended culture. Each block of four trays contained one replicate unit at each of the four densities (150, 300, 450, and 600 oysters tray⁻¹). All blocks were suspended at 5 m depth in Metcalf Bay off a shellfish aquaculture raft, following standard industry practices.

3.2.2 Environmental Factors

A YSI EXO2 sonde (YSI, Yellow Springs, OH, USA) was deployed at a 5-m depth in Fanny Bay (49.507°N, 124.829°W) (Fig. 3.1) for the duration of the experiment and measured temperature, salinity, turbidity, and oxygen saturation at 10-min intervals. An Onset® HOBO® pendent (Onset, Bourne, MA, USA) was attached to an experimental block and recorded temperatures at 10-min intervals. Daily water temperatures at Chrome Island lighthouse (49.496°N, 124.765°W) from 1969 to 2018 were downloaded from DFO (Anon, 2019a).

Water samples were collected for carbon chemistry analysis in 350-ml soda-lime glass bottles from surface water directly above the trays approximately weekly, with care being taken to limit the introduction of air bubbles (Evans *et al.*, 2019). Bottles were preserved with 200 µl of a saturated mercuric chloride solution and capped with polyurethane lined metal caps. Samples were analyzed using a Burke-o-Lator (Hales *et al.*, 2004) and partial pressure of carbon dioxide ($p\text{CO}_2$), temperature-adjusted hydrogen ion concentration (pH_T), and aragonite saturation state (Ω_{arag}) were computed using the CO2SYS program on MATLAB (Van Heuven *et al.*, 2011; Evans *et al.*, 2019).

3.2.3 Oyster Monitoring and Sample Collection

Approximately every two weeks between May 11 and September 17, 2018 the shell height, length, and width of 10 haphazardly-chosen oysters from each tray were measured. Dimensions used were as described by Galstoff (1964): height is the distance between the umbo and the ventral valve margin, length is the maximum distance between the anterior and posterior margin parallel to the hinge axis, and width is the greatest distance between the top and bottom shell halves. To assess mortality, 100 haphazardly-chosen oysters from each tray were examined,

with dead oysters being defined as those with no shell closing response. Starting on May 23, one haphazardly-chosen oyster from each tray was retained for histological analysis and DNA extraction at each sampling interval. The collected oysters were scrubbed of biofouling with a bristle brush and opened with a shucking knife and scalpel that were rinsed for approximately 2 min with 70% v/v EtOH between oysters. Oysters were cross sectioned at approximately one third of the way from the dorsal end through the visceral mass and a thin section was fixed in Davidson's solution for a minimum of 24 h before histology preparation (Howard *et al.*, 2004). A gill clipping was taken, preserved in 500 µl of RNALater (Invitrogen, Carlsbad, CA, USA) and stored at -80°C for DNA extractions.

3.2.4 Histology

Tissue was dehydrated and embedded in paraffin with a Tissue Tek-TEC embedder (Sakuras, Torrance, CA, USA) and using routine histological techniques. Paraffin-embedded tissues were trimmed in 30-µm sections via a microtome (Thermo Fisher Scientific, Waltham, MA, USA) to expose tissue for sectioning. Five-µm thick sections of tissue were deparaffinized, rehydrated, stained with H&E, mounted on slides, and cover slips sealed with toluene (Permount, Thermo Fisher Scientific, Hampton, NH, USA). The 16 samples from August 12, during the mortality event, were later re-sectioned and stained using a Richard-Allan Scientific™ Gram Stain Kit (Thermo Fisher Scientific).

Oyster cross sections stained in H&E were examined for histopathology of microscopic disease agents of regional concern (Bower, 2017) and to identify the gonad developmental phase of each oyster, which was categorized based on the phases described by Steele and Mulcahy (1999); undifferentiated (0), early active (1), late active (2), ripe (3), partially spent (4), totally

spent (5), post-spawning (6), and resorption (7). Images of each oyster cross section were captured via light microscopy and traces of gonad area (GA) and total oyster area (OA) were prepared on QGIS (Anon, 2020a). For each oyster, the GA, OA, and maximal gonadal length (GL) were quantified using ImageJ software (Schneider et al., 2012) and the gonadosomatic index (GSI) was calculated as the proportion of GA to OA.

3.2.5 DNA Extraction

In addition to the 16 gill clippings collected per sampling date, 2 weak oysters (slow shell closing response), and 4 moribund oysters (no shell closing response, but not yet undergoing liquefactive necrosis) were collected on August 12 for DNA extraction as previously described. Each gill clipping was transferred from RNALater to a 1.7-ml microcentrifuge tube containing 500 μ l of lysis buffer (1-M Tris-HCl, pH 8.0; 0.5-M EDTA, pH 8.0; 1% sodium dodecyl sulfate) and ~30 mg of silica beads and homogenized using a Mini Bead-beater (BioSpec Products, Bartlesville, OK, USA) for 30 s. Proteinase K (250 μ g) was added to each sample, followed by incubation in a shaker incubator (Excella E24, New Brunswick Scientific, Edison, NJ, USA) for 16 h at 37°C and 150 rpm. Chloroform:isoamyl alcohol (24:1, 500 μ l) was subsequently added to each sample, vortexed for 1 min, and centrifuged at 14,000 rcf for 5 min. The upper aqueous phase was removed and placed in a DNase free microcentrifuge tube for ethanol precipitation. Ice-cold ethanol (100%, 400 μ l) was added and samples were centrifuged at 14,000 rcf for 10 min. The supernatant was removed, and the pellet washed with 200 μ l of ethanol (80%). The samples were centrifuged at 14,000 rcf for 10 min and the supernatant removed. The pellet was air-dried and re-suspended in 50 μ l of 1 \times Tris EDTA buffer.

3.2.6 Microbial Composition

Five μl from each oyster $25 \text{ ng } \mu\text{l}^{-1}$ DNA sample were pooled across the four replicates for each density and time point. Additionally, the samples from weak oysters were pooled together, and the samples from moribund oysters were pooled together for a total of 38 samples for high-throughput sequencing analysis of microbial communities. Amplicons of the 16S rRNA gene region were generated by two rounds of PCR, both using a $20\text{-}\mu\text{l}$ reaction volume containing $10 \mu\text{l}$ of 2X GoTaq Green Master Mix (Promega Corporation, Madison, WI, USA), $2 \mu\text{l}$ ($1 \mu\text{M}$ final concentration) of both forward and reverse primers (see below), $1 \mu\text{l}$ of template DNA, and $7 \mu\text{l}$ dsH_2O using a SimpliAmp Thermal Cycler (Thermo Fisher Scientific). The first round of PCR used the primers F357 (5' TACGGGAGGCAGCAG) and R806 (5' GGACTACVSGGGTATCTAAT), with thermocycling settings of 95.0°C hot start for 4 min, followed by 25 cycles of 95.0°C for 30 s, 53.4°C for 45 s, and 72.0°C for 2 min, followed by a final elongation step for 5 min at 72.0°C (Fisher *et al.*, 2016). The forward primer for the second round of PCR included variable Ion Xpress barcoded region (bold) and a sequencing adaptors (underlined and bold) PCR F341 (5' CCATCTCATCCCTGCG TGTCTCCGACTCAGCTAAG **GTAACGAT**TACGGGAGGCAGCAG 3') and the reverse primer 806R, containing the P1 adaptor (underlined) (5' CCACTACGCCTCCGCTTTCCTCTC TATGGGCAGTCGGTGATGG ACTACVSGGGTATCTAAT 3'). The thermocycling settings were 95.0°C hot start for 4 min, followed by 20 cycles of 95°C for 30 s, 65.0°C for 45 s, and 72.0°C for 2 min, followed by a final elongation step for 5 min at 72.0°C . Following PCR amplification, each product was purified with the Agencourt AMPure XP magnetic bead cleanup protocol (Beckman Coulter, Inc., Brea,

CA, USA) using a magnetic PCR plate rack, and quantified on a Qubit 2 Fluorometer (Thermo Fisher Scientific) using the Quant-iT dsDNA BR Assay Kit (Thermo Fisher Scientific).

Following purification of the secondary PCR products, barcoded amplicons from each sample were pooled at equimolar amounts and the library dilution factor was determined based on quantification with an Ion Library Quantitation Kit on an ABI QuantStudio 3 Real-Time PCR System (Applied Biosystems, Foster City, CA, USA). An Ion 520 and Ion 530 Kit-Chef on an Ion Chef Instrument was used to prepare DNA for sequencing, which was completed on an Ion 530 chip with 400 bp chemistry on an Ion S5 XL System (Life Technologies Inc., Carlsbad, CA, USA). Sequencing data was processed in Torrent Suite 5.10.0 with Pre-BaseCaller and BaseCaller Args set to disable-all-filters. The resulting multiplexed BAM file was exported and passed to AMPtk v1.2.5 (Palmer *et al.*, 2018) for de-multiplexing with the AMPtk ion script using default parameters (minimum read length 100 bases, trim all reads to 300 bases, no barcode mismatches, 2 base primer mismatch allowed, USEARCH v9.2.64, VSEARCH v2.9.0). OTUs data were created by concatenated de-multiplexed data files and were clustered with an AMPtk OTU clustering ratio of 97% and filtered with AMPtk filter. Taxonomic designation was assigned using the AMPtk taxonomy script and the AMPtk bacterial 16S database, prepared from rdp_16S_v16 from drive5 Bioinformatics Software and Services.

3.2.7 Quantification of *Vibrio aestuarianus*

Isolates of *Vibrio* spp. obtained from oyster homogenate of sampled oysters collected in Baynes Sound, BC were identified as *Vibrio aestuarianus*, based on comparisons with confirmed recA nucleotide sequence (Chapter 2). These *V. aestuarianus* sequences were used to design species-specific recA primers and probes for use in quantitative polymerase chain reaction

(qPCR). Each 10- μ l qPCR reaction contained 5 μ l SSO Advanced Universal Probes Supermix (Bio-Rad, Hercules, CA, USA), 0.25 μ l of both forward (5' AGGTTCGATCATGCG CCTAG-3') and reverse (5' CTGACGATTCCGGGCCATAG 3') primers, 0.1 μ l probe (5' [HEX] TACGATGGATGTTGAAACCATCTCTACTG [BHQ1] 3'), 1.9 μ l of dsH₂O, and 2.5 μ l of extracted DNA from each sample. Sampled oyster were diluted to 25 ng μ l⁻¹ to normalize the concentration of DNA per sample. Reaction conditions included an initial denaturation phase of 5 min at 95°C, followed by 40 cycles of 15 s at 95°C and 15 s at 60°C. All samples were run with qPCR duplicates in a 384-well hard-shell PCR plate (Bio-Rad) on a CFX384 Real-Time System using the Bio-Rad CFX Maestro version 1.1 software (Bio-Rad). The standard curve was created by amplifying a dilution series from DNA extracted from a known concentration of *V. aestuarianus* cell culture. The resulting concentration of cells per μ l was converted to cells per ng of DNA using the concentration of DNA per qPCR reaction.

3.2.8 Potentially Harmful Phytoplankton

Samples were collected approximately weekly at Metcalf Bay for analysis of phytoplankton composition and biomass. One 15-m vertical tow, using a plankton net (20- μ m mesh), and one discrete water sample at 5-m depth, using a Van Dorn bottle, were taken and stored in 125-ml bottles. These were preserved with a final concentration of 0.3 and 0.04% v/v Lugol's iodine solution, respectively. Identification of all harmful phytoplankton species was done with a compound microscope using a Sedgewick-Rafter slide to the lowest practical taxonomic level, based on morphology (Hasle, 1978). Algal species suspected or known to be of concern for the shellfish industry, including *Alexandrium* spp., *Heterosigma akashiwo*, *Dityocha speculum*, and non-skeletal *Dityocha*, and the dominant phytoplankton species

were enumerated. The total phytoplankton biomass was subjectively scored on a qualitative scale from 1 to 5, which corresponds rough to a range from very low (1–2 cells ml⁻¹) to very high (>10,000 cells ml⁻¹).

3.2.9 Statistical Analyses and Visualization

All statistical analysis was performed in R statistical language (Anon, 2020b). Values in this study are represented as average \pm standard deviation unless otherwise indicated. Graphics were created using the packages ggplot2 (Wickham, 2016) in R and Microsoft Excel 2016. Maps of the field area were created using the maps (Becker *et al.*, 2018a), mapdata (Becker *et al.*, 2018b), PBSmapping (Schnute *et al.*, 2019), and prettymapR (Dunnington, 2017) packages in R statistical language. To examine the density dependent effects on oyster size, reproductive effort, and mortality, end values from each tray were compared with a linear mixed-effects regression (LMER), with density as a fixed factor and block as a random effect, using the lme4 package (Bates *et al.*, 2019). Pairwise comparisons were conducted using the Tukey HSD significance test in the emmeans package with $\alpha = 0.05$ (Lenth *et al.*, 2019). The assumptions of normality and homoscedasticity for a linear model were met based on Shapiro-Wilk test and Levene's test, respectively. Size and reproductive effort values were square-root transformed and final cumulative mortality was arcsine transformed to meet these assumptions.

Due to the repeated independent subsampling observations of mortality within each tray, a logistic regression or any transformed normal analysis over time would underestimate the variation of observed mortality and overestimate the correlations with observed environmental variables. Therefore, the analysis over time is an interpretation of graphed variables as they relate to the onset of the observed mortality event.

The 16S rRNA gene OTUs were investigated using the Vegan package (Dixon, 2003). Non-metric multidimensional scaling (NMDS) plots using Bray Curtis dissimilarity were generated for exploratory data analysis and a permutational multivariate analysis of variance (PERMANOVA) in the Vegan package was used to examine statistical differences in microbial composition between groups. Similarity percentage analysis (SIMPER) was used to further examine which OTUs contributed to the significant difference in microbial composition.

3.3 Results:

3.3.1 Effects of Stocking Density

At the end of the experiment, density significantly affected final cumulative mortalities with mortality increasing with density and the highest density having significantly lower mortalities than the lowest density ($p=0.023$) (Fig. 3.5). Density also had significant effects on oyster shell width ($p=0.001$) and length ($p=0.002$), with higher densities having significantly smaller oysters than lower densities (Fig. 3.3). Oyster shell height decreased with increasing stocking density, although the effect was marginally non-significant ($p=0.057$) (Fig. 3.3). Gonad length also decreased significantly with increasing density ($p=0.049$), with the lowest and highest stocking densities being significantly different (Fig. 3.4). Both gonad area and oyster area also decreased with increasing stocking density, but the effects were non-significant ($p=0.718$ and $p=0.070$, respectively) (Fig. 3.4).

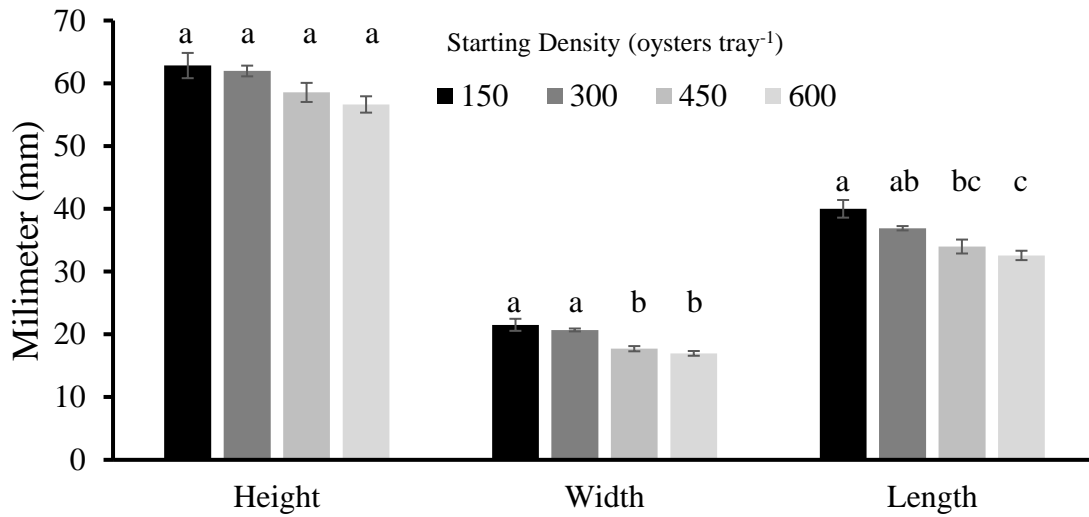


Figure 3.3: Final-end measurements of density dependent effects on Pacific oyster shell size. Oysters were grown at four starting stocking densities 150, 300, 450, and 600 oysters tray⁻¹ from May 11 to September 17, 2018. Values represent the average of four replicate trays at each density with 10 observations from each tray, and error bars represent standard error.

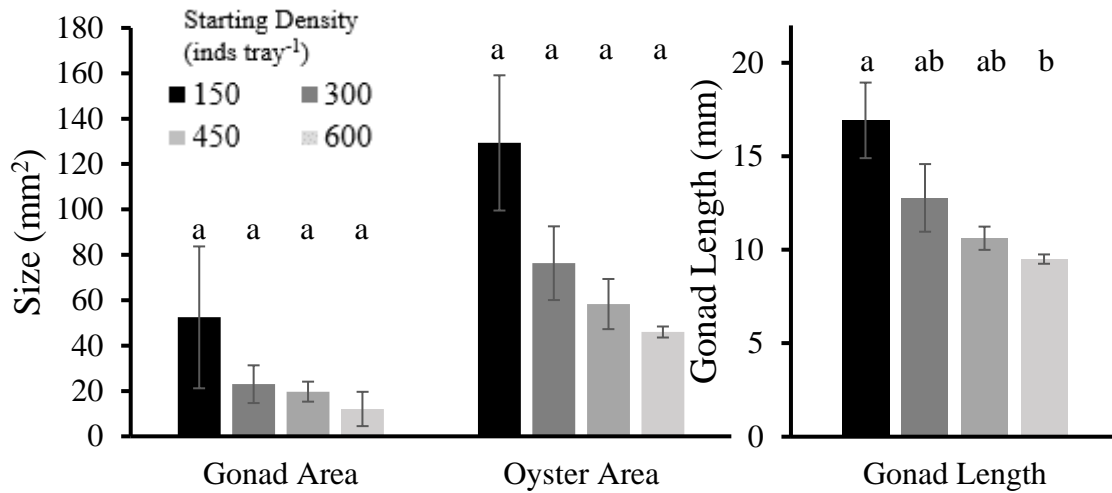


Figure 3.4: Final-end measurements of reproductive characteristics measured from Pacific oyster histological cross sections. Oysters were grown at four starting stocking densities (150, 300, 450, and 600 oysters tray⁻¹) from May 11 to September 17, 2018. Values represent the average of four replicate trays at each density with one observation from each tray, error bars represent standard error.

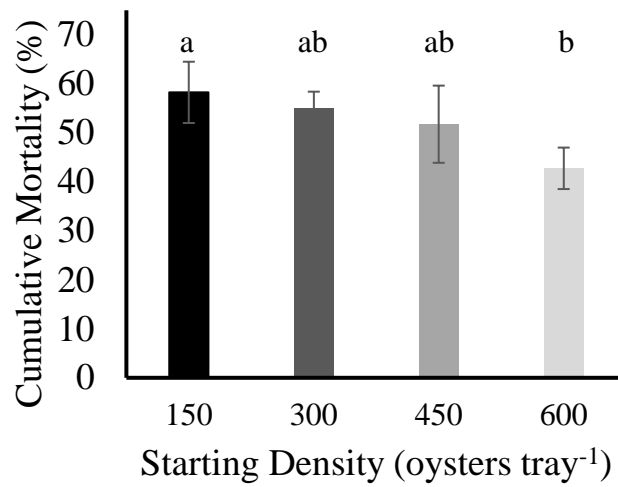


Figure 3.5: Final-end observations of Pacific oyster cumulative mortality observed in suspended culture at Metcalf Bay, Baynes Sound on September 17, 2018. Oysters were grown at four starting stocking densities (150, 300, 450, and 600 oysters tray⁻¹) from May 11 to September 17, 2018. Values represent the average of four replicate trays at each density with 100 observations from each tray, and error bars represent standard error.

3.3.2 Growth and Reproductive Development

Throughout the experiment, the average shell height, width, and length of the oysters increased, averaged across densities, from 14.2 ± 0.5 , 4.7 ± 0.2 , and 11.0 ± 0.3 mm to 60.0 ± 0.9 , 19.2 ± 0.6 , and 35.9 ± 0.9 mm, respectively. The relationship between height, width, and length was examined by a principal component analysis (PCA) (not shown), and principal component one (PC1) described 98.3% of the variation in these size measurements. Based on PC1, the oysters had an average of 320.0% increase in shell size from May 11 to July 30 at the onset of mortality. Similarly, oyster reproductive development shifted from predominantly undifferentiated gonads (14/16 individuals) with 1 male and 1 female on May 23 to predominantly late active and ripe gonads (15/16 individuals) with 8 males and 8 females on July 30 at the onset of the mortality event. Over the same time period, a change in gonad area from 0.04 ± 0.14 to 14.49 ± 12.79 mm² was observed and the gonadosomatic index increased from 0.48 ± 1.66 to 24.23 ± 11.90 % gonad occupation. A PCA (not shown) of reproductive effort assessed the correlation between developmental stage, gonad area, gonad length, and gonadosomatic index with PC1 describing 79.4% of the variation in reproductive effort. There was a linear relationship between log-transformed values of oyster size (PC1) and reproductive development (PC1) throughout the summer (Fig. 3.6) ($R^2=0.652$, $p<0.001$).

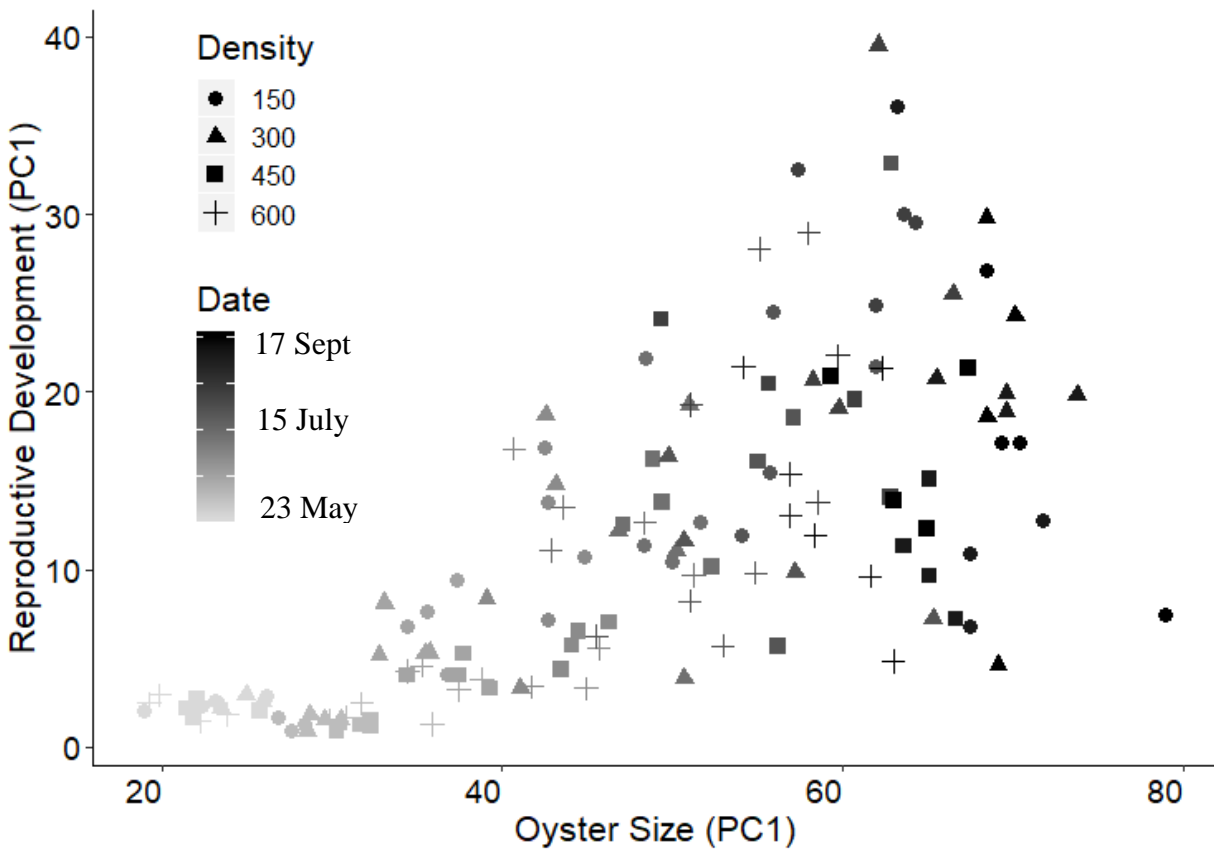


Figure 3.6: Each point represents a replicate tray containing 150, 300, 450, or 600 Pacific oysters. PC1 of oyster size variables described 98.3% of the variation in shell height, width, and length. PC1 of oyster reproductive development described 79.4% of variation in oyster gonad length, gonad area, gonadosomatic index, and gonad developmental phase.

3.3.3 Observed Mortality

From May 11 to July 15 there was no observed mortality in any of the replicate trays. Mortality was first observed on July 30 with $10.75 \pm 1.97\%$ mortality across all densities, which coincided with a period of elevated temperature (Fig. 3.7). Cumulative mortalities (average \pm SD) measured on September 17 were $52.9 \pm 11.8\%$ across all densities. The average water temperature at Chrome Island for the 10 d preceding the first observation of the mortality event (July 20 to July 30) was $20.11 \pm 0.58^\circ\text{C}$, which includes 5 d above the 80th percentile for the last 30 years for their respective dates.

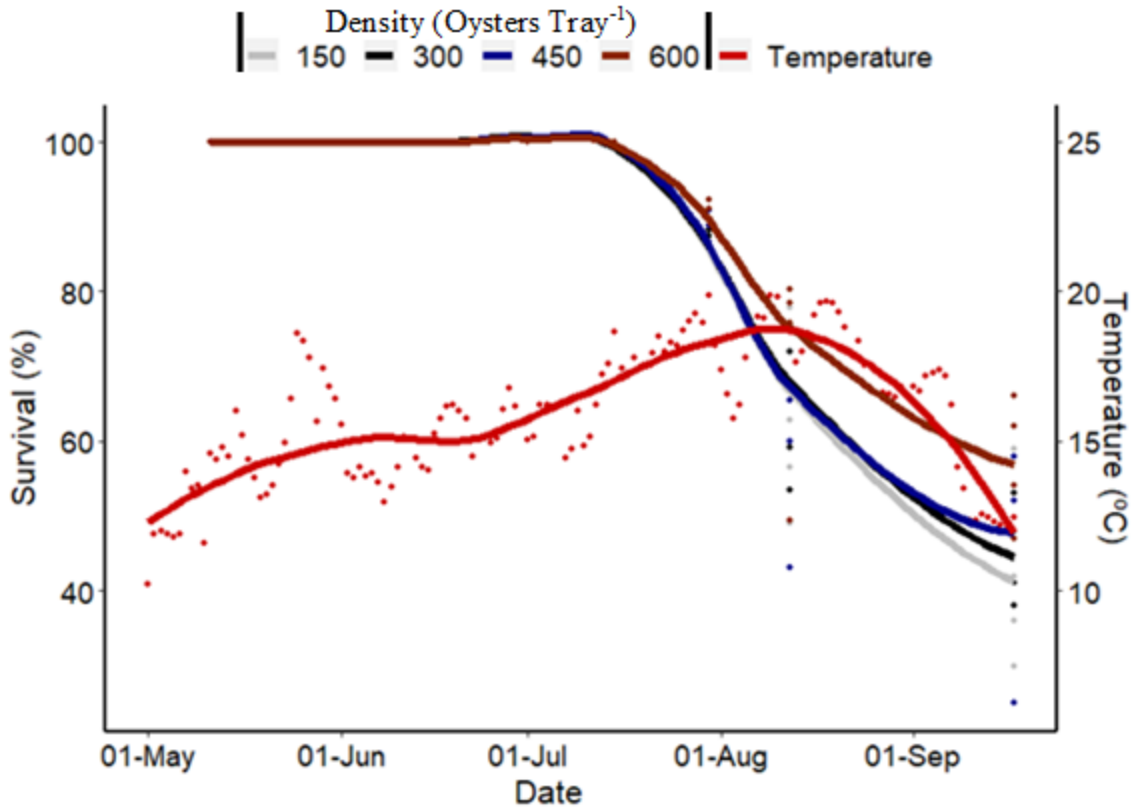


Figure 3.7: Pacific oyster survival by starting stocking density and water temperature during summer, 2018. Densities were 150, 300, 450, and 600 oysters tray⁻¹ at the onset of the experiment on May 11, 2018. Daily water temperatures were acquired from DFO monitoring at Chrome Island Lighthouse (Fig. 3.1) (Anon, 2019a). Fitted curves are smoothed conditional means using local polynomial regression fitting.

3.3.4 Environmental Observations

The sonde recorded data from May 11 to August 2. The average daily temperature was $15.7 \pm 2.0^{\circ}\text{C}$, oxygen saturation was $114.1 \pm 11.3\%$, salinity was $26.2 \pm 1.1\%$, chlorophyll was $35.37 \pm 64.13 \mu\text{g l}^{-1}$, and turbidity was 5.26 ± 9.67 FNU. Eleven surface carbonate chemistry samples were collected at Metcalf Bay from July 18 to September 18. The pH, pCO_2 , and aragonite saturation throughout the study was 8.17 ± 0.02 , $258.5 \pm 15.7 \mu\text{ATM}$, and 2.34 ± 0.10 , respectively. Air temperatures during the period of oyster sampling and observation on the boat were higher than the submerged temperature. For example, July 30 sampling on the boat occurred from 10:24 AM to 12:14 PM and the average air temperature was 36.8°C . In contrast, the average daily maximum water temperature recorded, excluding sampling periods, for July and August was $19.2 \pm 2.0^{\circ}\text{C}$.

3.3.5 Histopathology

All oysters collected for histopathology appeared healthy macroscopically meaning they had strong adductor muscle response, no shell deformities, no lesions, and no liquefactive necrosis. No pathologies of pathogens or parasites of regional concern were observed through macroscopic or microscopic observations (Bower, 2017). An unknown rickettsia-like infection was observed in one oyster slide from August 12. Three of 16 histological samples collected from oysters on August 12, during the mortality event, had necrotic gill epithelium and mixed microbial infections in peripheral tissue (Fig. 3.8).

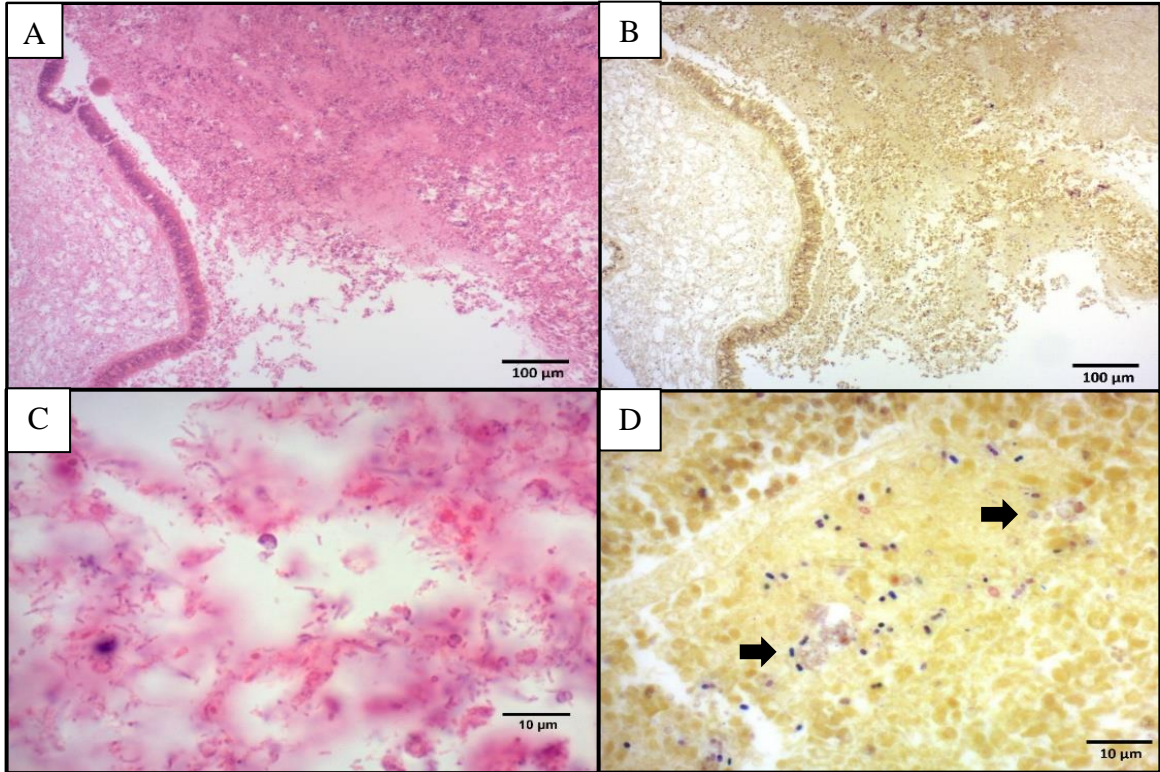


Figure 3.8: Histopathology cross sections from August 12, 2018 sampling of the Pacific oyster summer mortality event. Top: low magnification of necrosis in gills and epithelium with healthy labial palps on the left. Bottom: high magnification of mixed microbial infection in peripheral tissue necrosis. Staining done with H&E (A and C) and Gram stain (B and D). In the Gram stain gram-negative bacteria are pink to light purple and gram-positive bacteria are blue.

3.3.6 Analysis of Microbial Composition

Read number varied from 13 to 185,473. Seventeen samples below 9,150 reads samples were removed, and the remaining 21 samples were rarefied to 9,150 reads. A total of 1,054 OTUs were present and the average per sample was 310.6 ± 111.0 OTUs. Of the 1,054 OTUs, 983 were identified to class and 340 were identified to genus, based on the AMPtk bacterial 16S database. The most common classes were Gammaproteobacteria (310 OTUs), Alphaproteobacteria (165), Flavobacteria (89), and Deltaproteobacteria (84), while the most common genera were *Arcobacter* (17 OTUs), *Vibrio* (11), and *Psychromonas* (8). Eight of the most abundant OTUs, primarily of the genera *Vibrio*, *Serratia*, *Pseudomonas*, and *Psychromonas*, made up 48.6% of the read counts across all samples (Fig. 3.9).

The NMDS of Bray Curtis dissimilarity clustered by density (not shown) suggested there was no significant difference in microbial composition based on stocking density and the PERMANOVA supports this observation ($p=0.599$, $R^2=0.156$). There was, however, a significant difference in bacterial composition among groups of samples associated with observed low ($<0.1\% \text{ d}^{-1}$), medium ($0.1\text{--}2\% \text{ d}^{-1}$), and high ($>2\% \text{ d}^{-1}$) percent mortalities (Fig. 3.10) ($p=0.009$, $R^2=0.349$). The PERMANOVA analysis suggests there was a significant difference between the low and medium mortality groups ($p=0.003$, $R^2=0.169$) and the low and high ones ($p=0.012$, $R^2=0.244$), but not between the medium and high mortality groups ($p=0.079$, $R^2=0.172$). Differences in microbial composition were assessed using a SIMPER analysis. The variation between clusters of samples from low, medium, and high mortality groups was driven predominantly by OTU1. For example, OTU1 explained 36.0% of the variation among samples that appeared healthy and the combined weak and moribund samples in

the PERMANOVA ($p=0.028$, $R^2=0.111$). It is important to note that OTU1 shared 99.7% nucleotide identity with *Vibrio aestuarianus* (GenBank: KY923252.1) (Saulnier *et al.*, 2017).

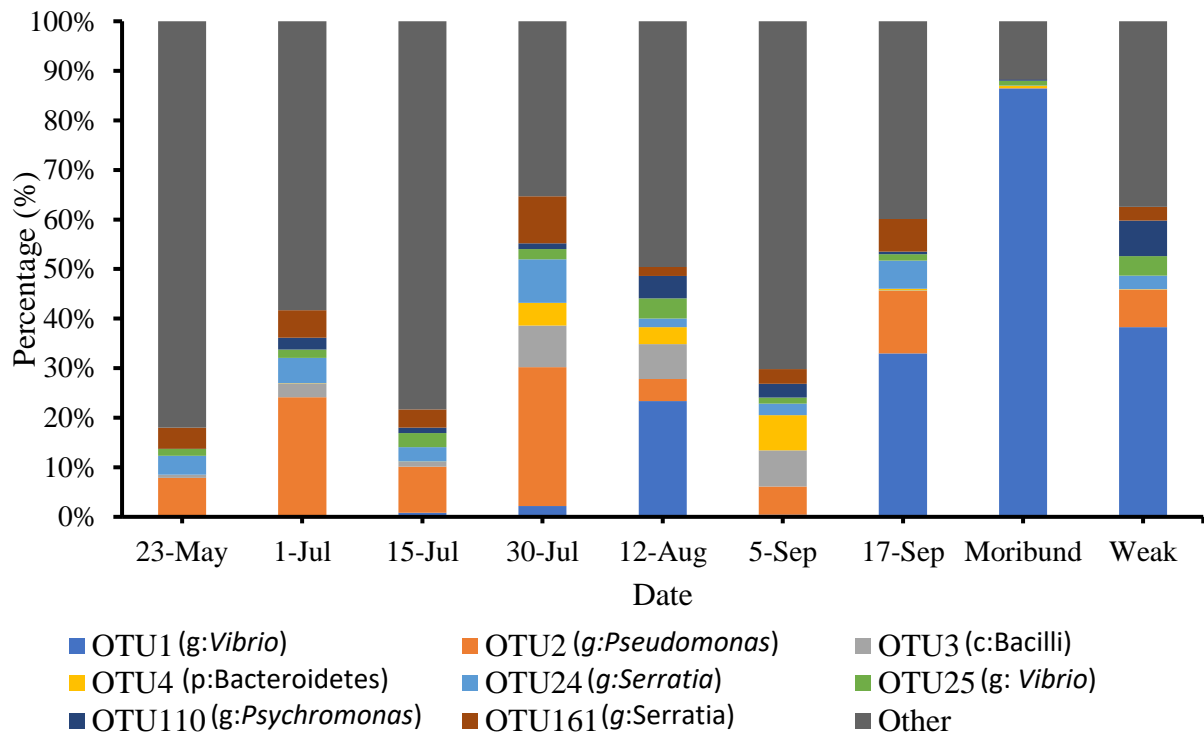


Figure 3.9: Stacked bar plot of Pacific oyster bacterial microbiome. Shown identities are the nearest result from AMPtk 16S rRNA gene data base using AMPtk taxonomy with 97% nucleotide clustering.

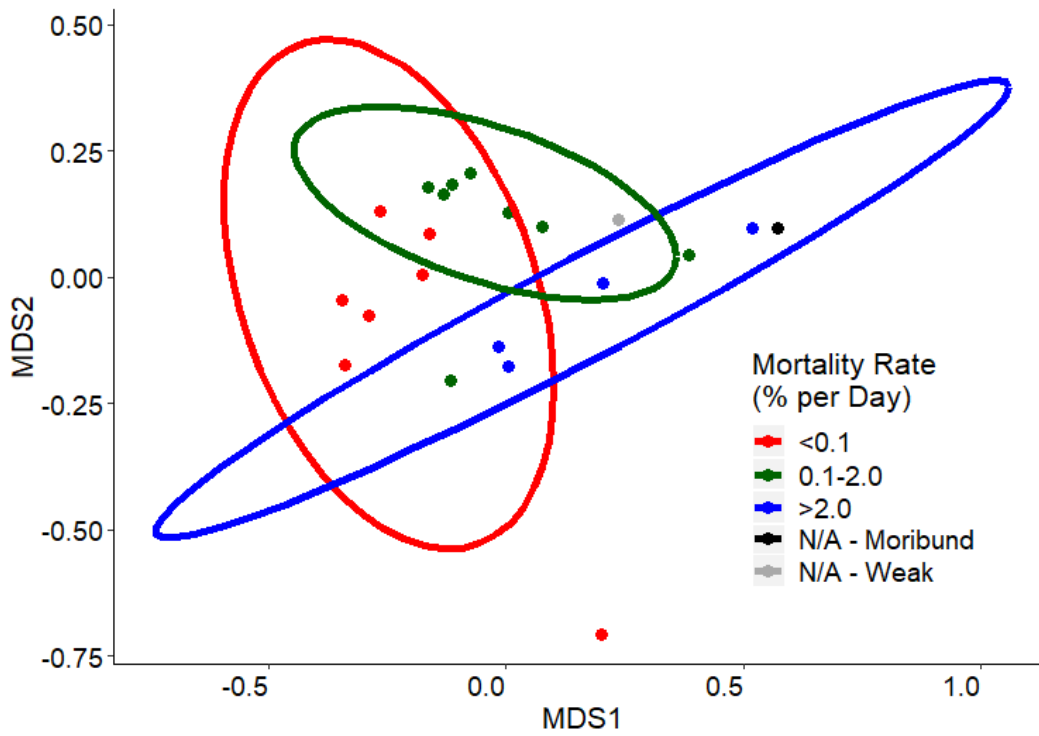


Figure 3.10: Bacterial composition using Bray Curtis dissimilarities of the V4 region of the 16S rRNA gene rarified to 9150 reads. Ellipses indicate 95% confidence intervals for each cluster.

3.3.7 Quantification of *Vibrio aestuarianus*

Vibrio aestuarianus abundance was quantified by qPCR using species-specific primers designed to amplify the *recA* gene. An example amplicon (5' TCTGACGATTCCGGGCCATA GACTTCAACAATACGNCCCATTGGTAAGCCACCAGCACCCAATGCAATATCCAGAG AAAGTGAACCAGTAGAGATGGTTTCAACATCCATCGTACGGTTATCACCTAGGCGCA TGATCGAACCT 3') was sequenced following the methodology in chapter 2, and had 99.3% nucleotide identity with *V. aestuarianus* (GenBank: AJ580855.1) and 90.9% identity to the next closest match, *V. scophthlami* (GenBank: CP016307.1). The standard curve had the equation $y = -3.308x + 44.388$, $R^2 = 0.991$, and an amplification efficiency of 1.006. Twenty four of 144 samples were above the limit of detection of $1.78 \log_{10}$ cells ng^{-1} of DNA, which was the lowest detectable concentration in the standard curve (Fig. 3.11). The concentration of *V. aestuarianus* was highest in moribund oysters and was elevated during periods of observed mortality from July 30 to September 17.

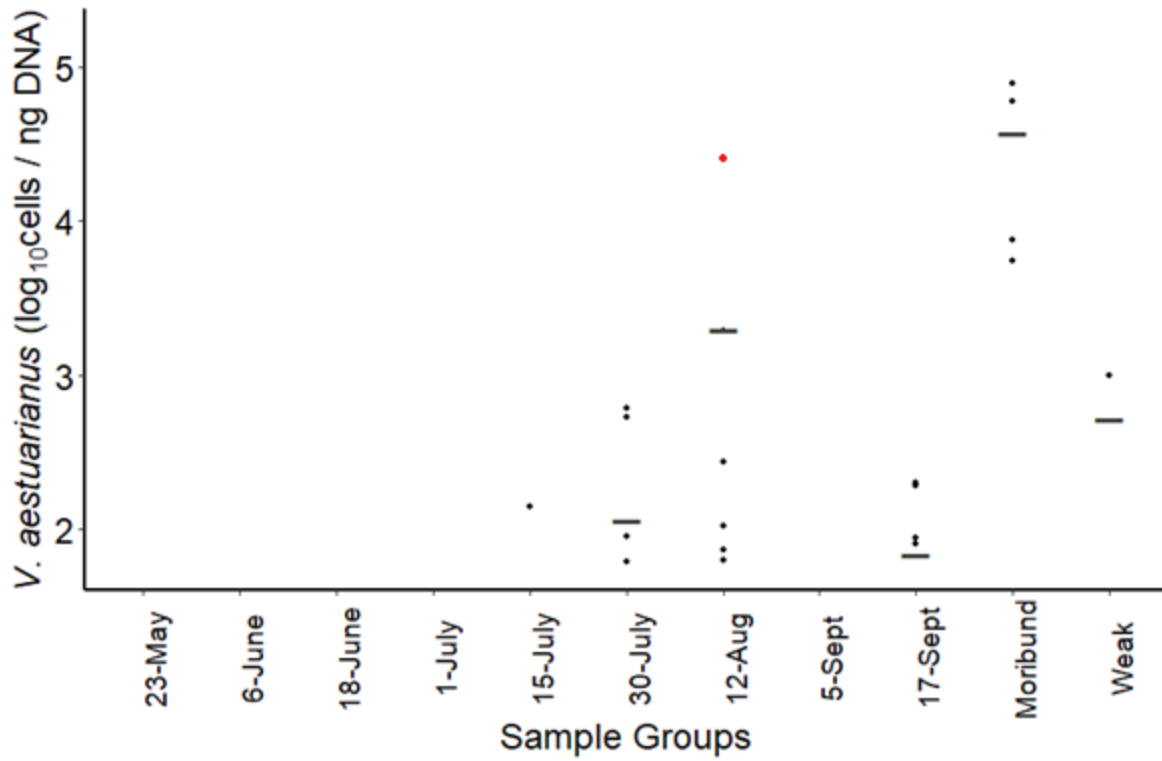


Figure 3.11: Quantitative polymerase chain reaction results for juvenile Pacific oyster gill tissue. Group averages are shown with gray bars. Four moribund and two weak individuals were collected during the mortality event on August 12, 2018. The red point is from the same oyster with a mixed microbial infection shown in Figure 3.8.

3.3.8 Phytoplankton

Rhizosolenia setigera was the most abundant potentially harmful phytoplankton species present in Baynes Sound in 2018, with an average of 476 ± 35 cells ml^{-1} across all samples (Fig. 3.12). Other potentially harmful species present in samples were *Alexandrium* spp., *Heterosigma akashiwo*, *Dichtyocha speculum*, and non-skeletal *Dichtyocha*. The average concentration of phytoplankton collected was $3,500 \pm 1,000$ cells ml^{-1} .

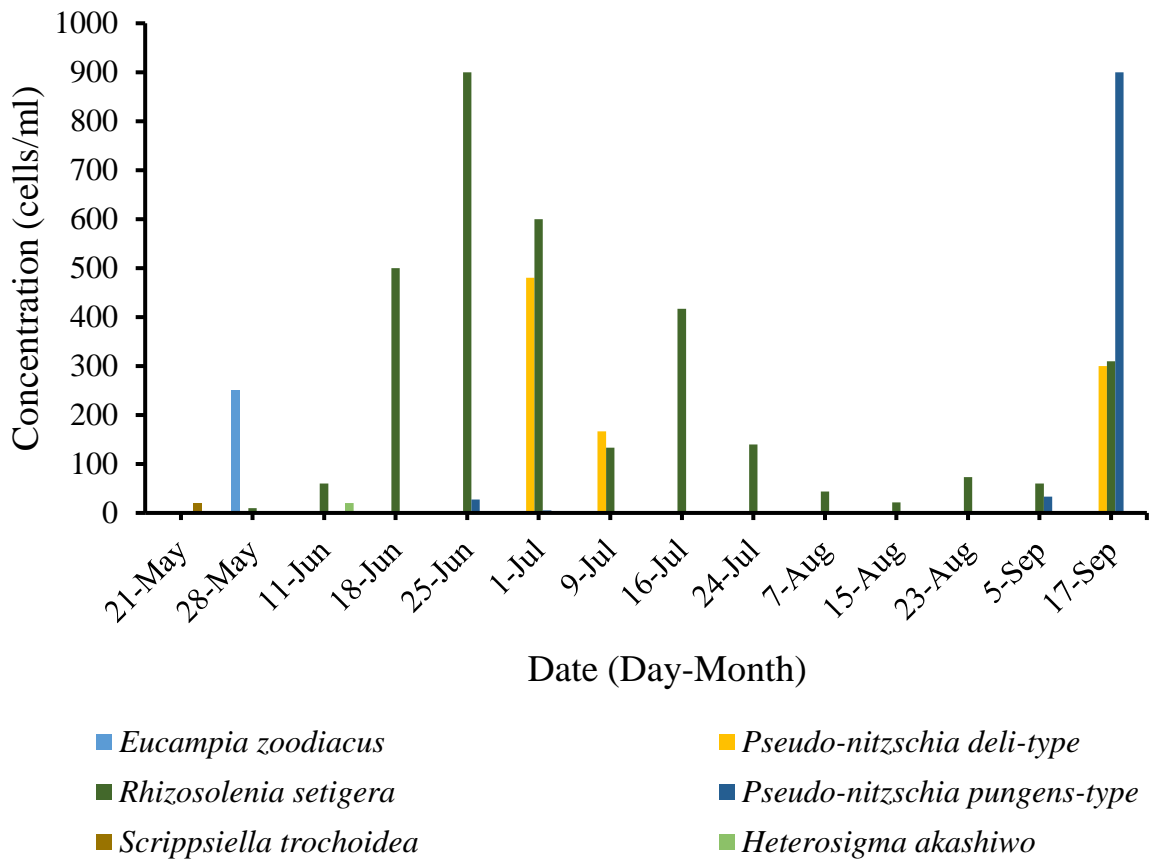


Figure 3.12: Concentration of the most abundant species per samples and all potentially harmful plankton species detected at 5 m depth in Metcalf Bay.

3.4 Discussion

3.4.1 Effect of Stocking Density

In the present study there was a negative relationship between stocking density and size, reproductive effort, and mortality of oysters. Similarly, Chávez-Villalba *et al.* (2010), working with various densities (25 to 600 oysters tray⁻¹) of Pacific oysters in a subtropical lagoon in Mexico, showed reduced somatic growth at their highest tested density. Interestingly, they did not observe a significant effect of stocking density on Pacific oyster survival, showing that they can be grown in densities as high as 600 oysters tray⁻¹ with no ill effects on survival. The density effects on survival in these two studies are, at first, counter-intuitive, but are most likely explained by the following. Field observations suggest that reducing food availability with higher stocking densities will reduce gonad development (Royer *et al.*, 2008; Chávez-Villalba *et al.*, 2010), which will reduce physiological stress associated with reproduction. Combined, these two field studies on Pacific oyster density manipulation provide evidence that limiting food availability may indirectly reduce mortalities through a reduction in oyster growth and reproductive effort. Observations from controlled laboratory studies on Pacific oysters confirm this hypothesis, with increased food availability causing significantly higher summer mortalities (Lipovsky and Chew, 1972; Delaporte *et al.*, 2007). From a practical commercial perspective there are likely more effective methods of limiting food availability than by altering the culture density of oysters. For instance, lowering the shellfish below the chlorophyll maxima in the water column before gametogenesis begins could reduce both food availability and temperature, which may be an effective way of reducing summer mortalities of Pacific oysters.

3.4.2 Environmental Factors

The May temperature spike can be defined as a marine heatwave since it had more than five consecutive days above the 90th percentile for the 30-year historical dataset collected at Chrome Island (Hobday *et al.*, 2016). There was no observed mortality at that point, which could be due to the small size and very little gametogenesis observed in the oysters during May. High water temperatures (>19°C) occurred at the end of July and coincided with the onset of summer mortality. Elevated temperatures can increase the proliferation and virulence of pathogens while simultaneously increasing physiological stress and susceptibility of the hosts (Malham *et al.*, 2009; Kimes *et al.*, 2012; Wendling *et al.*, 2014; Solomieu *et al.*, 2015). Mortalities of the juvenile oysters occurred during a period of rapid growth with an increase in shell size of 320% between May 11 and July 30. This was their first summer of gametogenesis, with most oysters developing gonads between May 23 and July 30. The correlation of oyster growth and reproductive development with the susceptibility of Pacific oysters to infection by opportunistic pathogens and increased summer mortality has been previously described (e.g. Cotter *et al.*, 2010; De Decker *et al.*, 2011; Wendling and Wegner, 2013). The observed accumulation of *V. aestuarianus* and OTU1 during the mortality event in the present study was likely a result of increased host susceptibility associated with elevated temperature, rapid growth, and the onset of gametogenesis. No other observed environmental factors in this study were outside of the optimal range for Pacific oyster health.

Handling effects throughout this experiment may also have contributed to mortality. For example, the data collection conducted on July 30, at the onset of the mortality, took two hours to complete with an average air temperature of 36.8°C – however, how well the rapid warming of the temperature probe reflects the warming of oyster tissue and liquor is unknown. The LT₅₀ of

Pacific oysters has been reported as 1 hr exposure to 42.3°C (Shamseldin *et al.*, 1997).

Scheduling industry handling practises for cooler periods of the day may mitigate some of the observed mortalities.

3.4.3 Bacterial Composition and the Occurrence of *Vibrio aestuarianus*

Amplicon sequencing of the V4 hypervariable region of the 16S rRNA gene demonstrated a reduction in diversity of OTUs and an increase in OTU1 associated with elevated mortalities. A reduction in microbial diversity is commonly associated with a diseased state (Kamada *et al.*, 2013) and has been observed in Pacific oyster summer mortalities (Lokmer and Wegner, 2015; Green *et al.*, 2019; King *et al.*, 2019a, 2019b). Evidence from terrestrial vertebrates suggests microbiomes can protect the host from colonization by pathogens (Kamada *et al.*, 2013). In Pacific oysters, bacterial taxa can provide protection or promotion of OsHV-1 infections, suggesting that the microbial composition plays a significant role in disease-resistance and progression (King *et al.*, 2019c). Lokmer and Wegner (2015) demonstrated that the composition of healthy Pacific oyster microbiomes changes significantly with temperature, but not a challenge with a virulent *Vibrio* sp. alone. Similarly, a study with a simulated marine heatwave of $\Delta 5^{\circ}\text{C}$ resulted in a cumulative Pacific oyster mortality of 77.4% over six days, a reduction in microbial diversity, and a 324-fold increase in *V. harveyi* concentration (Green *et al.*, 2019).

OTU1 shared 99.7% nucleotide similarity with *V. aestuarianus*, based on NCBI BLAST, and when viewed in respect to the qPCR results, there is strong evidence that it is *V. aestuarianus*. Characterization of *Vibrio* communities based on 16S rRNA gene high-throughput sequencing has provided researchers confidence in differentiating *V. aestuarianus* from other

Vibrio spp. (Jesser and Noble, 2018). The V4 hypervariable region is likely the optimal sub-region of the 16S rRNA gene to study bacterial phylogenies (Yang *et al.*, 2016). Due to the structural importance of the 16S rRNA gene product, however, the rate of nucleotide change is much lower than protein-coding genes (Ochman and Wilson, 1987). The substitution rate for 16S and 18S genes is roughly 1% per 50 million years, whereas the silent substitution rate for protein-coding genes is approximately 0.7–0.8% per million years; this increased nucleotide variability for the latter allows for more effective resolution of closely related taxa (Ochman and Wilson, 1987; Jesser and Noble, 2018). Therefore, the resolution of *Vibrio* spp. could have been improved by using a protein-coding gene. The heat-shock protein 60 was recently used for high-throughput sequencing to characterize *Vibrio* community ecology (Jesser and Noble, 2018; King *et al.*, 2019b). Furthermore, the use of a protein-coding gene could reduce potential bias in relative abundance estimates for high-throughput sequencing analysis, which can be associated with variable 16S rRNA copy number. For instance, the average 16S rRNA gene copy number is 9 for the genus *Vibrio*, but only 3.5 for proteobacteria (Kormas, 2011), suggesting that the 16S rRNA high-throughput sequencing assay may have over-estimated the relative abundance of *Vibrio* OTUs in the present study.

Vibrio aestuarianus was first isolated from seawater, clams, oysters, and crabs along the Oregon coast and later reported as a pathogen of Pacific oysters in France (Tison and Seidler, 1983; Labreuche *et al.*, 2006a). Following the association of *V. aestuarianus* with Pacific oyster summer mortality in France (Garnier *et al.*, 2007), the species was split into two sub-species classifications, *V. aestuarianus* subsp. *aestuarianus* (Tison and Seidler, 1983) and *V. aestuarianus* subsp. *francensis* (Garnier *et al.*, 2008). Due to the significance of Pacific oyster summer mortality in France, *V. aestuarianus* subsp. *francensis* has been well-studied (Labreuche

et al., 2006b, 2010; Parizadeh *et al.*, 2018). Like most pathogenic *Vibrio* spp., the virulence of *V. aestuarianus* to Pacific oysters is strain-dependent (Garnier *et al.*, 2008; Baker-Austin *et al.*, 2018). Investigations into a highly pathogenic strain of *V. aestuarianus* subsp. *francensis* (01/32) revealed an extracellular zinc metalloprotease that confers the cytotoxicity and virulence (Labreuche *et al.*, 2006a; 2006b, 2010). This metalloprotease induces morphological changes in oyster haemocytes, causing reduced function and survival, leading to host immunosuppression.

In the present study, *V. aestuarianus* abundance increased in association with observed mortalities and declining oyster health. In the histological analysis of oysters that appeared healthy from August 12 there were mixed microbial infections in peripheral necrotic tissue, although I cannot differentiate between opportunistic and causative pathogens. Further characterization of *V. aestuarianus* strains isolated in this region is required to assess the mechanism(s) of virulence and the role of this bacteria in the observed summer mortalities. At 5°C, *V. aestuarianus* can infect oysters with concentrations below detectable limits that can be revealed with thermal stress (Parizadeh *et al.*, 2018). This suggests that *V. aestuarianus* was likely present in oysters throughout May and June until favorable environmental and physiological conditions developed.

3.4.4 Reproductive Effort

This study provides evidence for the association of reproductive effort with summer mortality. This association has been observed in field studies conducted in other regions of the world (Imai *et al.*, 1965; Lipovskey and Chew, 1972; Perdue, 1983; Cotter *et al.*, 2010), as well as in laboratory trials (Delaporte *et al.*, 2007; Huvet *et al.*, 2010; Wendling and Wegner, 2013), but not for cultivated oysters in coastal waters of BC. At the onset of summer mortality on July

30 I observed a GSI of 24%, whereas during the marine heatwave in May, the oysters had a GSI of 0.48%. Many summer mortality studies have focused on Pacific oysters in their second summer, when they typically have a much higher GSI and summer mortalities (Perdue, 1983; Azéma *et al.*, 2016). Mature gametes in Pacific oysters are associated with oyster size, not age, and the amount of reproductive effort is a product of food availability (Quayle, 1988; Enríquez-Díaz *et al.*, 2009). There also appears to be a higher proportion of female oysters associated with increased food supply and oyster age (Quayle, 1988). Pacific oysters are protandrous hermaphrodites and are thought to all be male for their first summer of reproductive development (Pauley *et al.*, 1988). In contrast, I observed a large proportion of females (e.g. 50% on July 30) throughout their first summer. A number of studies support the observation that reproductive effort has a positive correlation with summer mortality, however, the mechanism by which gametogenesis might increase susceptibility is not well understood (De Decker *et al.*, 2011).

Does gametogenesis increase susceptibility to opportunistic pathogens such as *V. aestuarianus*? The process of gametogenesis may directly reduce immune response of oysters by reducing the number of circulating haemocytes (Delaporte *et al.*, 2006). Additionally, De Decker *et al.* (2011) observed that *Vibrio splendidus* preferentially infects gonad tissue, although I observed *V. aestuarianus* infections in gill epithelium. Gonad tissue may not allow adequate haemocyte infiltration to clear developing infections of opportunistic bacteria. The lack of observed infection in gonad tissue in my study may be a result of survivorship bias. For instance, disease progression could occur more rapidly in gonad tissue, causing liquefactive necrosis.

Triploid Pacific oysters grow more rapidly than diploids and represent 30% of global Pacific oyster production (Suquet *et al.*, 2016). They are often considered partially sterile with approximately 0.06% the reproductive potential than diploid oysters (Allen and Downing, 1986;

Suquet *et al.*, 2016; Houssin *et al.*, 2019). Their GSI is also significantly lower than diploids (Jeung *et al.*, 2016). Suquet *et al.* (2016) observed gametes in 92.9% of diploid oysters and 42.0% of triploid oysters. Despite their potentially reduced reproductive effort, Wadsworth (2018) observed significantly higher mortalities in triploid Eastern oysters (*Crassostrea virginica*) than in diploids. Comparisons between diploid and triploid Pacific oysters may present an opportunity to differentially examine the of role reproductive effort and energy utilization in summer mortality (Allen and Downing, 1986).

3.4.5 Conclusion

This study demonstrated that summer mortalities of $52.9 \pm 11.8\%$ can occur during the first summer of growth for juvenile Pacific oysters grown in suspended culture in Baynes Sound. Under these conditions, I demonstrated an association among the variables of *V. aestuarianus* abundance, elevated water temperature, and rapid growth/gametogenesis that culminated with high summer mortality. The positive effect of stocking density on mortality suggests limiting food availability could alter Pacific oyster susceptibility to summer mortality (through reduced reproductive effort). Improved understanding of oyster energetics during periods of gametogenesis may identify improved management strategies for oyster farmers in the region.

Chapter 4 Conclusion and Perspectives

4.1 Summary of Pacific Oyster Summer Mortality in Baynes Sound

This thesis examined factors that may contribute to Pacific oyster summer mortality events in Baynes Sound, BC. The questions initially posed were:

- 1) How prevalent are Pacific oyster summer mortalities in Baynes Sound?

Cumulative mortality of adult Pacific oysters (initial height: 96.0 mm, age: 15 months) grown in the intertidal was 22.7% from July 5, 2017 to September 15, 2017 (Chapter 2). Whereas, juvenile Pacific oysters (initial height: 14.2 mm, age: 8 months) grown in suspended culture had a cumulative mortality of $52.9 \pm 11.8\%$ from May 11 to September 17, 2018 (Chapter 3).

- 2) What potentially pathogenic *Vibrio* spp. are present during the observed mortalities and are they more abundant during periods of mortality?

Culturing and sequencing the *recA* gene in 2017 suggested that a number of potentially pathogenic *Vibrio* spp. are present in Pacific oysters that have not previously been described for this region. Quantification of *V. aestuarianus* with qPCR and high-throughput sequencing of the 16s rRNA gene showed an increased abundance of *V. aestuarianus* in oyster gill tissue and a decrease in microbiome diversity during periods of summer mortality in 2018.

- 3) Are there elevated concentrations of potentially harmful phytoplankton species associated with mortality events?

There were no harmful algal blooms observed in either year, and the abundance of potentially harmful species, such as *Alexandrium* spp. and *Heterosigma akashiwo*, was far below threshold values causing adverse health effects for Pacific oysters.

- 4) What environmental factors appear to contribute to the incidence of summer mortality in Baynes Sound?

There was very limited evidence that any environmental factors were implicated in the observed summer mortalities in 2017; however, in 2018 the onset of the mortality event was associated with a period of warming and water temperatures above 19°C.

4.2 Mitigating Pacific Oyster Summer Mortalities

Future research and development directions should prioritize mitigating mortalities and improving outcomes for oyster farmers. Selective breeding, intertidal conditioning, changing food availability, and moving farm locations or tray depths are potential mitigative strategies that will be discussed in the context of the mechanisms of summer mortality in BC proposed in this thesis (Fig. 4.1).

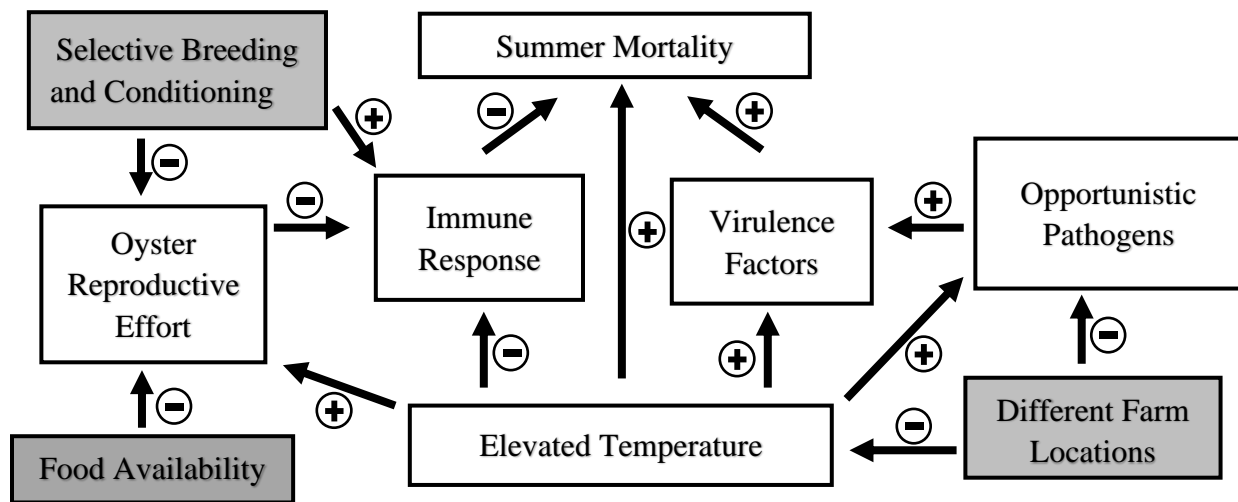


Figure 4.1: Hypothesized mechanisms of Pacific oyster summer mortality and potential mitigative actions (shown in grey filled boxes). Positive (+) and negative (-) interactions between factors are indicated.

There is both field (Imai *et al.*, 1965; Lipovskey and Chew, 1972; Perdue, 1983; Cotter *et al.*, 2010) and laboratory (Delaporte *et al.*, 2007; Huvet *et al.*, 2010; Wendling and Wegner, 2013) evidence demonstrating that by limiting food availability, growers could reduce oyster reproductive effort and correspondingly reduce the impact of summer mortality (Fig. 4.1). Increasing oyster culture density is one option to reduce food availability, but this strategy is limited by space; even in the highest density of 600 oysters tray⁻¹, which nearly filled the tray, only a small effect was observed. Alternative options, such as increasing culture depth below the chlorophyll maximum, or transporting oysters to different depths throughout the tidal range could also alter the food availability, exposure temperature, and microbial communities.

There appears to be a critical period during the end of July to mid-August, during the hottest days of the year, in which summer mortality typically occurs in Baynes Sound. This corresponds to the warmest daily water temperatures recorded in the historic Chrome Island dataset. Another mitigation technique would be harvesting before this critical period of elevated temperature could reduce the losses. This is not always possible, for example, the oysters studied in Chapter 3 incurred summer mortality, but were not marketable due to their smaller shell thickness and meat size. Moving farm operations to an area with colder water, lower nutrients, or the absence of pathogenic *Vibrio* spp. could eliminate summer mortality. This presents a number of challenges such as increased regulatory barriers, growing times, increased transport, and negative social stigma.

Breeding for Pacific oyster resistance to summer mortality has had promising results in France with realized heritabilities above 0.55 for survival in each of the first two generations (Dégremont *et al.*, 2010). The invasive success of Pacific oysters has been, in part, attributed to its ability to rapidly develop resistance to local *Vibrio* spp. (Wendling and Wegner, 2015). This

may contribute to the lack of reported summer mortalities in farmed oysters derived from wild populations in BC. Most of BC hatchery produced Pacific oyster seed may have originated from the Molluscan Broodstock Program, based out of Oregon State University. This program increased oyster growth rates and survival under standard operating conditions free of summer mortality (de Melo *et al.*, 2016). The genetic background of oysters grown in Baynes Sound and how it may influence summer mortalities it is not well understood. This knowledge gap could be addressed by comparing and contrasting the summer mortalities of wild set s and hatchery produced Pacific oyster in BC aquaculture.

Future research could focus on better understanding the mechanisms of summer mortalities through controlled laboratory work. Whole genome sequencing of *V. aestuarianus* strains from Baynes Sound would allow for a more thorough comparison with other regions. It would also be informative to examine the differences in immune response and disease progression between oysters cultured in suspended and intertidal culture. There is evidence that the elevated nutrients in suspended culture contributes to higher mortalities (Imai *et al.*, 1965; Lipovskey and Chew, 1972; Perdue, 1983; Cotter *et al.*, 2010; Delaporte *et al.*, 2007; Huvet *et al.*, 2010; Wendling and Wegner, 2013); however, the intertidal temperatures (both maxima and daily variability) are much higher than in suspended culture (Fig 4.1). Additionally, the repeated exposure to elevated temperatures and pathogens in May and June experienced by intertidal oysters could condition the metabolism and immune system of oysters thereby reducing mortalities during the July and August heatwaves (Fig. 4.1). These conditions could be simulated in a laboratory setting to reduce environmental variability, and provide evidence for the relative contribution of temperature, reproductive development, and *V. aestuarianus* in observed mortalities.

4.3 Conclusion

Historically, Quayle (1988) observed that “in British Columbia there [was] little evidence of [summer mortalities] in the Pacific oyster since it was first introduced”. This thesis provides evidence that summer mortalities of Pacific oysters are occurring in Baynes Sound, BC, and they are associated with similar characteristics that have been described in other regions of the world. I demonstrated the association of Pacific oyster mortality with elevated water temperature, increased reproductive effort, size, and the abundance of *V. aestuarianus* in Baynes Sound.

Literature Cited:

- Abi-Khalil, C., Lopez-Joven, C., Abadie, E., Savar, V., Amzil, Z., Laabir, M., Rolland, J., 2016. Exposure to the paralytic shellfish toxin producer *Alexandrium catenella* increases the susceptibility of the oyster *Crassostrea gigas* to pathogenic vibrios. *Toxins*. 8, 1-24. <https://doi.org/10.3390/toxins8010024>.
- Allen, S.K., Downing, L.E., 1986. Performance of triploid Pacific oysters, *Crassostrea gigas* (Thunberg). I. Survival, growth, glycogen content, and sexual maturation in yearlings. *J. Exp. Mar. Biol. Ecol.* 102, 197-208. [https://doi.org/10.1016/0022-0981\(86\)90176-0](https://doi.org/10.1016/0022-0981(86)90176-0).
- Allen, S.M., Burnett, L.E., 2008. The effects of intertidal air exposure on the respiratory physiology and the killing activity of hemocytes in the Pacific oyster, *Crassostrea gigas* (Thunberg). *Exp. Mar. Biol. Ecol.* 357, 165-171. <https://doi.org/10.1016/j.jembe.2008.01.013>.
- Anon., 2013. Socio-economic impact of aquaculture in Canada. Fisheries and Ocean Canada. Downloaded on March 2, 2020 from <https://www.dfo-mpo.gc.ca/aquaculture/sector-secteur/socio/index-eng.htm>.
- Anon., 2015. Oyster mortality EFSA panel on animal health and welfare (AHAW). *EFSA J.* 13, 4122. <https://doi.org/10.2903/j.efsa.2015.4122>.
- Anon., 2016a. The state of world fisheries and aquaculture. Food and Agriculture Organization of the United Nations. Downloaded on March 3, 2020 from <http://www.fao.org/publications/sofia/2016/en/>.
- Anon., 2016b. Aquaculture production quantities and values. Fisheries and Oceans Canada. Downloaded on March 2, 2020 from <http://www.dfo-mpo.gc.ca/stats/aqua/aqua16-eng.htm>.

- Anon., 2016c. Recommendations from the national working group for *Vibrio parahaemolyticus* control in BC oysters for raw consumption. British Columbia Center for Disease Control. Downloaded on March 2, 2020 from <http://www.bccdc.ca/health-info/food-your-health/fish-shellfish/vibrio>.
- Anon., 2017a. Surveillance Programs. National Aquatic Animal Health Program. Fisheries and Oceans Canada. Downloaded on March 3, 2020 from <http://www.dfo-mpo.gc.ca/science/aah-saa/surveillance-eng.html>.
- Anon., 2017b. Denman Island (#7955) 7 days tidal predictions. Fisheries and Oceans Canada. Downloaded on March 9, 2020 from <https://www.tides.gc.ca/eng/station?sid=7955>.
- Anon., 2018. FishStatJ statistics. Fisheries and Aquaculture Department, Organization of the United Nations. Downloaded on March 3, 2020 from <http://www.fao.org/fishery/statistics/en>.
- Anon., 2019a. British Columbia lightstation sea surface temperature and salinity data (Pacific), 1914-present. Government of Canada. Downloaded on March 3, 2020 from <https://open.canada.ca/data/en/dataset/719955f2-bf8e-44f7-bc26-6bd623e82884>.
- Anon., 2019b. Molluscan Broodstock Program. Oregon State University. Downloaded on March 3, 2020 from <https://marineresearch.oregonstate.edu/comes/aquaculture/molluscan-broodstock-program>.
- Anon., 2020a. QGIS geographical information system. Open source geospatial foundation project. Downloaded on March 4, 2020 from <https://www.qgis.org/>.

- Anon., 2020b. R Core Team. R: A language and environment for statistical computing. The R project for statistical computing, Vienna, Australia. Downloaded on March 3, 2020 from <https://www.r-project.org/>.
- Austin, B., Pride, A.C., Rhodie, G.A., 2003. Association of a bacteriophage with virulence in *Vibrio harveyi*. J. Fish Dis. 26, 55-58. <https://doi.org/10.1046/j.1365-2761.2003.00413.x>.
- Azéma, P., Travers, M., Benabdelmouna, A., Dégremont, L., 2016. Single or dual experimental infections with *Vibrio aestuarianus* and OsHV-1 in diploid and triploid *Crassostrea gigas* at the spat, juvenile and adult stages. J. Invertebr. Pathol. 139, 92-101. <https://doi.org/10.1016/j.jip.2016.08.002>.
- Baghurst, B.C., Mitchell, J.G., 2002. Sex-specific growth and condition of the Pacific oyster (*Crassostrea gigas* Thunberg). Aquac. Res. 33, 1253-1263.
- Baker-Austin, C., Trinanes, J., Gonzalez-Escalona, N., Martinez-Urtaza, J., 2017. Non-cholera *Vibrios*: the microbial barometer of climate change. Trends Microbiol. 25, 76-84. <https://doi.org/10.1016/j.tim.2016.09.008>.
- Baker-Austin, C., Oliver, J.D., Alam, M., Ali, A., Waldor, M.K., Qadri, F., Martinez-Urtaza, J., 2018. *Vibrio* spp. infections. Nat. Rev. Dis. Primers. 2, 1-19. <https://doi.org/10.1038/s41572-018-0005-8>.
- Barton, A., Hales, B., Waldbusser, G.G., Langdon, C., Feely, R.A., 2012. The Pacific oyster, *Crassostrea gigas*, shows negative correlation to naturally elevated carbon dioxide levels: Implications for near-term ocean acidification effects. Limnol. Oceanogr. 57, 698-710. <https://doi.org/10.4319/lo.2012.57.3.0698>.

- Bartoń, K., 2020. MuMIn: multi-model inference. Package ‘MuMIn’ for the statistical software R. Downloaded on March 3, 2020 from <https://cran.r-project.org/web/packages/MuMIn/index.html>.
- Bates, D., Maechler, M., Bolker, B., Walker, S., 2019. Fitting linear mixed-effects models using lme4. *J. Stat. Softw.* 67, 1-48. <https://doi.org/10.18637/jss.v067.i01>.
- Bayne, B., d’Auriac, M.A., Backeljau, T., Beninger, P., Boudry, P., Carnegie, R., Davis, J., Guo, X., Hedgecock, D., Krause, M., Langdon, C., Lapègue, S., Manahan, D., Mann, R., Powell, E., Shumway, S., 2019. A scientific name for Pacific oysters. *Aquaculture*. 499, 373. <https://doi.org/10.1016/j.aquaculture.2018.08.048>.
- Becker, R.A., Wilks, A.R., Brownrigg, R., Minka, T.P., Deckmyn, A., 2018a. Maps: Draw Geographical maps. Package ‘maps’ for the statistical software R. Downloaded on March 3, 2020 from <https://cran.r-project.org/web/packages/maps/index.html>.
- Becker, R.A., Wilks, A.R., Brownrigg, R., Minka, T.P., Deckmyn, A., 2018b. Mapdata: extra map databases. Downloaded on March 3, 2020 from <https://cran.r-project.org/web/packages/mapdata/index.html>.
- Bendell, L., 2019. Baynes sound; its unique nature and the need to recognize the region as a marine protected area. Chapter 4 in *Sterwarding the sound the challenge of managing sensitive coastal ecosystems*. Eds: Bendell, L., Gallagher, P., McKeachie, S., Wood, L. CRC Press Taylor and Francis Group, Boca Raton, FL. <https://doi.org/10.1201/9780429025303>.
- Boulais, M., Chenevert, K., Demey, A., Darrow, E., Robison, M., Roberts, J., Volety, A., 2017. Oyster reproduction is compromised by acidification experienced seasonally in coastal regions. *Sci. Rep.* 7, 13276. <https://doi.org/10.1038/s41598-017-13480-3>.

- Bougrier, S., Geairon, P., Deslous-Paoli, J.M., Bacher, C., Jonquière, G., 1995. Allometric relationships and effects of temperature on clearance and oxygen consumption rates of *Crassostrea gigas* (Thunberg). *Aquaculture*. 134, 143-154. [https://doi.org/10.1016/0044-8486\(95\)00036-2](https://doi.org/10.1016/0044-8486(95)00036-2).
- Bower, S.M., Hervio, D., Meyer, G.R., 1997. Infectivity of *Mikrocytos mackini*, the causative agent of Denman Island disease in Pacific oysters *Crassostrea gigas*, to various species of oysters. *Dis. Aquat. Org.* 29, 111-116. <https://doi.org/10.3354/dao029111>.
- Bower, S.M., 2017. Synopsis of infectious diseases and parasites of commercially exploited shellfish. Fisheries and Oceans Canada. Downloaded on March 3, 2020 from <http://www.dfo-mpo.gc.ca/science/aah-saa/diseases-maladies/toc-eng.html#oys>.
- Brown, B.F., 1977. The role of Vibrios as pathogens for the Pacific oyster. Doctoral Dissertation. University of Washington.
- Burge, C.A., Griffin, F.J., Friedman, C.S., 2006. Mortality and herpesvirus infections of the Pacific oyster *Crassostrea gigas* in Tomales Bay, California, USA. *Dis. Aquat. Org.* 72, 31-43. <https://doi.org/10.3354/dao072031>.
- Burge, C.A., Friedman, C.S., Getchell, R., House, M., Kafferty, K.D., Mydlarz, L.D., Prager, K.C., Sutherland, K.P., Renault, T., Kiryu, I., Vega-Thurber, R., 2016. Complementary approaches to diagnosing marine diseases: a union of the modern and the classic. *Philos. Trans. R. Soc. Lond. B. Biol. Sci.* 371, 1689. <https://doi.org/10.1098/rstb.2015.0207>.
- Cannuel, R., Beninger, P.G., 2006. Gill development, functional and evolutionary implications in the Pacific oyster *Crassostrea gigas* (Bivalvia: Ostreidae). *Mar. Biol.* 149, 547-563. <https://doi.org/10.1007/s00227-005-0228-6>.

- Cassis, D., 2005. The effect of harmful algae on the summer mortality of juvenile Pacific oysters (*Crassostrea gigas*). Master of Science Thesis. University of British Columbia.
Downloaded on March 8, 2020 from
<https://open.library.ubc.ca/cIRcle/collections/ubctheses/831/items/1.0052590>.
- Cassis, D., Pearce, C.M., Maldonado, M.T., 2011. Effects of the environment and culture depth on growth and mortality in juvenile Pacific oysters in the Strait of Georgia, British Columbia. *Aquac. Environ. Interact.* 1, 259-274. <https://doi.org/10.3354/aei00025>.
- Chávez-Villalba, J., Villelas-Ávila, R., Cáceres-Martínez, C., 2007. Reproduction, condition and mortality of the Pacific oyster *Crassostrea gigas* (Thunberg) in Sonora, México. *Aquac. Res.* 38, 268-278. <https://doi.org/10.1111/j.1365-2109.2007.01662.x>.
- Chávez-Villalba, J., Arreola-Lizárraga, A., Burrola-Sánchez, S., Hoyos-Chairez, F., 2010. Growth, condition, and survival of the Pacific oyster *Crassostrea gigas* cultivated within and outside a subtropical lagoon. *Aquaculture.* 300, 128-136.
<https://doi.org/10.1016/j.aquaculture.2010.01.012>.
- Cheney, D.P., Macdonald, B.F., Elston, R.A., 2000. Summer mortality of Pacific oysters, *Crassostrea gigas* (Thunberg): initial findings on multiple environmental stressors in Puget Sound, Washington, 1998. *J. Shellfish Res.* 19, 353-359.
[https://doi.org/10.2983/0730-8000\(2007\)26\[163:SSMOTP\]2.0.CO;2](https://doi.org/10.2983/0730-8000(2007)26[163:SSMOTP]2.0.CO;2).
- Cheslett, D., McKiernan, F., Hickey, C., Collins, E., 2009. Viral gametocytic hypertrophy of the Pacific oyster *Crassostrea gigas* in Ireland. *Dis. Aquat. Organ.* 83, 181-185.
<https://doi.org/10.3354/dao02020>.

- Choi, K., Lewis, D.H., Powell, E.N., Ray, S.M., 1993. Quantitative measurements of reproductive output in the American oyster, *Crassostrea virginica* (Gmelin), using an enzyme-linked immunosorbent assay (ELISA). *Aquac. Res.* 24, 299-322.
<https://doi.org/10.1111/j.1365-2109.1993.tb00553.x>.
- Coen, L.D., Brumbaugh, R.D., Bushek, D., Grizzle, R., Luckenbach, M.W., Posey, M.H., Powers, S.P., Tolley, S.G., 2007. Ecosystem services related to oyster restoration. *Mar. Ecol. Prog. Ser.* 341, 303-307. <https://doi.org/doi:10.3354/meps341303>.
- Colwell, R.R., Grimes, D.J., 1984. *Vibrio* diseases of marine fish populations. *Helgol. Mar. Res.* 37, 265-287. <https://doi.org/10.1007/BF01989311>.
- Cotter, E., Malham, S.K., O'Keefe, S., Lynch, S.A., Latchford, J.W., King, J.W., Beaumont, A.R., Culloty, S.C., 2010. Summer mortality of the Pacific oyster, *Crassostrea gigas*, in the Irish Sea: the influence of growth, biochemistry and gametogenesis. *Aquaculture.* 303, 8-21. <https://doi.org/10.1016/j.aquaculture.2010.02.030>.
- De Decker, S., Normand, J., Saulnier, N., Pernet, F., Castagnet, S., Boudry, P., 2011. Response of diploid and triploid Pacific oysters *Crassostrea gigas* to *Vibrio* infections in relation to their reproductive status. *J. Invertebr. Pathol.* 106, 179-191.
<https://doi.org/10.1016/j.jip.2010.09.003>.
- de Kantzow, MC., Hick, P.M., Dhand, N.K., Whittington, R.J., 2017. Risk factors for mortality during the first occurrences of Pacific oyster mortality syndrome due to *Ostreid herpesvirus – 1* in Tasmania, 2016. *Aquaculture.* 468, 328-336.
<https://doi.org/10.1016/j.aquaculture.2016.10.025>.

- de Lorgeril, J., Lucasson, A., Petton, B., Toulza, E., Montagnani, C., Clerissi, C., Vidal-Dupirol, J., Chaparro, C., Galinier, R., Escoubas, J., Haffner, P., Dégremont, L., Charrière, G.M., Lafont, M., Delort, A., Vergnes, A., Chiarello, M., Faury, N., Rubio, T., Leroy, M., Pérignon, A., Régler, D., Morga, B., Alunno-Bruscia, M., Boudry, P., Le Roux, F., Destoumieux-Garzón, D., Gueguen, Y., Mitta, G., 2018. Immune-suppression by OsHV-1 viral infection causes fatal bacteraemia in Pacific oysters. *Nat. Commun.* 9, 4215. <https://doi.org/10.1038/s41467-018-06659-3>.
- de Melo, C.M.R., Durland, E., Langdon, C., 2016. Improvements in desirable traits of the Pacific oyster, *Crassostrea gigas*, as a result of five generations of selection on the West Coast, USA. *Aquaculture*. 460, 105-115. <https://doi.org/10.1016/j.aquaculture.2016.04.017>.
- Dégremont, L., Bédier, E., Boudry, P., 2010. Summer mortality of hatchery-produced Pacific oyster spat (*Crassostrea gigas*). II. Response to selection for survival and its influence on growth and yield. *Aquaculture*. 299, 21-29. <https://doi.org/10.1016/j.aquaculture.2009.11.017>.
- Delaporte, M., Soudant, P., Lambert, C., Moal, J., Pouvreay, S., Samain, J., 2006. Impact of food availability on energy storage and defense related hemocyte parameters of the Pacific oyster *Crassostrea gigas* during an experimental reproductive cycle. *Aquaculture*. 254, 571-582. <https://doi.org/10.1016/j.aquaculture.2005.10.006>.
- Delaporte, M., Philippe, S., Lambert, C., Jegaden, M., Moal, J., Pouvreau, S., Dégremont, L., Boudry, P., Samain, J., 2007. Characterisation of physiological and immunological differences between Pacific oysters (*Crassostrea gigas*) genetically selected for high or low survival to summer mortalities and fed different rations under controlled conditions. *J. Exp. Mar. Biol. Ecol.* 353, 45-57. <https://doi.org/10.1016/j.jembe.2007.09.003>.

- Dixon, P., 2003. VEGAN, a package of R functions for community ecology. *J. Veg. Sci.* 14, 927-930. <https://doi.org/10.1111/j.1654-1103.2003.tb02228.x>.
- Dowle, M., Srinivasan, A., 2019. Package 'data.table'. Downloaded on March 2, 2020 from <https://rdatatable.gitlab.io/data.table/>.
- Dubert, J., Barja, J.L., Romalde, J.L., 2017. New insights into pathogenic Vibrios affecting bivalves in hatcheries: present and future prospects. *Front. Microbiol.* 8, 762. <https://doi.org/10.3389/fmicb.2017.00762>.
- Dunnington, D., 2017. Prettymapr: scale bar, north arrow, and pretty margins in R. Package 'prettymapr' for the statistical software R. Downloaded on March 3, 2020 from <https://cran.r-project.org/web/packages/prettymapr/index.html>.
- Dupuy, C., Vaquer, A., Lam-Höai, T., Rougier, C., Mazouni, N., Lautier, J., Collos, Y., Le Gall, S., 2000. Feeding rate of the oyster *Crassostrea gigas* in a natural planktonic community of the Mediterranean Thau Lagoon. *Mar. Ecol. Prog. Ser.* 250, 171-184. <https://doi.org/10.3354/meps205171>.
- Elston, R.A., Beattie, J.H., Friedman, C., Hedrick, R., Kent, M.L., 1987. Pathology and significance of fatal inflammatory bacteraemia in the Pacific oyster, *Crassostrea gigas* Thünberg. 10, 121-132. *J. Fish Dis.* <https://doi.org/10.1111/j.1365-2761.1987.tb00727.x>.
- Emmet, B., 2002. Activities and potential environmental effects associated with shellfish aquaculture in Baynes Sound. Government of British Columbia. Archipelago Marine Research LTD. 525 Head St. Victoria British Columbia. Downloaded on March 3, 2020 from https://www2.gov.bc.ca/assets/gov/farming-natural-resources-and-industry/natural-resource-use/land-water-use/crown-land/land-use-plans-and-objectives/coastal-marine/baynes-sound-coastal-plan/activity_review.pdf.

- Enríquez-Díaz, M., Pouvreau, S., Chávez-Villalba, J., Le Pennec, M., 2009. Gametogenesis, reproductive investment, and spawning behaviour of the Pacific giant oyster *Crassostrea gigas*: evidence of an environment-dependent strategy. *Aquac. Int.* 17, 491-506.
<https://doi.org/10.1007/s10499-008-9219-1>.
- Evans, W., Pocock, K., Hare, A., Weekes, C., Hales, B., Jackson, J., Gurney-Smith, H., Mathis, J.T., Alin, S.R., Feely, R.F., 2019. Marine CO₂ patterns in the northern Salish Sea. *Front. Mar. Sci.* 5, 536. <https://doi.org/10.3389/fmars.2018.00536>.
- Fisher, M.A., Güllert, S., Neulinger, S.C., Streit, W.R., Schmitz, R.A., 2016. Evaluation of 16S rRNA gene primer pairs for monitoring microbial community structures showed high reproducibility within and low comparability between datasets generated with multiple archaeal and bacterial primer pairs. *Front. Microbiol.* 7, 1297.
<https://doi.org/10.3389/fmicb.2016.01297>.
- Flachowsky, G., Meyer, U., Südekum, K., 2017. Land use for edible protein of animal origin – a review. *Animals.* 7, 1-19. <https://doi.org/10.3390/ani7030025>.
- Friedman, C.S., Beattie, J.H., Elston, R.A., Hendrick, R.P., 1991. Investigation of the relationship between the presence of a Gram-positive bacterial infection and summer mortality of the Pacific oyster, *Crassostrea Gigas* Thunberg. *Aquaculture.* 94, 1-15.
[https://doi.org/10.1016/0044-8486\(91\)90124-P](https://doi.org/10.1016/0044-8486(91)90124-P).
- Friedman, C.S., Hendrick, R.P., 1991. Pacific oyster nocardiosis: isolation of the bacterium and induction of laboratory infections. *J. Invertebr. Pathol.* 57, 109-120.
[https://doi.org/10.1016/0022-2011\(91\)90047-T](https://doi.org/10.1016/0022-2011(91)90047-T).

- Friedman, C.S., Beaman, Blaine.L., Chun, J., Goodfellow, M., Gee, A., Hedrick, R.P., 1998. *Nocardia crassostreae* sp. nov., the causal agent of nocardiosis in Pacific oysters. Int. J. Syst. Bact. 48, 237-246. <https://doi.org/10.1099/00207713-48-1-237>.
- Galstoff, P.S., 1964. Morphology and structure of shell. Chapter 2 in The American Oyster *Crassostrea virginica* Gmelin. Fishery Bulletin, 64, 2. Downloaded on March 4, 2020 from <https://www.nefsc.noaa.gov/publications/classics/galtsoff1964/galtsoff1964.pdf>.
- Garcia, C., Robert, M., Arzul, I., Chollet, B., Joly, J., Miossec, L., Comtet, T., Berthe, F., 2006. Viral gametocytic hypertrophy of *Crassostrea gigas* in France: from occasional records to disease emergence? Dis. Aquat. Organ. 70, 193-199. <https://doi.org/10.3354/dao070193>.
- Garcia, S.M., Rosenberg, A.A., 2010. Food security and marine capture fisheries: characteristics, trends, drivers, and future perspectives. Phil. Trans. R. Soc. B. 365, 2869-2880. <https://doi.org/10.1098/rstb.2010.0171>.
- Garnier, M., Labreuche, Y., Garcia, C., Robert, M., Nicolas, J.L., 2007. Evidence for the involvement of pathogenic bacteria in summer mortality of Pacific oyster *Crassostrea gigas*. Microb. Ecol. 53, 187-196. <https://doi.org/10.1007/s00248-006-9061-9>.
- Garnier, M., Labreuche, Y., Nicolas, J., 2008. Molecular and phenotypic characterization of *Vibrio aestuarianus* subsp *francensis* subsp. nov., a pathogen of the oyster *Crassostrea gigas*. Syst. Appl. Microbiol. 31, 358-365. <https://doi.org/10.1016/j.syapm.2008.06.003>.
- Gazeau, F., Quiblier, C., Jansen, J.M., Gattuso, J.P., Middelburg, J.J., Heip, C.H., 2007. Impact of elevated CO₂ on shellfish calcification. Geophys. Res. Lett. 34, L07603. <https://doi.org/10.1029/2006GL028554>.

- Gillespie, G., Bower, S., Marcus, K., Kiese, D., 2012. Biological synopsis for three exotic mollusks, manila clam (*Venerupis philippinarum*), Pacific oysters (*Crassostrea gigas*) and Japanese Scallop (*Mizuhopecten vessoensis*) licensed for aquaculture in British Columbia. DFO. Can. Sci. Advis. Sec. Res. Doc. 2012/2013. Downloaded on March 3, 2020 from <http://publications.gc.ca/pub?id=9.575685&sl=1>.
- Go, J., Deutscher, A., Spiers, Z., Dahle, K., Kirkland, P., Jenkins, C., 2017. Mass mortalities of unknown aetiology in Pacific oysters *Crassostrea gigas* in Port Stephens, New South Wales, Australia. Dis. Aquat. Organ. 125, 227-242. <https://doi.org/10.3354/dao03146>.
- Godfray, H., Beddington, J., Crute, I., Haddad, L., Lawrence, D., Muir, J., Pretty, J., Robinson, S., Thomas, S., Toulmin, C., 2010. Food security: the challenge of feeding 9 billion people. Food. Sec. 327, 812-818. <https://doi.org/10.1126/science.1185383>.
- Gouletquer, P., Soletchnik, P., Le Moine, D., Razet, D., Geairon, P., Faury, N., Taillade, S., 1998. Summer mortality of the Pacific cupped oyster *Crassostrea gigas* in the Bay of Marennes-Oléron (France). ICES Statutory Meeting. IFREMER shellfish aquaculture laboratory of Poitou-Charentes. Downloaded on March 3, 2020 from <http://citeseerx.ist.psu.edu/viewdoc/download?doi=10.1.1.334.3103&rep=rep1&type=pdf>.
- Green, T.J., Siboni, N., King, W.L., Labbate, M., Seymour, J.R., Raftos, D., 2019. Simulated marine heat wave alters abundance and structure of *Vibrio* populations associated with the Pacific oyster resulting in a mass mortality event. Microb. Ecol. 77, 736-747. <https://doi.org/10.1007/s00248-018-1242-9>.

- Guo, X., Hedgecock, D., Hershberger, W.K., Cooper, K., Allen, S.K., 1998. Genetic determinants of protandric sex in the Pacific oyster, *Crassostrea gigas* Thunberg. *Evolution*. 52, 394-402. <https://doi.org/10.1111/j.1558-5646.1998.tb01640.x>.
- Hales, B., Chipman, D., Takahashi, T., 2004. High-frequency measurement of partial pressure and total concentration of carbon dioxide in seawater using microporous hydrophobic membrane contactors. *Limnol. Oceanogr. Methods*. 2, 356-364. <https://doi.org/10.4319/lom.2004.2.356>.
- Hall, T., 2005. BioEdit: Biological sequence alignment editor for windows 95/98/NT/XO. Downloaded on March 3, 2020 from <http://www.oalib.com/references/5555736>.
- Hasle, G.R., 1978. Identification problems. General recommendations. In: Sournia, A. (Ed.), *Phyto-plankton manual. Monographs on oceanographic methodology*. UNESCO Publishing. 6, 135-128. Downloaded on March 3, 2020 from <https://unesdoc.unesco.org/ark:/48223/pf0000030788>.
- Hobday, A.J., Alexander, L.V., Perkins, S.E., Smale, D.A., Straub, S.C., Oliver, E.C.J., Benthuisen, J.A., Burrows, M.T., Donat, M.G., Feng, M., Holbrook, N.J., Moore, P.J., Scannell, H.A., Gupta, A.S., Wernberg, T., 2016. A hierarchical approach to defining marine heatwaves. *Prog. Oceanogr.* 141, 227-238. <https://doi.org/10.1016/j.pocean.2015.12.014>.
- Horner, R.A., 2002. A taxonomic guide to some common phytoplankton. *Harmful Algae*. 2, 161-162. [https://doi.org/10.1016/S1568-9883\(03\)00024-6](https://doi.org/10.1016/S1568-9883(03)00024-6).

- Houssin, M., Trancart, S., Denechere, L., Oden, E., Adeline, B., Lepoitevin, M., Pitel, P., 2019. Abnormal mortality of triploid adult Pacific oysters: Is there a correlation with high gametogenesis in Normandy, France? *Aquaculture*. 505, 63-71. <https://doi.org/10.1016/j.aquaculture.2019.02.043>.
- Howard, D.W., Lewis, E.J., Keller, B.J., Smith, C.S., 2004. Histological techniques for marine bivalve molluscs and crustaceans. NOAA Technical Memorandum NOS NCCOS. 5, 218. Downloaded on March 3, 2020 from <https://nefsc.noaa.gov/nefsc/publications/tm/pdfs/tmfnc25.pdf>.
- Huvet, A., Normand, J., Fleury, E., Quillen, V., Fabioux, C., Bourdy, P., 2010. Reproductive effort of Pacific oysters: a trait associated with susceptibility to summer mortality. *Aquaculture*. 304, 95-99. <https://doi.org/10.1016/j.aquaculture.2010.03.022>.
- Imai, T., Kenichi, N., Juichi, O., Shigeru, S., 1965. The search for the cause of mass mortality and the possibility of its prevention by transplantation experiments. The bulletin Tohokoku Regional Fisheries Research Laboratory. 25, 27-38.
- Jenkins, C., Hick, P., Gabor, M., Spiers, Z., Fell, S.A., Gu, X., Read, A., Go, J., Dove, M., O'Connor, W., Kirkland, P.D., Frances, J., 2013. Identification and characterisation of an ostreid herpesvirus-1 microvariant (OsHV-1 μ -var) in *Crassostrea gigas* (Pacific oysters) in Australia. *Dis. Aquat. Org.* 105, 109-126. <https://doi.org/10.3354/dao02623>.
- Jesser, K.J., Noble, R.T., 2018. *Vibrio* ecology in the Neuse River estuary, North Carolina characterized by next-generation amplicon sequencing of the gene encoding heat shock protein 60 (*hsp60*). *Appl. Environ. Microbiol.* 18, e00333-18. <https://doi.org/10.1016/10.1128/AEM.00333-18>.

- Jeung, H., Keshavmurthy, S., Lim, H., Kim, S., Choi, K., 2016. Quantification of reproductive effort of the triploid Pacific oyster, *Crassostrea gigas* raised in intertidal rack and bag oyster culture system off the west coast of Korea during spawning season. *Aquaculture*. 464, 374-380. <https://doi.org/10.1016/j.aquaculture.2016.07.010>.
- Joseph, S.W., Colwell, R.R., Kaper, J.B., 1982. *Vibrio parahaemolyticus* and related halophilic vibrios. *Crit. Rev. Microbiol.* 10, 77-124. <https://doi.org/10.3109/10408418209113506>.
- Kamada, N., Chen, G.Y., Inohara, N., Núñez, G., 2013. Control of pathogens and pathobionts by the gut microbiota. *Nat. Immunol.* 14, 685-690. <https://doi.org/doi:10.1038/ni.2608>.
- Katkansky, S.C., Warner, R.W., 1974. Pacific oyster disease and mortality studies in California. California Department of Fish and Game. Marine Resources Technical Report No. 25. Downloaded on March 3, 2020 from http://aquaticcommons.org/678/1/Technical_Report_1974_No._25_A.pdf.
- Kelly, M.T., Stroh, E.M., 1989. Urease-positive, kanagawa-negative *Vibrio parahaemolyticus* from patients and the environment in the Pacific Northwest. *J. Clin. Microbiol.* 27, 2820-2822. Downloaded on March 3, 2020 from <https://jcm.asm.org/content/27/12/2820>.
- Keppler, C.J., Hogue, J., Smith, K., Ringwood, A.H., Lewitus, A.J., 2005. Sublethal effects of the toxic alga *Heterosigma akashiwo* on the southeastern oyster (*Crassostrea virginica*). *Harmful Algae.* 4, 275-285. <https://doi.org/10.1016/j.hal.2004.05.002>.
- Kimes, N.E., Grim, C.J., Johnson, W.R., Hasan, N.A., Tall, B.D., Kothary, M.H., Kiss, H., Munk, A.C., Tapia, R., Green, L., Detter, C., Bruce, D.C., Brettin, T.S., Colwell, R.R., Morris, P.J., 2012. Temperature regulation of virulence factors in the pathogen *Vibrio coralliityicus*. *ISME. J.* 6, 835-846. <https://doi.org/10.1038/ismej.2011.154>.

- King, W.L., Jenkins, C., Go, J., Siboni, N., Seymour, J.R., Labbate, M., 2019a. Characterisation of the Pacific oyster microbiome during a summer mortality event. *Microbiol. Ecol.* 77, 502-512. <https://doi.org/10.1007/s00248-018-1226-9>.
- King, W.L., Siboni, N., Kahle, T., Green, T.J., Labbate, M., Seymour, J.R., 2019b. A new high throughput sequencing assay for characterizing the diversity of natural *Vibrio* communities and its application to a Pacific oyster mortality event. *Front. Microbiol.* 10, 2907. <https://doi.org/10.3389/fmicb.2019.02907>.
- King, W.L., Siboni, N., Williams, N.L., Kahlke, T., Nguyen, K.V., Jenkins, C., Dove, M., O'Connor, W., Seymour, J.R., Labbate, M., 2019c. Variability in the composition of Pacific oyster microbiomes across oyster families exhibiting different levels of susceptibility to OsHV-1 μ var disease. *Front. Microbiol.* 10, 473. <https://doi.org/10.3389/fmicb.2019.00473>.
- Kormas, K.A., Interpreting diversity of proteobacteria based on the 16S rRNA gene copy number. 2011. In *Proteoabacteria: phylogeny, metabolic diversity and ecological effects*. Ed, Sezenna, M.L. Nova Publishers, Hauppauge, NY, USA. ISBN: 978-1-61761-810-9. Downloaded on March 3, 2020 from <http://kkormas.users.uth.gr/kormas2011proteobacteria.pdf>.
- Kumar, S., Stecher, G., Tamura, K., 2015. MEGA7: molecular evolutionary genetics analysis version 7.0. *Mol. Biol. Evol.* 33, 1870-4. <https://doi.org/10.1093/molbev/msw054>.
- Labreuche, Y., Lamber, C., Soudant, P., Boulo, V., Huvet, A., Nicolas, J.L., 2006a. Cellular and molecular hemocyte responses of the Pacific oyster, *Crassostrea gigas*, following bacterial infection with *Vibrio aestuarianus* strain 01/32. *Microbes Infect.* 8, 2715-2724. <https://doi.org/10.1016/j.micinf.2006.07.020>.

- Labreuche, Y., Soudant, P., Goncalves, M., Lambert, C., Nicolas, J.L., 2006b. Effects of extracellular products from the pathogenic *Vibrio aestuarianus* strain 01/32 on lethality and cellular immune responses of the oyster *Crassostrea gigas*. *Dev. Comp. Immunol.* 30, 367-379. <https://doi.org/10.1016/j.dci.2005.05.003>.
- Labreuche, Y., Le Roux, F., Henry, J., Zatylny, C., Huvet, A., Lambert, C., Soudant, P., Mazel, D., Nicolas, J.L., 2010. *Vibrio aestuarianus* zinc metalloprotease causes lethality in the Pacific oyster *Crassostrea gigas* and impairs the host cellular immune defenses. *Fish Shellfish Immunol.* 29, 753-758. <https://doi.org/10.1016/j.fsi.2010.07.007>.
- Lacoste, A., Jalabert, F., Malham, S., Cueff, A., Gélébart, F., Cordevant, C., Lange, M., Poulet, S.A., 2001. A *Vibrio splendidus* strain is associated with summer mortality of juvenile oysters *Crassostrea gigas* in the Bay of Morlaix. *Dis. Aquat. Organ.* 46, 139-145. <https://doi.org/10.3354/dao046139>.
- Lango-Reynoso, F., Chávez-Villaba, J., Le Penec, M., 2006. Reproductive patterns of the Pacific oyster *Crassostrea gigas* in France. *Invertebr. Reprod. Dev.* 49, 41-50. <https://doi.org/10.1080/07924259.2006.9652192>.
- Lemasson, A.J., Fletcher, S., Hall-Spencer, J.M., Knights, A.M., 2017. Linking the biological impacts of ocean acidification on oysters to changes in ecosystem services: A review. *J. Exp. Mar. Bio. Ecol.* 492, 49-62. <https://doi.org/10.1016/j.jembe.2017.01.019>.
- Le Moullac, G., Quéau, I., Le Souchu, P., Pouvreau, S., Moal, J., Le Coz, J.R., Samain, J.F., 2007. Metabolic adjustments in the oysters *Crassostrea gigas* according to oxygen level and temperature. *Mar. Biol. Res.* 3, 357-366. <https://doi.org/10.1080/17451000701635128>.

- Lenth, R., Signmann, H., Love, J., Buerkner, P., Herve, M., 2020. Estimated marginal means, aka least-squares means. Package ‘emmeans’ for the statistical software R. Downloaded on March 3, 2020 from <https://github.com/rvlenth/emmeans>.
- Li, Y., Qin, J.G., Abbott, C.A., Li, X., Benkendorff, K., 2007. Synergistic impacts of heat shock and spawning on the physiology and immune health of *Crassostrea gigas*: an explanation for summer mortality in Pacific oysters. *Phys. Reg. Integr. Comp. Physiol.* 293, 2353-2362. <https://doi.org/10.1152/ajpregu.00463.2007>.
- Li, L., Li, A., Song, K., Meng, J., Guo, X., Li, S., Li, C., Wit, P.D., Que, H., Wu, F., Wang, W., Qi, H., Xu, F., Cong, R., Huang, B., Li, Y., Wang, T., Tang, X., Liu, S., Li, B., Shi, R., Liu, Y., Bu, C., Zhang, C., He, W., Zhao, S., Li, H., Zhang, S., Zhang, L., Zhang, G., 2018. Divergence and plasticity shape adaptive potential of the Pacific oyster. *Nat. Ecol. Evol.* 2, 1751-1760. <https://doi.org/10.1038/s41559-018-0668-2>.
- Lipovsky, V.P., Chew, K.K., 1972. Mortality of Pacific oysters (*Crassostrea gigas*): the influence of temperature and enriched seawater on survival. *Proc. Nat. Shellfish. Ass.*, 62, 72-82. Downloaded on March 2, 2020 from <https://www.biodiversitylibrary.org/page/2164272#page/84/mode/1up>.
- Lokmer, A., Wegner, K.M., 2015. Hemolymph microbiome of Pacific oysters in response to temperature, temperature stress and infection. *ISME. J.* 9, 670-682. <https://doi.org/10.1038/ismej.2014.160>.
- Malham, S.K., Cotter, E., O’Keeffe, S., Lynch, S., Culloty, S.C., King, J.W., Latchford, J.W., Beaumont, A.R., 2009. Summer mortality of Pacific oyster, *Crassostrea gigas*, in the Irish Sea: the influence of temperature and nutrients on health and survival. *Aquaculture.* 287, 128-138. <https://doi.org/10.1016/j.aquaculture.2008.10.006>.

- Mat, A., Klopp, C., Payton, L., Jaziorski, C., Chalopin, M., Amzil, Z., Tran, D., Wikfors, G., Hégaret, H., Soudant, P., Huvet, A., Fabioux, C., 2018. Oyster transcriptome response to *Alexandrium* exposure is related to saxitoxin load and characterized by disrupted digestion, energy balance, and calcium and sodium signaling. *Aquat. Toxicol.* 199, 127-137. <https://doi.org/10.1016/j.aquatox.2018.03.030>.
- Meyer, G., 2013. Summary of 2013 diagnostic test results and investigation of mortalities in Pacific oysters from Redonda Bay (Deer Passage, NW Redonda Island). Fisheries and Oceans Canada.
- Moore-Maley, B., Ianson, D., Allen, S., 2017. Wind-driven upwelling and seawater chemistry in British Columbia's shellfish aquaculture capital. Canadian Meteorological and Oceanographic Society. Downloaded on June 6, 2020 from <https://bulletin.cmos.ca/upwelling-seawater-chemistry-bc-shellfish-aquaculture/>.
- Morrison, D.B., Saksida, S., 2013. Trends in antimicrobial use in Marine Harvest Canada farmed salmon production in British Columbia (2003-2011). *Can. Vet. J.* 54, 1160-1163. Downloaded on June 2, 2020 from <https://pubmed.ncbi.nlm.nih.gov/24293677/>.
- Mroch, R.M., Eggleston, D.B., Puckett, B.J., 2012. Spatiotemporal variation in oyster fecundity and reproductive output in a network of no-take reserves. *J. Shellfish. Res.* 31, 1091-1101. <https://doi.org/10.2983/035.031.0420>.
- Ochman, H., Willson, A.C., 1987. Evolution in bacteria: evidence for universal substitution rate in cellular genomes. *J. Mol. Evol.* 26, 74-86. <https://doi.org/10.1007/BF02111283>.
- Palmer, J.M., Jusino, M.A., Banik, M.T., Lindner, D.L., 2018. Non-biological synthetic spike-in controls and the AMPtk software pipeline improve mycogionome data. *PeerJ.* 6, e4925. <http://dx.doi.org/10.7717/peerj.4925>.

- Parizadeh, L., Tourbiez, D., Garcia, C., Haffner, P., Dégremont, L., Le Roux, F., Tavers, M., 2018. Ecologically realistic model of infection for exploring the host damage caused by *Vibrio aestuarianus*. *Environ. Microbiol.* 20, 4343-4355. <https://doi.org/10.1111/1462-2920.14350>.
- Patrick, S., Faury, N., Gouletquer, P., 2006. Seasonal changes in carbohydrate metabolism and its relationship with summer mortality of Pacific oyster *Crassostrea gigas* (Thunberg) in Marennes–Oléron bay (France). *Aquaculture.* 252, 328-338. <https://doi.org/10.1016/j.aquaculture.2005.07.008>.
- Pauley, G., Raay, B., Troutt, D., 1988. Species profiles: life histories and environmental requirements of coastal fishes and invertebrates (Pacific Northwest) – Pacific oyster. U.S. Fish wildlife biological report. U.S. Army Corps of Engineers. 82, 11-82. Downloaded on March 3, 2020 from <https://apps.dtic.mil/dtic/tr/fulltext/u2/a203409.pdf>.
- Pauly, D., Christensen, V., Guénette, S., Pitcher, T.J., Sumaila, U.R., Walter, C.J., Watson, R., Zeller, D., 2002. Towards sustainability in world fisheries. *Nature.* 418, 689-695. <https://doi.org/10.1038/nature01017>.
- Pazos, A.J., Ventoso, P., Martínez-Escauriaza, R., Pérez-Parallé, M., Blanco, J., Triviño, J.C., Sánchez, J.L., 2017. Transcriptional response after exposure to domoic acid-producing *Pseudo-nitzschia* in the digestive gland of the mussel *Mytilus galloprovincialis*. *Toxicon.* 140, 60 -71. <https://doi.org/10.1016/j.toxicon.2017.10.002>.
- Percival, S., Williams, D., 2014. *Vibrio*. Chapter 12 in *Microbiology of Waterborne Diseases: Microbiological Aspects and Risks*. Eds, Percival, S.L., Williams, D.W., Gray, N.F., Yates, M.V., Chalmers, R.M. Elsevier Sciences & Technology. <https://doi.org/10.1016/C2010-0-67101-X>.

- Perdue, J.A., Beattie, J.H., Chew, K.K., 1981. Relationships between gametogenic cycle and summer mortality phenomenon in the Pacific oyster (*Crassostrea gigas*) in Washington state. J. Shellfish Res. 1, 9-16. Downloaded on March 4, 2020 from <https://www.biodiversitylibrary.org/page/2156379#page/15/mode/1up>.
- Perdue, J.A., 1983. The relationship between the gametogenic cycle of the Pacific oyster, *C. gigas*, and the summer mortality phenomenon in strains of selectively bred oysters. Doctoral Dissertation. University of Washington.
- Quayle, D., 1988. Pacific oyster culture in British Columbia. Department of Fisheries and Oceans – Canadian Bulletin of Fisheries and Aquatic Sciences. 218. Downloaded on March 4, 2020 from <https://waves-vagues.dfo-mpo.gc.ca/Library/109165.pdf>.
- Renault, T., Ford, S., Samain, J.F., 2005. Information on the distribution, causes and significance of the summer mortality syndrome in the Pacific oyster (*Crassostrea gigas*) and in other bivalve species. ICES working group on pathology and diseases of marine organisms (WGPDMO) and ACME deliberations. WGPDMO Report, annex 6. Downloaded on March 4, 2020 from <http://www.ices.dk/sites/pub/Publication%20Reports/Advice/2005/may/Summer%20Mortality%20syndrome.pdf>.
- Royer, J., Segueineau, C., Park, K., Pouvreau, S., Choi, K., Costil, K., 2008. Gameteogenic cycle and reproductive effort assessed by two methods in 3 age classes of Pacific oysters, *Crassostrea gigas*, reared in Normandy. Aquaculture. 277, 313-320. <https://doi.org/10.1016/j.aquaculture.2008.02.033>.

- Salvi, D., Macali, A., Mariottini, P., 2014. Molecular phylogenetics and systematics of the bivalve family ostreidae based on rRNA sequence-structure models and multilocus species tree. PLoS one. 9, e116014. <https://doi.org/10.1371/journal.pone.0116014>.
- Samain, J.F., Dégremont, L., Soletchnik, P., Haure, J., Bédier, E., Ropert, M., Moal, J., Huvet, A., Bacca, H., Van Wormhoudt, A., Delaport, M., Costil, K., Pouvreau, S., Lambert, C., Boulo, V., Soudant, P., Nicolas, J.L., Le Roux, F., Renault, T., Gagnaire, B., Geret, F., Boutet, I., Burgeot, T., Boudry, P., 2007. Genetically based resistance to summer mortality in Pacific oyster (*Crassostrea gigas*) and its relationship with physiological, immunological characteristics and infection processes. Aquaculture. 268, 227-243. <https://doi.org/10.1016/j.aquaculture.2007.04.044>.
- Saulnier, D., De Decker, S., Tourbiez, D., Travers, M.A., 2017. Development of duplex Taqman real-time PCR assay for rapid identification of *Vibrio splendidus*-related and *V. aestuarianus* strains from bacterial cultures. J. Microbiol. Methods. 140, 67-69. <https://doi.org/10.1016/j.mimet.2017.07.002>.
- Schneider, C.A., Rasband, W.S., Eliceiri, K.W., 2012. NIH image to ImageJ: 25 years of image analysis. Nat. Methods. 9, 671-675. <https://doi.org/10.1038/nmeth.2089>
- Schnute, J.T., Boers, N., Haigh, R., Couture-Beil, A., Chabot, D., Grandin, C., Johnson, A., Wessel, P., Antonio, F., Lewin-Koh, N.J., Bivand, R., 2019. PBSmapping: mapping fisheries data and spatial analysis tools. Package ‘PBSmapping’ for the statistical software R. Downloaded on March 3, 2020 from <https://cran.r-project.org/web/packages/PBSmapping/index.html>.

- Shamseldin, A., Clegg, J., Friedman, C., Cherr, G., Pillai, M., 1997. Induced thermotolerance in the Pacific oyster *C. gigas*. *J. Shellfish Res.* 16, 487-91 Downloaded on March 4, 2020 from <http://hdl.handle.net/10211.1/812>.
- Shumway, S., Davis, C., Downey, R., Karney, R., Karney, R., Kraeuter, J., Parsons, J., Rheault, R., Wikfors, G., 2003. Shellfish aquaculture – in praise of sustainable economies and environments. *World Aquaculture.* 34, 15-17. AGR: IND43645777.
- Smith, M., Roheim, C., Crowder, L., Halpern, B., Turnipseed, M., Anderson, J., Asche, F., Bourillón, L., Guttormsen, A., Khan, A., Liguori, L., McNevin, A., O'Connor, M., Squires, D., Tyedmers, P., Brownstein, C., Carden, K., Klinger, D., Sagarin, R., Selkoe, K., 2010. Sustainability and global seafood. *Science.* 327, 784-786.
<https://doi.org/10.1126/science.1185345>.
- Solomieu, V.B., Renault, T., Travers, M., 2015. Mass mortality in bivalves and the intricate case of the Pacific oyster, *Crassostrea gigas*. *J. Invertebr. Pathol.* 131, 2-10.
<https://doi.org/10.1016/j.jip.2015.07.011>.
- Steele, S., Mulcahy, M., 1999. Gametogenesis of the oyster *Crassostrea gigas* in southern Ireland. *J. Mar. Biol. Ass. U.K.* 79, 673-686.
<https://doi.org/10.1017/S0025315498000836>.
- Stenzel, H.B., 1963. Aragonite and calcite as constituents of adult oyster shells. *Science.* 142, 232-233. <https://doi.org/10.1126/science.142.3589.232>.
- Strand, Å., Lindegarh, S., 2014. Japanska ostron i svenska vatten. Report from Vattenbrukscentrum Väst at the University of Göteborgs. Downloaded on March 3, 2020 from https://swemarc.gu.se/digitalAssets/1492/1492246_japanska-ostron-i-svenska-vatten.pdf.

- Suquet, M., Malo, F., Quere, C., Ledu, C., Le Grand, J., Benabdelmouna, A., 2016. Gamete quality in triploid Pacific oyster (*Crassostrea gigas*). *Aquaculture*. 451, 11-15.
<https://doi.org/10.1016/j.aquaculture.2015.08.032>.
- Sussarellu, R., Dudognon, T., Fabious, C., Soudant, P., Moraga, D., Kraffe, E., 2013. Rapid mitochondrial adjustments in response to short-term hypoxia and re-oxygenation in the Pacific oyster, *Crassostrea gigas*. *J. Exp. Biol.* 216, 1561-1569.
<https://doi.org/10.1242/jeb.075879>.
- Thompson, F., Gevers, D., Thompson, C., Dawyndt, P., Naser, S., Hoste, B., Munn, C., Swings, J., 2005. Phylogeny and molecular identification of *Vibrios* on the basis of multilocus sequence analysis. *Appl. Envir. Microbiol.* 71, 5107-5115.
<https://doi.org/10.1128/AEM.71.9.5107-5115.2005>.
- Tison, D.L., Seidler, R.J., 1983. *Vibrio aestuarianus*: a new species isolated from estuarine waters and shellfish. *Int. J. Syst. Bacteriol.* 33, 699-702.
<https://doi.org/10.1099/00207713-33-4-699>.
- Travers, M., Miller, K.B., Roque, A., Friedman, C., 2015. Bacteria disease in marine bivalves. *J. Invertebr. Pathol.* 131, 11-31. <https://doi.org/10.1016/j.jip.2015.07.010>.
- Troost, K., 2010. Causes and effects of a highly successful marine invasion: case-study of the introduced Pacific oyster *Crassostrea gigas* in continental NW European estuaries. *J. Sea Res.* 64, 145-165. <https://doi.org/10.1016/j.seares.2010.02.004>.
- Van Heuven, S., Pierrot, D., Rae, J.W.B., Lewis, E., Wallace, D.W.R., 2011. MATLAB program developed for CO₂ system calculations. In ORNL/CDIAC-105b, ed. Published by Carbon Dioxide Information Analysis Center Department of Energy, Oak Ridge, Tennessee, USA.

- Vezzulli, L., Grande, C., Reid, P.C., Hélaouët, P., Edwards, M., Höfle, M.G., Brettar, I., Colwell, R.R., Pruzzo, C., 2016. Climate influence on *Vibrio* and associated human diseases during the past half-century in the coastal North Atlantic. PNAS. 113, 62-71
<https://doi.org/10.1073/pnas.1609157113>.
- Wadsworth, P.C., 2018. Comparing triploid and diploid growth and mortality in farmed, *Crassostrea virginica*, in the northern Gulf of Mexico. Master of Science Thesis. Auburn University, AL, USA. Downloaded on March 4, 2020 from
https://etd.auburn.edu/bitstream/handle/10415/6074/Wadsworth_Pandora_MSthesis2018.pdf?sequence=2&isAllowed=y.
- Waldbusser, G.G., Hales, B., Langdon, C., Haley, B., Schrader, P., Brunner, E., Gray, M., Miller, C., Gimenez, I., 2014. Saturation-state sensitivity of marine bivalve larvae to ocean acidification. Nat. Clim. Chang. 5, 273-280. <https://doi.org/10.1038/nclimate2479>.
- Waldbusser, G.G., Hales, B., Haley, B.A., 2016. Calcium carbonate saturation state: on myths and this or that stories. ICES J. Mar. Sci. 73, 563-568.
<https://doi.org/10.1093/icesjms/fsv174>.
- Watermann, B.T., Herlyn, M., Daehne, B., Bergmann, S., Meemken, M., Kolodzey, H., 2008. Pathology and mass mortality of Pacific oysters, *Crassostrea gigas* (Thunberg), in 2005 at the East Frisian coast, Germany. J. Fish Dis. 31, 621-630.
<https://doi.org/10.1111/j.1365-2761.2008.00953.x>.
- Wendling, C., Wegner, K., 2013. Relative contribution of reproductive investment, thermal stress and *Vibrio* infection to summer mortality phenomena in Pacific oysters. Aquaculture. 412, 88-96. <https://doi.org/10.1016/j.aquaculture.2013.07.009>.

- Wendling, C.C., Batista, F.M., Wegner, K.M., 2014. Persistence, seasonal dynamics and pathogenic potential of *Vibrio* communities from Pacific oyster hemolymph. PLoS one. 9.4:1-12. <https://doi.org/10.1371/journal.pone.0094256>.
- Wendling, C.C., Wegner, K.M., 2015. Adaptation to enemy shifts: rapid resistance evolution to local *Vibrio* spp. In invasive Pacific oysters. Proc. R. Soc. B. 282: 20142244. <https://doi.org/10.1098/rspb.2014.2244>.
- Whittington, R., Hick, P., Evans, O., Rubio, A., Dhand, N., Paul-Pont, I., 2016. Pacific oyster mortality syndrome: a marine herpesvirus active in Australia. Microbiol. Australia. 126-128. <https://doi.org/10.1071/MA16043>.
- Wickham, H., ggplot2: Elegant Graphics for Data Analysis. Springer-Verlag New York, 2016. Downloaded on March 3, 2020 from <https://ggplot2.tidyverse.org/>.
- Yang, B., Wang, Y., Qian, P., 2016. Sensitivity and correlation of hypervariable regions in 16S rRNA genes in phylogenetic analysis. BMC Bioinformatics. 17, 135. <https://doi.org/10.1186/s12859-016-0992-y>.
- Zhang, N., Xu, F., Guo, X., 2014. Genomic analysis of the Pacific oyster (*Crassostrea gigas*) reveals possible conservation of vertebrate sex determination in a mollusk. G3 (Bethesda). 4, 2207-2217. <https://doi.org/10.1534/g3.114.013904>.
- Zhang, G., Li, L., Meng, J., Qi, H., Qu, T., Xu, F., Zhang, L., 2016. Molecular basis for adaptation of oysters to stressful marine intertidal environments. Annu. Rev. Anim. Biosci. 4, 357-381. <https://doi.org/10.1146/annurev-animal-022114-110903>.